

MODELING THE TRANSMISSION DYNAMICS AND CONTROL OF CASSAVA MOSAIC DISEASE WITH NON-CASSAVA HOST PLANTS

Bahati Erick

**A Dissertation Submitted in Partial Fulfilment of the Requirements for the Master's
Degree in Mathematical and Computer Sciences and Engineering of the Nelson Mandela
African Institution of Science and Technology**

Arusha, Tanzania

August, 2023

ABSTRACT

For many years cassava mosaic disease hinders cassava production in Africa. In this study, the mathematical model for the transmission dynamics and control of cassava mosaic disease in cassava and non-cassava host plant populations was formulated and analysed. The next-generation matrix technique was employed to obtain the basic reproduction number (\mathcal{R}_0). The local stability of the disease-free equilibrium point was determined using the Linearization method while the normalized forward sensitivity index technique was utilized to analyse the sensitivity of the model parameters. The optimality control technique, based on the Pontryagin Maximum Principle, with roguing activities and insecticide application as control strategies, has been applied to achieve the optimality of objective function. Moreover, the Incremental Cost-effectiveness Ratio approach was used to perform a cost-effectiveness analysis on control strategies in combating cassava mosaic disease. Lastly, the numerical simulation for the formulated models to assess sensitive parameters, global stability and the optimal solution was performed. The findings reveal the existence and global stability of both disease-free and endemic equilibrium points when $\mathcal{R}_0 \leq 1$ and $\mathcal{R}_0 > 1$ respectively. The most sensitive parameters for the dynamics of cassava mosaic disease were found to be whitefly mortality rate (ω) and the whitefly carrying capacity per m^2 (κ_w). The findings from numerical simulation and cost-effectiveness analysis on the optimality system conclude that the combined method of roguing and insecticide application has higher impacts with a lower cost of controlling the disease compared to the single control approach of roguing activities or insecticide application. Therefore, for effective and efficient mitigation of cassava mosaic disease, results from this study suggest the integrated approach of roguing and insecticides application.

DECLARATION

I, Bahati Erick do hereby declare to the Senate of the Nelson Mandela African Institution of Science and Technology that this dissertation is my own original work and that it has neither been submitted nor being concurrently submitted for degree award in any other institution.



Bahati Erick

21/08/2023

Date

The above declaration is confirmed



Dr. Maranya Mayengo

21/08/2023

Date



Prof. Dmitry Kuznetsov

21/08/2023

Date

COPYRIGHT

This dissertation is copyright material protected under the Berne Convention, the Copyright Act of 1999 and other international and national enactments, in that behalf, on intellectual property. It must not be reproduced by any means, in full or in part, except for short extracts in fair dealing; for researcher private study, critical scholarly review or discourse with an acknowledgement, without a written permission of the Deputy Vice Chancellor for Academic, Research and Innovation, on behalf of both the author and the Nelson Mandela African Institution of Science and Technology.

DECLARATION

I, Bahati Erick do hereby declare to the Senate of the Nelson Mandela African Institution of Science and Technology that this dissertation is my own original work and that it has neither been submitted nor being concurrently submitted for degree award in any other institution.

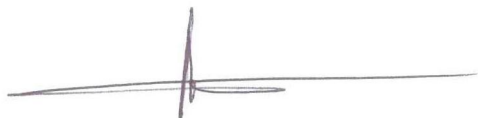


Bahati Erick

21/08/2023

Date

The above declaration is confirmed



Dr. Maranya Mayengo

21/08/2023

Date



Prof. Dmitry Kuznetsov

21/08/2023

Date

ACKNOWLEDGEMENTS

I am thankful to God Almighty for providing me with the chance, health, and capability to enrol in and successfully complete my Master's degree at the Nelson Mandela African Institution of Science and Technology (NM-AIST).

The School of Communication and Computational Science and Engineering (CoCSE) at NM-AIST, specifically Dr. Maranya Mayengo and Prof. Dmitry Kuznetsov, deserve special thanks for their dedication, encouragement, support, guidance, and supervision, which helped this study advance quickly over time after it began.

My employer, the Ministry of Education, Science and Technology in Tanzania (MoEST), deserves a lot of thanks for paying for my education and providing me with study leave so I could enrol in the MCSE program at NM-AIST.

My sincere gratitude goes out to Mr. Charles Pascal, Mr. Gilbert Mlacky, Mr. John Gweba, Mr. Mohamed Mwanga, Ms. Eva Lusekelo, and Mr. Faraja Luhanda, for their collaboration, support, and inspiration during the coursework and research part of my studies. Throughout my time at NM-AIST, I really value their contributions.

My profound appreciation to everyone in my family, especially to my devoted wife Devota Mushi, my son Ian, and my daughter Gianna, for their unfailing love, support, and prayers. Without them, this work could not have been accomplished successfully.

The community around NM-AIST played significant contributions to my studies. They were kind, considerate, and helpful throughout the whole time I was a student at NM-AIST. I owe them all the utmost appreciation.

DEDICATION

Ms. Devota Mushi

&

Gianna and Ian

I dedicate this work to you, my beloved wife, and my kids.

TABLE OF CONTENTS

ABSTRACT	i
DECLARATION	ii
COPYRIGHT	iii
CERTIFICATION	iv
ACKNOWLEDGEMENTS	v
DEDICATION	vi
TABLE OF CONTENTS	vii
LIST OF TABLES	ix
LIST OF FIGURES	x
LIST OF APPENDICES	xi
ABBREVIATIONS	xii
CHAPTER ONE	1
INTRODUCTION	1
1.1 Background of the problem	1
1.2 Statement of the problem	3
1.3 Rationale of the study	3
1.4 Objectives	3
1.4.1 General objective	3
1.4.2 Specific objectives	3
1.5 Research questions	4
1.6 Significance of the study	4
1.7 Delineation of the study	4
CHAPTER TWO	6
LITERATURE REVIEW	6
2.1 Introduction	6
2.2 Mathematical models for CMD	6
CHAPTER THREE	9
MATERIALS AND METHODS	9
3.1 Introduction	9
3.2 Model formulation	9
3.3 Basic model properties	11

3.3.1	Invariant region	11
3.3.2	Positivity of the solution	12
3.3.3	Existence of equilibrium points	13
3.3.4	The basic reproduction number	14
3.3.5	Local stability analysis for the disease-free equilibrium point	17
3.4	Sensitivity analysis	18
3.5	Global stability	19
3.5.1	Global stability of DFE	20
3.6	Control model formulation	22
3.7	Basic model properties for the control model	23
3.7.1	Invariant region	23
3.7.2	Positivity of the model solution	25
3.7.3	Disease-free equilibrium	25
3.7.4	The effective reproduction number	26
3.8	Optimal control	26
CHAPTER FOUR		30
RESULTS AND DISCUSSION		30
4.1	Introduction	30
4.2	Numerical simulation and results	30
4.3	Numerical simulation for the global stability analysis	32
4.4	Numerical simulation for optimal control model	33
4.4.1	Strategy 1: Roguing	34
4.4.2	Strategy 2: Insecticides application	35
4.4.3	Strategy 3: Roguing and insecticides application	36
4.5	Cost-effectiveness analysis	37
CHAPTER FIVE		42
CONCLUSION AND RECOMMENDATIONS		42
5.1	Conclusion	42
5.2	Recommendations	43
REFERENCES		45
APPENDICES		52
RESEARCH OUTPUTS		96

LIST OF TABLES

Table 1:	Sensitivity indices of model parameters	19
Table 2:	The range and baseline values for the model parameter	35
Table 3:	Total infection averted with their respective ICER in ascending order	39
Table 4:	Recalculated ICER for strategy 3 and 1	39

LIST OF FIGURES

Figure 1:	Cassava leaves infected by cassava mosaic disease	2
Figure 2:	Transmission mechanisms for cassava mosaic disease (Technical Centre for Agricultural and Rural Cooperation, 1990)	2
Figure 3:	Cassava mosaic disease flow diagram	10
Figure 4:	Cassava mosaic disease flow diagram with control measure	23
Figure 5:	Cassava population dynamics	30
Figure 6:	Whitefly population dynamics	31
Figure 7:	Non-cassava hosts population dynamics	32
Figure 8:	The impact of altering the whitefly mortality rate (ω) on the infected pop- ulation. Subplots (a), (b) and (c) represent the simulation of the infectious cassava plants, whiteflies and non-cassava host plants respectively	33
Figure 9:	The impact of altering the whitefly carrying capacity (κ_w) on the infected population. Subplots (a), (b) and (c) represent the simulation of the infec- tious cassava plants, whiteflies and non-cassava host plants respectively . . .	34
Figure 10:	A graphical depiction of global stability for DFE	36
Figure 11:	A graphical depiction of global stability for EEP	37
Figure 12:	Infected population dynamics when roguing activities are implemented . . .	38
Figure 13:	The control profile for roguing activities	39
Figure 14:	Infected population dynamics for optimal insecticides application	40
Figure 15:	The control profile for insecticides application	40
Figure 16:	The dynamics of the infected population when roguing and insecticides ap- plication was implemented	41
Figure 17:	The control profile for roguing implementation and insecticides application .	41

LIST OF APPENDICES

Appendix 1: Code for the basic model simulation.	52
Appendix 2: Main file for global stability simulation.	57
Appendix 3: Main file for optimal control model.	72
Appendix 4: Maple code for sensitivity indices.	80

ABBREVIATIONS

CBSD	Cassava Brown Streak Disease
CMD	Cassava Mosaic Disease
CMG	Cassava Mosaic Gemini-viruses
CoCSE	Computational and Communication Science and Engineering
DFE	Disease-free Equilibrium Point
EEP	Endemic Equilibrium Point
ICER	Incremental Cost-effectiveness Ratio
MoEST	Ministry of Education Science and Technology
NM-AIST	The Nelson Mandela Institution of Science and Technology
ODE	Ordinary Differential Equation
RHS	Right-Hand Side

CHAPTER ONE

INTRODUCTION

1.1 Background of the problem

Cassava (*Manihot esculenta* Crantz) is a perennial tropical woody plant in the Euphorbiaceae family that produces consumable starchy roots (Alves, 2002). European traders introduced these cassava plants in Africa from South America in the 16th century (Alaux & Fauquet, 1990). The starchy root is the most commonly used part of cassava and is rich in carbohydrates. Moreover, cassava leaves are also consumable and contain proteins, minerals, vitamins B1, B2, C and carotenes (Fasuyi, 2005). Cassava has been praised as a possible climate change crop due to its tolerance for unfavourable climatic conditions including irregular rainfall (Howeler, 2002).

In Tanzania, cassava is a crucial subsistence crop, especially in mostly dryland where cereal crops fail to thrive (Mtunguja *et al.*, 2019). Statistics show that in Tanzania, cassava production accounts for more than 37% of the economy of rural farmers (Mtunguja *et al.*, 2019). But, the existence and persistence of plant pests and diseases, such as Cassava Mosaic Disease (CMD) and Cassava Brown Streak Disease (CBSD) hinder the production of cassava in Africa (Hillocks, 1997). For instance, an average of 34 million tonnes of cassava yields are lost annually due to CMD (Chapwanya & Dumont, 2021; James *et al.*, 2006). The history of CMD in Africa can be traced back to 1894 when it was first reported in Tanzania (Chapwanya & Dumont, 2021).

More than eleven distinct Cassava Mosaic Gemini viruses (CMGs) are the known causes of CMD (James *et al.*, 2015; Tiendrebeogo *et al.*, 2012). These viruses spread through the whitefly vector ingestion from the host plant to the healthy cassava plant (Anitha *et al.*, 2020; Macfadyen *et al.*, 2018). The viruses can also be transported from one area to another through the use of contaminated stem cuttings (James & Thresh, 2000). Studies also show that yield loss due to contaminated cuttings ranges between 55% to 77% and when the plant is contaminated by whitefly the yield loss range between 35% to 60% (Technical Centre for Agricultural and Rural Cooperation, 1990). The symptoms of infected cassava plants depend on CMGs variant, climatic conditions, and the susceptibility of the cassava cultivar (Mabasa, 2007).



Figure 1: Cassava leaves infected by cassava mosaic disease

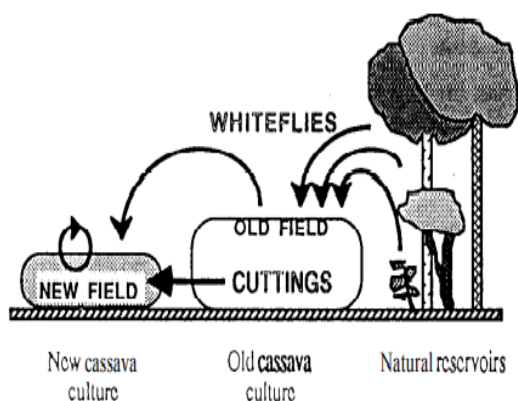


Figure 2: Transmission mechanisms for cassava mosaic disease (Technical Centre for Agricultural and Rural Cooperation, 1990)

Various studies have revealed the existence of alternative non-cassava host plants that could operate as a source of inoculum for whiteflies. For instance, Alabi *et al.* (2008) studied alternative host plants for CMD. The study establishes that castor oil plant (*Ricinus communis*), river tamarind plant (*Leucana leucocephala*), soybeans (*Glycine max*), coffee senna (*Senna occidentalis*), and a wild cassava species (*Manihot glaziovii*) can host both African Cassava Mosaic Virus (ACMV) and East African Cassava Mosaic Cameroon virus (EACMCV). These findings were also supported by Badamasi *et al.* (2020) where ACMV, EACMV and co-infection were found on Asthma-plant (*Euphorbia hirta* (L)) and *Combretum hispidum* which are commonly found as weeds in cassava plants. Further, Euphorbiaceae plants and 64 species of Solanaceae plants were found to host Srilankan Cassava Mosaic Virus (SCMV) variant in the study by Anitha *et al.* (2020). The results from these studies highlight that these non-cassava host plants can provide inoculum to the whitefly vector (Milenovic *et al.*, 2019; Sseruwagi *et al.*, 2006;

Tairo *et al.*, 2017).

1.2 Statement of the problem

Since reported in 1894 as shown by Chapwanya and Dumont (2021), CMD has continuously caused more yield loss that affects the welfare of African farmers. The transmission dynamics and control of CMD have been studied using a variety of mathematical models (Chapwanya & Dumont, 2021; Fahad *et al.*, 2021; Fahad & Roy, 2018; Holt *et al.*, 1997; Magoyo *et al.*, 2019). However, most of these models did not account the presence of non-cassava host plants in their model formulation and analyses. This calls for mathematical models incorporating non-cassava host plants to understand CMD transmission dynamics and potential control methods. Thus, this study develops the mathematical model and its analysis for the transmission dynamics and control of CMD with a non-cassava host plant population.

1.3 Rationale of the study

Since 1894, CMD has been one of the significant threats to Africa's capability to produce cassava. The transmission dynamics and control methods of CMD can be understood with the use of mathematical models. Therefore, the present study informs the farmers, policymakers, and other stakeholders in raising disease awareness and planning for the best time and variety of measures to reduce disease transmission.

1.4 Objectives

1.4.1 General objective

Generally, this study develops and analyses a mathematical model for transmission dynamics and control of CMD that incorporates non-cassava host plants.

1.4.2 Specific objectives

To fulfil the stated general objective, the subsequent specific objectives were formulated:

- (i) To formulate a deterministic mathematical model for transmission dynamics of CMD which includes non-cassava host plants population.
- (ii) To perform theoretical analysis for the formulated CMD Model, like the positivity of the

model solution, parameter sensitivity and stability of equilibrium points.

- (iii) To estimate the control parameters and their significance by conducting a numerical simulation.
- (iv) To find the most cost-effective method for disease control.

1.5 Research questions

To accomplish the stated research objectives, the following research questions were proposed and answered:

- (i) How to formulate a mathematical model which represents the dynamics of CMD and incorporates non-cassava host plants?
- (ii) How to theoretically analyse the formulated CMD dynamics model?
- (iii) What control measure parameters help to contain the CMD disease when conducting a numerical simulation?
- (iv) What ideal control approach for CMD control is the most efficient and economical?

1.6 Significance of the study

The obtained findings of this study:

- (i) Add to our understanding of how non-cassava host plants influence CMD transmission dynamics.
- (ii) Provides the best information regarding costs and effectiveness to stakeholders such as policy and decision-makers, farmers and researchers on managing CMD.
- (iii) Provides a foundation for future research.

1.7 Delineation of the study

Developing and analysing a mathematical model for the transmission dynamics and control of CMD that incorporates the non-cassava host plant population is an extensive and sensitive

study. This study does not aim to examine every aspect of the CMD's transmission dynamics and optimal disease management strategies. However, it focused on simulating the dynamics of CMD transmission while considering the influence of non-cassava host plants on the transmission dynamics and management of the disease. Further, not all CMD control methods are covered in the formulation of the optimality system. Instead, it solely employed control methods, which reduces the impact of the more sensitive parameters.

CHAPTER TWO

LITERATURE REVIEW

2.1 Introduction

Numerous deterministic model studies on the transmission dynamics and control of CMD have been conducted. In this chapter, some studies are examined to show how CMD Models have been developed thus far and what gaps exist.

2.2 Mathematical models for CMD

Holt *et al.* (1997) examined the effects of various parameters on the transmission dynamics of CMD by using the mathematical model. The model incorporates the whitefly vector population and cassava population. The system of ordinary differential equations (ODE) comprising healthy and diseased cassava plants, and non-infective and infective whiteflies compartments was used to model disease propagation. The study found that the disease's occurrence depends little on the use of contaminated cutting tools and roguing of infected cassava.

Magoyo *et al.* (2019) amended the framework by Holt *et al.* (1997) by incorporating cultivars which are susceptible to CMG through contaminated cutting and susceptible breeds that can acquire CMD virus through the use of infected cassava stem and whitefly contact. The findings reveal that CMD transmission was highly influenced by the whitefly mortality rate, whitefly infection rate, vector density, and the roguing rate of infected cassava plants.

Chapwanya and Dumont (2021) studied the dynamics of crop vector-borne disease by using CMD as a case. The study developed the mathematical model by considering the crop growth rate and the vector dynamics. According to the study, the most efficient approach to control CMD is to uproot affected plants (roguing). Further, the study recommends that to reduce epidemiological risk, the proportion of cassava cultivars which are less susceptible to the virus can be integrated into a plot.

Jittamai *et al.* (2021) formulated a deterministic mathematical model to investigate the dynamics of CMD. The model considers infected stem cuttings and whitefly transmission to determine the most effective and efficient disease management strategy. The findings indicated that the whiteflies' visitation rate on cassava plants and the whiteflies' density have impacts on the dis-

ease's spread. Additionally, the computer simulations showed how whitefly treatment might reduce disease management costs while effectively suppressing outbreaks.

Fahad *et al.* (2021) investigated the implications of the time used for vector maturation on CMD transmission dynamics where young and matured whitefly vectors were included, as well as a temporal delay that indicates vector maturation. The findings suggest that delaying vector maturation can help to stabilize the transmission otherwise cyclic epidemiological dynamics occur.

Different disease management strategies such as using resistant cassava cultivars, using insecticides to control whitefly, roguing (uprooting infected plants) and promoting the use of virus-free cuttings have been recommended to control CMD (Chikoti *et al.*, 2019; Tadesse & Regessa, 2017). Also, mathematical models have been employed in different scenarios to examine the efficacy of control measures for plant virus diseases such as CMD.

For example, Kinene *et al.* (2015) studied the spread of Cassava Brown Streak Disease (CBSD) by developing a deterministic mathematical model. The simulation results for roguing of infected cassava and killing of whitefly in the plantation as the control strategies reveal that roguing of infected cassava plants was the optimal solution.

Further, Gao *et al.* (2016) included impulsive roguing activities as a control strategy when developing a compartmental model to describe the plant disease dynamics in an irregular environment and found that the disease can never be eradicated by implementing roguing activities alone when there is a high infection rate and suggested the necessity of effective identification of the latent plant for disease control.

Additionally, the influence of roguing and insecticide application on mosaic disease in *Jatropha curcas* plant was studied by Al-Basir *et al.* (2017). The study found that the disease can be controlled with roguing activities but to ensure a smooth supply of *Jatropha* oil to the industry for biodiesel production the study recommends the use of an integrated approach of spraying and roguing because it uses less time in controlling the disease compared to roguing alone.

Moreover, Tadesse and Regessa (2017) review on CMD and mealybug revealed that the use of resistant cultivars, biological control, Phyto-sanitation practices and sound agronomic practices as a combined pest control strategy is the best control option for combating the disease.

Further, the study signified that the effectiveness of these integrated cassava pest control methods depends on well-planned training and raising farmers' awareness, agricultural development agents, extension officers, and policymakers.

In addition, Rakshit *et al.* (2019) developed a mathematical model to explore the role of uprooting infected plants as a biological control measure in the transmission dynamics of plant mosaic diseases. The model compartments include an uninfected and infectious vector, as well as a healthy, exposed, and infected plant. The study observes that infection rate is inversely associated with illness transmission, whitefly growth, and whitefly infection rate. In other words, it implies that even when infection rates are low, the dynamic system becomes unstable when they exceed their threshold values. Furthermore, the study found that if the proper rates and intervals for roguing can be identified, uprooting infected plants is the most cost-effective way for mosaic disease management in plants.

Furthermore, Bokil *et al.* (2019) studied the disease management strategies for vector plant diseases by considering frequency and abundance replanting strategies. The study found that the combined strategy of roguing and insecticide was the most effective disease-control strategy than a single control but the best control methods with the frequency-replanting model can differ greatly from those with the abundance-replanting model.

The reviewed literature shows how different researchers developed their models to understand the transmission dynamics and control of the CMD. All these researchers included cassava and whitefly vector population only in their model. Since current studies reveal the presence of many non-cassava host plants which can act as a source of inoculum to whitefly vector, there is a need to develop a mathematical model which incorporates the non-cassava host plant population. Therefore, this study addresses that gap by developing a mathematical model which includes non-cassava hosts.

CHAPTER THREE

MATERIALS AND METHODS

3.1 Introduction

This chapter illustrates the methods and procedures that were employed to achieve research objectives. Model formulation approaches, theoretical analysis of the formulated CMD Model and the estimation of control parameters are all covered. The study covered all non-cassava host plants which are used regularly by humans or found as weeds in cassava-growing regions in Tanzania.

3.2 Model formulation

In the model formulation, the model suggested by Bokil *et al.* (2019) was modified to include the exposed cassava compartment and the non-cassava host plant population. The exposed cassava plant compartment was added because it takes up to 5 weeks for CMD symptoms to appear and during that time an exposed plant can contaminate other cassava plants with the CMGs (Fargette *et al.*, 1994). Therefore the formulated model consists of cassava plant (N_c), non-cassava plant (N_h) and whitefly (N_w) population. The assumptions were made so that all susceptible plants and whiteflies are recruited logistically such that the recruitment rate is greater than their harvesting/mortality rate.

The parameters (r_c) , (r_w) and (r_h) describe the recruitment rate of susceptible compartments of cassava plants (S_c), whitefly (S_w) and non-cassava host plants (S_h) respectively while parameter (ψ) , (η) and (ω) symbolises the harvesting/mortality rate for cassava, non-cassava and whitefly respectively. Additionally, exposed cassava plants (E_c) were assumed to be the result of infected whitefly (I_w) ingestion rate (a) on susceptible cassava plants and the logistical recruitment of harvested exposed stem cuttings relying on the probability of selection (ρ). The rate at which susceptible non-cassava host plants (S_h) acquire mosaic viruses from infected whitefly (I_w) is presented by parameter (d) while the rate at which susceptible whitefly (S_w) acquire mosaic viruses from the infected/exposed cassava and non-cassava host (I_h) is symbolised by the parameter (b) and (c) respectively.

Lastly, parameters (ε) , (ϕ) , (κ_c) , (κ_w) and (κ_h) were used to symbolize exposure to infected latent rate, recovering rate of infected cassava (I_c), the carrying capacity of cassava plants, the

carrying capacity of whiteflies and the carrying capacity for non-cassava host plants respectively. As commented before, flow diagram Fig. 3 and system of differential equations (1) were designed to summarise the formulated model of CMD transmission dynamics provided $r_c - \psi > 0$, $r_w - \omega > 0$, and $r_h - \eta > 0$.

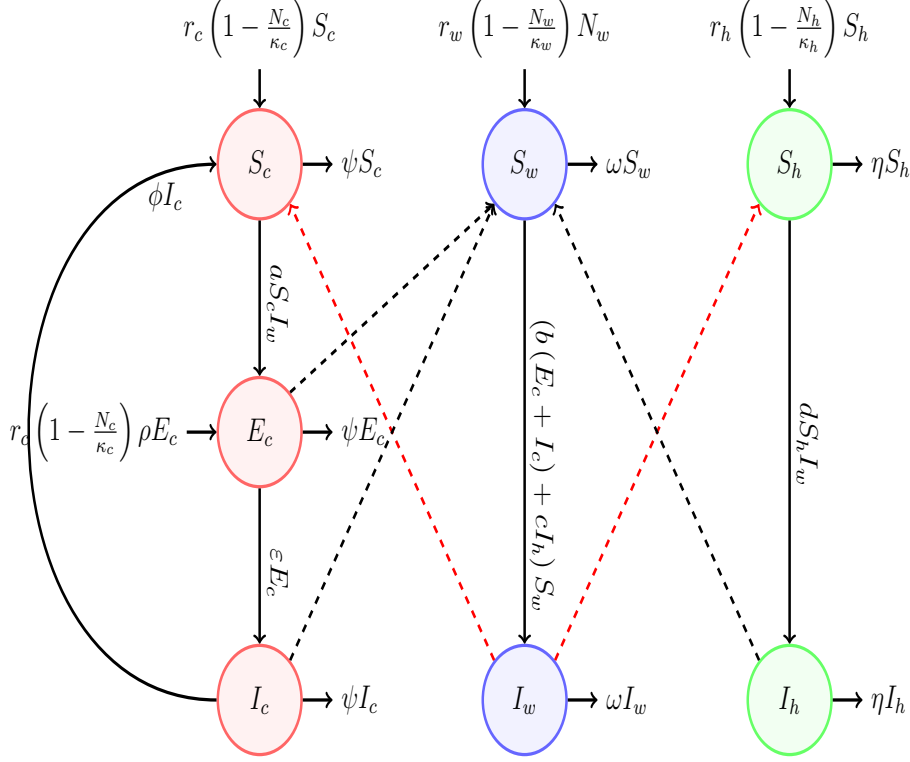


Figure 3: Cassava mosaic disease flow diagram

$$\begin{cases} \frac{dS_c}{dt} = r_c \left(1 - \frac{N_c}{\kappa_c}\right) S_c + \phi I_c - a S_c I_w - \psi S_c \\ \frac{dE_c}{dt} = r_c \left(1 - \frac{N_c}{\kappa_c}\right) \rho E_c + a S_c I_w - (\psi + \varepsilon) E_c \\ \frac{dI_c}{dt} = \varepsilon E_c - (\psi + \phi) I_c \\ \frac{dS_w}{dt} = \left(1 - \frac{N_w}{\kappa_w}\right) r_w N_w - (b(E_c + I_c) + c I_h) S_w - \omega S_w \\ \frac{dI_w}{dt} = (b(E_c + I_c) + c I_h) S_w - \omega I_w \\ \frac{dS_h}{dt} = r_h \left(1 - \frac{N_h}{\kappa_h}\right) S_h - d S_h I_w - \eta S_h \\ \frac{dI_h}{dt} = d S_h I_w - \eta I_h \end{cases} \quad (1)$$

with initial conditions, $S_c(0) > 0$, $E_c(0) \geq 0$, $I_c(0) \geq 0$, $S_w(0) > 0$, $I_w(0) \geq 0$, $S_h(0) > 0$, $I_h(0) \geq 0$.

3.3 Basic model properties

3.3.1 Invariant region

Lemma 3.1

Given the model system (1) in \mathbb{R}_+^7 with the initial conditions $S_c(0) > 0, E_c(0) \geq 0, I_c(0) \geq 0, S_w(0) > 0, I_w(0) \geq 0, S_h(0) > 0, I_h(0) \geq 0$, its solution enters the invariant region $\Omega = (S_c, E_c, I_c, S_w, I_w, S_h, I_h) \geq 0$ in \mathbb{R}_+^7 .

Proof: As used in the study of Chuma (2019) and Daudi *et al.* (2021) and Nyerere *et al.* (2020a), the box invariant method was employed to assess the feasibility of the formulated CMD Model system. We assume the continuity and the Lipschitz properties of its solution for our dynamic system $\frac{dX}{dt} = \mathcal{G}(X, t), X$ in \mathbb{R}^n . The model system (1) is reduced to the form,

$$\frac{dX}{dt} = \mathcal{A}X + Z$$

Where, column vector $X = (S_c, E_c, I_c, S_w, I_w, S_h, I_h)^T$ and

$$Z = \left(r_c \left(1 - \frac{N_c}{\kappa_c} \right) S_c, r_c \left(1 - \frac{N_c}{\kappa_c} \right) \rho E_c, 0, \left(1 - \frac{N_w}{\kappa_w} \right) r_w N_w, 0, r_h \left(1 - \frac{N_h}{\kappa_h} \right) S_h, 0 \right)^T$$

and the Metzler matrix $\mathcal{A} \forall X \in \mathbb{R}_+^7$ is defined as:

$$\mathcal{A} = \begin{pmatrix} -(\psi + aI_w) & 0 & \phi & 0 & 0 & 0 & 0 \\ 0 & -(\psi + \varepsilon) & 0 & 0 & aS_c & 0 & 0 \\ 0 & \varepsilon & -(\psi + \phi) & 0 & 0 & 0 & 0 \\ 0 & 0 & 0 & -P_1 & 0 & 0 & 0 \\ 0 & 0 & 0 & P_2 & -\omega & 0 & 0 \\ 0 & 0 & 0 & 0 & 0 & -(dI_w + \eta) & 0 \\ 0 & 0 & 0 & 0 & 0 & dI_w & -\eta \end{pmatrix} \quad (2)$$

provided, $P_1 = b(E_c + I_c) + cI_h + \omega$ and $P_2 = b(E_c + I_c) + cI_h$ are simplifying factors.

Since we have negative values in the major diagonal of the matrix \mathcal{A} in Equation (2) and the rest are non-negative values we can conclude that all variable solutions will enter and remain in the feasible area Ω . This indicates that the developed model system (1) is properly posed and

epidemiologically meaningful in the invariant region Ω .

3.3.2 Positivity of the solution

Utilizing the model equation (1) we have:

$$\frac{dS_c}{dt} = r_c \left(1 - \frac{N_c}{\kappa_c} \right) S_c + \phi I_c - a S_c I_w - \psi S_c \quad (3)$$

$$\frac{dS_c}{dt} \geq - (a I_w + \psi) S_c$$

employing separating the variables integration technique, we obtain:

$$\int \frac{dS_c}{S_c} \geq \int - (a I_w + \psi) dt$$

$$\ln S_c \geq - (a I_w + \psi) t + \mathcal{C}$$

$$S_c(t) \geq \mathcal{B} e^{-(a I_w + \psi) t}$$

substituting $t = 0$ as our initial condition, we obtain:

$$S_c(0) \geq \mathcal{B}$$

Thus:

$$S_c(t) \geq S_c(0) e^{-(a I_w + \psi) t} \geq 0 \quad \forall t \geq 0$$

Using the same approach for all equations of the model system (1) for all $t \geq 0$, we obtain the following results:

$$\begin{aligned} E_c(t) &\geq E_c(0) e^{-(\psi + \varepsilon) t} \geq 0 \\ I_c(t) &\geq I_c(0) e^{-(\psi + \phi) t} \geq 0 \\ S_w(t) &\geq S_w(0) e^{-(b(E_c + I_c) + c I_h + \omega) t} \geq 0 \\ I_w(t) &\geq I_w(0) e^{-\omega t} \geq 0 \\ S_h(t) &\geq S_h(0) e^{-(d I_w + \eta) t} \geq 0 \\ I_h(t) &\geq I_h(0) e^{-\eta t} \geq 0 \end{aligned} \quad (4)$$

Therefore, this assures that the formulated model system (1) has the positive solution for all $t \geq 0$.

3.3.3 Existence of equilibrium points

(i) Disease-free equilibrium point

In this sub-section, we obtain the Disease-free Equilibrium Point (DFE) by solving the system the CMD model (1) when the rate of change of model variables is equal to zero. As a result, we have:

$$\begin{aligned}
r_c \left(1 - \frac{N_c^*}{\kappa_c}\right) S_c^* + \phi I_c^* - a S_c^* I_w^* - \psi S_c^* &= 0 \\
r_c \left(1 - \frac{N_c^*}{\kappa_c}\right) \rho E_c^* + a S_c^* I_w^* - (\psi + \varepsilon) E_c^* &= 0 \\
\varepsilon E_c^* - (\psi + \phi) I_c^* &= 0 \\
\left(1 - \frac{N_w^*}{\kappa_w}\right) r_w N_w^* - (b(E_c^* + I_c^*) + c I_h^*) S_w^* - \omega S_w^* &= 0 \\
(b(E_c^* + I_c^*) + c I_h^*) S_w^* - \omega I_w^* &= 0 \\
r_h \left(1 - \frac{N_h^*}{\kappa_h}\right) S_h^* - d S_h^* I_w^* - \eta S_h^* &= 0 \\
d S_h^* I_w^* - \eta I_h^* &= 0
\end{aligned} \tag{5}$$

where $(S_c^*, E_c^*, I_c^*, S_w^*, I_w^*, S_h^*, I_h^*)$ is the set of solution to the system (5). When $E_c^* = 0, I_c^* = 0, I_w^* = 0, I_h^* = 0$ we obtain the DFE point, $DFE = (S_c^0, E_c^0, I_c^0, S_w^0, I_w^0, S_h^0, I_h^0)$ given by:

$$DFE = \left(\frac{\kappa_c(r_c - \psi)}{r_c}, 0, 0, \frac{\kappa_w(r_w - \omega)}{r_w}, 0, \frac{\kappa_h(r_h - \eta)}{r_h}, 0 \right) \tag{6}$$

(ii) Disease endemic equilibrium

The Disease Endemic Equilibrium Point (EEP) refers to the equilibrium point when disease infection occurs in the population of the model system (Kung'aro, 2016). Considering the system model equation (1), we obtain $EEP = (S_c^*, E_c^*, I_c^*, S_w^*, I_w^*, S_h^*, I_h^*)$, where:

$$\begin{aligned}
S_c^* &= \frac{I_c^* \kappa_c \phi + r_c (\kappa_c - N_c^*)}{\kappa_c (a I_w^* + \phi)}, \quad E_c^* = \frac{a \kappa_c S_c^* I_w^*}{N_c^* r_c \rho + \kappa_c ((\psi + \varepsilon) - r_c \rho)}, \quad I_c^* = \frac{\varepsilon E_c^*}{(\psi + \phi)}, \\
S_w^* &= \frac{r_w N_w^* (\kappa_w - N_w^*)}{\kappa_w ((b(E_c^* + I_c^*) + c I_h^*) + \omega)}, \quad I_w^* = \frac{(b(E_c^* + I_c^*) + c I_h^*) S_w^*}{\omega} \text{ and } S_h^* = \frac{\eta I_h^*}{d I_w^*}
\end{aligned}$$

Considering equation 5, we obtain:

$$r_c \left(1 - \frac{N_c^*}{\kappa_c} \right) S_c^* + \phi I_c^* - a S_c^* I_w^* - \psi S_c^* = 0$$

implying that $r_c \left(\frac{\kappa_c - N_c^*}{\kappa_c} \right) S_c^* + \phi I_c^* > 0$, consequently, we have $\kappa_c - N_c^* > 0$. Similar to this, employing equation number four and six of the system (5) we confirm that $\kappa_w - N_w^* > 0$ and $\kappa_h - N_h^* > 0$, respectively. Further, the second equation of the system (5) verifies that $r_c \rho N_c^* + (\psi + \varepsilon) - r_c \rho > 0$.

3.3.4 The basic reproduction number

The concept of Basic Reproduction Number (\mathcal{R}_0) was first introduced in demographic studies. Later, the concept was expanded to vector-borne diseases and human infection. Currently, the idea is widely used in studies of infectious diseases, especially in models of in-host population dynamics (Heffernan *et al.*, 2005). The definition of (\mathcal{R}_0) is contextual but generally, the (\mathcal{R}_0) refers to the anticipated number of offspring that a person will generate throughout the course of their lifespan (Heffernan *et al.*, 2005). When $\mathcal{R}_0 < 1$, it indicates that the disease will disappear in the environment but whenever $\mathcal{R}_0 \geq 1$, the disease will spread (Driessche & Watmough, 2008).

Different approaches can be used in obtaining \mathcal{R}_0 . In the deterministic model, \mathcal{R}_0 can be found by using the survival function method or next-generation matrix. This study employs the next-generation matrix concepts as presented by Driessche and Watmough (2008) to compute \mathcal{R}_0 . The infected compartments of the model were written as:

$$\frac{dX}{dt} = \mathcal{F}_i - \mathcal{V}_i, i = 1, \dots, n,$$

where \mathcal{F}_i is the increased secondary infections rate at i^{th} disease compartment and \mathcal{V}_i is the disease progression and death decrease rate at i^{th} compartment. The Spectral radius of the matrix $\mathcal{F}\mathcal{V}^{-1}$ gives the \mathcal{R}_0 , thus $\mathcal{R}_0 = \rho(\mathcal{F}\mathcal{V}^{-1})$ where, $\mathcal{F} = \left[\frac{\partial \mathcal{F}_i}{\partial x_j} \right]$ and $\mathcal{V} = \left[\frac{\partial \mathcal{V}_i}{\partial x_j} \right]$ evaluated at DFE point when $x = (E_c, I_c, I_w, I_h)$. Now, referring to the model system (1), we

find the infected subsystem to be:

$$\begin{cases} \frac{dE_c}{dt} = r_c \left(1 - \frac{N_c}{\kappa_c}\right) \rho E_c + a S_c I_w - (\psi + \varepsilon) E_c \\ \frac{dI_c}{dt} = \varepsilon E_c - (\psi + \phi) I_c \\ \frac{dI_w}{dt} = (b(E_c + I_c) + c I_h) S_w - \omega I_w \\ \frac{dI_h}{dt} = d S_h I_w - \eta I_h \end{cases} \quad (7)$$

Thus:

$$\mathcal{F}_i = \begin{pmatrix} r_c \left(1 - \frac{N_c}{\kappa_c}\right) \rho E_c + a S_c I_w \\ 0 \\ (b(E_c + I_c) + c I_h) S_w \\ d S_h I_w \end{pmatrix} \quad (8)$$

and,

$$\mathcal{V}_i = \begin{pmatrix} (\psi + \varepsilon) E_c \\ (\psi + \phi) I_c - \varepsilon E_c \\ \omega I_w \\ \eta I_h \end{pmatrix}. \quad (9)$$

The Jacobian matrix for \mathcal{F}_i and \mathcal{V}_i evaluated at DFE are given by:

$$\mathcal{F} = \begin{pmatrix} r_c \left(1 - \frac{S_c^0}{\kappa_c}\right) \rho & 0 & a S_c^0 & 0 \\ 0 & 0 & 0 & 0 \\ b S_w^0 & b S_w^0 & 0 & c S_w^0 \\ 0 & 0 & d S_h^0 & 0 \end{pmatrix} \quad (10)$$

and

$$\mathcal{V} = \begin{pmatrix} (\psi + \varepsilon) & 0 & 0 & 0 \\ -\varepsilon & \psi + \phi & 0 & 0 \\ 0 & 0 & \omega & 0 \\ 0 & 0 & 0 & \eta \end{pmatrix}. \quad (11)$$

computing \mathcal{V}^{-1} we get:

$$\mathcal{V}^{-1} = \begin{pmatrix} \frac{1}{\psi + \varepsilon} & 0 & 0 & 0 \\ \frac{\varepsilon}{(\psi + \phi)(\psi + \varepsilon)} & \frac{1}{\psi + \phi} & 0 & 0 \\ 0 & 0 & \frac{1}{\omega} & 0 \\ 0 & 0 & 0 & \frac{1}{\eta} \end{pmatrix} \quad (12)$$

accordingly:

$$\mathcal{FV}^{-1} = \begin{pmatrix} \frac{\psi\rho}{\psi + \varepsilon} & 0 & a\frac{(r_c - \psi)\kappa_c}{\omega r_c} & 0 \\ 0 & 0 & 0 & 0 \\ b\frac{(r_w - \omega)\kappa_w}{(\psi + \varepsilon)r_w} \left(1 + \frac{\varepsilon}{\psi + \phi}\right) & b\frac{(r_w - \omega)\kappa_w}{(\psi + \phi)r_w} & 0 & c\frac{(r_w - \omega)\kappa_w}{\eta r_w} \\ 0 & 0 & d\frac{(r_h - \eta)\kappa_h}{\omega r_h} & 0 \end{pmatrix}. \quad (13)$$

If we let:

$$g_{11} = \frac{\psi\rho}{\psi + \varepsilon}, g_{13} = a\frac{(r_c - \psi)\kappa_c}{\omega r_c}, g_{31} = b\frac{(r_w - \omega)\kappa_w}{(\psi + \varepsilon)r_w} \left(1 + \frac{\varepsilon}{\psi + \phi}\right), \\ g_{32} = b\frac{(r_w - \omega)\kappa_w}{(\psi + \phi)r_w}, g_{34} = c\frac{(r_w - \omega)\kappa_w}{\eta r_w} \text{ and } g_{43} = d\frac{(r_h - \eta)\kappa_h}{\omega r_h}$$

and compute $\mathcal{R}_0 = \rho(\mathcal{FV}^{-1})$ we obtain:

$$\mathcal{R}_0 = \max \left\{ \frac{X}{6} + \frac{2}{X}X_2 + \frac{1}{3}g_{11}, -\frac{X}{12} - \frac{X_2}{X} + \frac{1}{3}g_{11} \pm \frac{\sqrt{3}}{2}i \left(\frac{X}{6} - \frac{2X_2}{X} \right) \right\} \quad (14)$$

where, $X = (X_0 + 12\sqrt{X_1})^{\frac{1}{3}}$, $X_0 = 4(9g_{31}g_{13} - 18g_{43}g_{34} + 2(g_{11})^2)g_{11}$ and

$$X_1 = -3(g_{11})^2(4g_{34}g_{43}(1 - 2g_{34}g_{43}) + g_{13}g_{31}(g_{13}g_{31} + 20g_{34}g_{43})) \\ - 12(g_{13}g_{31})^2(g_{13}g_{31} + 3g_{34}g_{43}) - 12(g_{34}g_{43})^2(3g_{13}g_{31} + g_{34}g_{43})$$

$$X_2 = g_{31}g_{13} + g_{43}g_{34} + \frac{1}{3}(g_{11})^2$$

3.3.5 Local stability analysis for the disease-free equilibrium point

Theorem 3.1

The disease-free equilibrium point (DFE) of the CMD Model system (1) is locally asymptotic stable when $\mathcal{R}_0 < 1$ and unstable otherwise.

Proof: The concept of decomposing the system Jacobian matrix evaluated at DFE and investigating the eigenvalues of diagonal sub-matrix as used by Mayengo *et al.* (2022), was used to verify the local stability of the model system (1). Therefore, matrix (15) is the obtained Jacobian matrix at DFE.

$$J_{DFE} = \begin{pmatrix} -(r_c - \psi) & -(r_c - \psi) & P_3 & 0 & -aS_c^0 & 0 & 0 \\ 0 & P_4 & 0 & 0 & aS_c^0 & 0 & 0 \\ 0 & \varepsilon & -(\psi + \phi) & 0 & 0 & 0 & 0 \\ 0 & -bS_w^0 & -bS_w^0 & P_5 & -r_w + 2\omega & 0 & -cS_w^0 \\ 0 & bS_w^0 & bS_w^0 & 0 & -\omega & 0 & cS_w^0 \\ 0 & 0 & 0 & 0 & -dS_h^0 & -(r_h - \eta) & -(r_h - \eta) \\ 0 & 0 & 0 & 0 & dS_h^0 & 0 & -\eta \end{pmatrix} \quad (15)$$

Where, $P_3 = -(r_c - \psi) + \phi$, $P_4 = -(\psi(1 - \rho) + \varepsilon)$, and $P_5 = -(r_w - \omega)$

When decomposing matrix J_{DFE} we obtain a block matrix of the form:

$$J_{DFE} = \begin{pmatrix} J_{11} & J_{12} & \mathbf{0} \\ J_{21} & J_{22} & J_{23} \\ \mathbf{0} & J_{32} & J_{33} \end{pmatrix} \quad (16)$$

Where $\mathbf{0}$ are zero matrices and

$$J_{11} = \begin{pmatrix} -(r_c - \psi) & -(r_c - \psi) & -(r_c - \psi) + \phi \\ 0 & -(\psi(1 - \rho) + \varepsilon) & 0 \\ 0 & \varepsilon & -(\psi + \phi) \end{pmatrix},$$

$$J_{22} = \begin{pmatrix} -(r_w - \omega) & -r_w + 2\omega \\ 0 & -\omega \end{pmatrix}, \quad J_{33} = \begin{pmatrix} -(r_h - \eta) & -(r_h - \eta) \\ 0 & -\eta \end{pmatrix}.$$

From diagonal sub-matrix J_{11} with eigenvalues $-(\psi + \phi)$, $-(\psi(1 - \rho) + \varepsilon)$ and $-(r_c - \psi)$, J_{22} with eigenvalues $-(r_w - \omega)$ and $-\omega$, and J_{33} with eigenvalues $-(r_h - \eta)$ and $-\eta$, if we utilize the stated assumption ($r_c - \psi > 0$, $r_w - \omega > 0$ and $r_h - \eta > 0$) of the model system (1) we can observe that our diagonal sub-matrices have real and negative eigenvalues. Since that property guarantees the stability of diagonal sub-matrices it in turn assures the local stability of the matrix (15) when $\mathcal{R}_0 < 1$.

3.4 Sensitivity analysis

The concept of normalized forward sensitivity index technique as used by Kung'aro (2016) was used to examine parameter contribution on the transmission of CMD using \mathcal{R}_0 . Therefore, we establish that:

$$\tau_{u_i}^{\mathcal{R}_0} = \frac{\partial \mathcal{R}_0}{\partial u_i} \times \frac{u_i}{\mathcal{R}_0} \quad (17)$$

where u_i represents the i^{th} model parameters as elaborated on Table 1.

With the help of Maple 15 software and the baseline values shown in Table 1 the sensitivity indices of model parameters of the model system (1) were computed (Appendix 4). The results are highlighted in Table 1.

The column of sensitivity index in Table 1 shows that the whitefly death rate (ω) has the most negative index while whitefly carrying capacity (κ_w) has the most positive index than other parameters.

Since the increase of the rate of negative indices, parameter causes the decrease of disease transmission rate and vice versa, these results signify that the increase of whitefly mortality rate (ω) or the decrease of whitefly carrying capacity will reduce the disease transmission rate. This signifies that for effective control strategies during the outbreak, CMD stakeholders should implement strategies which accelerate the whitefly death rate and reduce the carrying capacity of whiteflies. Other negative indices results which can also be accelerated to reduce the transmission rate of CMD include non-cassava host plant harvesting rate (η), cassava plant harvesting rate (ψ), the cassava plant latent rate (ε) and the cassava plant recovering rate (ϕ).

Table 1: Sensitivity indices of model parameters

Parameter	Range	Baseline Value	Reference	Index
r_c	0.025-0.1	0.05 day^{-1}	Jeger <i>et al.</i> (2004)	0.0177
r_w	0.1-0.3	0.2 day^{-1}	Holt <i>et al.</i> (1997)	0.0117
r_h	-	0.02 day^{-1}	Assumed	0.2141
ρ	0-1	0.1	Holt <i>et al.</i> (1997)	0.0006
a	0.002-0.032	0.008 $plant^{-1}day^{-1}$	Holt <i>et al.</i> (1997)	0.2779
b	0.002-0.032	0.008 $white\ fly^{-1}day^{-1}$	Holt <i>et al.</i> (1997)	0.2779
c	-	0.008 $white\ fly^{-1}day^{-1}$	Assumed	0.2218
d	-	0.008 $plant^{-1}day^{-1}$	Assumed	0.2218
ε	-	0.033 day^{-1}	Jeger <i>et al.</i> (2004)	-0.0202
ω	0.06-0.18	0.06 day^{-1}	Holt <i>et al.</i> (1997)	-0.7138
η	-	0.001 day^{-1}	Assumed	-0.2334
ψ	0.002-0.004	0.003 day^{-1}	Holt <i>et al.</i> (1997)	-0.1579
κ_c	0.01-1	0.7 m^{-2}	Holt <i>et al.</i> (1997)	0.2779
κ_w	0-350	90 m^{-2}	Bokil <i>et al.</i> (2019)	0.4997
κ_h	0.01-1	0.1 m^{-2}	Assumed	0.2218
ϕ	0.002-0.004	0.003 day^{-1}	Jeger <i>et al.</i> (2004)	-0.1176

Lastly, we find that the probability of replanting exposed cassava stem (ρ) has less sensitivity index compared to other parameters. This implies that the probability of using the exposed stem cutting does not contribute much to the disease spreading rate and therefore when used as a disease management strategy it will not bring pleasing results.

3.5 Global stability

The analysis of global asymptotic stability on equilibrium points of dynamical models is one of the mathematical tools that enable understanding the disease persistence over time. In global stability analysis, whenever the DFE is globally asymptotic stable, the eradication of the disease is assured in spite of the initial number of infected individuals introduced into the population, and if the EEP is globally asymptotic stable, the infection will permanently persist in the population if no control strategies implemented (Driessche & Watmough, 2002; Wangari, 2020). This information helps stakeholders to plan appropriately on prevention and intervention strate-

gies for the disease.

Different global stability analysis approaches such as Poincaré–Bendixson theory, Lyapunov functions, Bendixson and Dulac criteria, the concept of monotone flows, the geometric approach and the Volterra–Lyapunov matrix theory have been developed and used over time (Liao & Wang, 2012; Parsaei *et al.*, 2017; Zahedi & Kargar, 2017). The use of these methods highly depends on the strengths and limitations of the method and the nature of the problem at hand (Zahedi & Kargar, 2017). The Lyapunov function approach has been frequently utilized and successful in providing global stability findings for various epidemiological models, despite the difficulties in determining the proper function coefficients (Liao & Wang, 2012; Zahedi & Kargar, 2017). To overcome that challenge of determining the proper function coefficients, Li and Shuai (2010) highlighted the use of graph theory in the construction and estimation of the derivatives of the Lyapunov functions. Additionally, the introduced family of Lyapunov functions by Korobeinikov and Maini (2004) and Korobeinikov and Wake (2002) helps in analyzing the global stability of equilibrium points for many epidemiological models. Thus, the Lyapunov function method is simple to implement and requires little theoretical background knowledge (Liao & Wang, 2012).

In this section, the concept by Castillo-Chavez *et al.* (2002) was employed to verify the global stability of the DFE for the model system (1). Furthermore, we performed a numerical simulation of model population variables on the model system (1) to portray the stability of DFE and EEP. The numerical simulation results are presented in Chapter Four.

3.5.1 Global stability of DFE

As highlighted in the study by Chuma and Mwanga (2019) and Renald (2020), the CMD Model system (1) is written in the form:

$$\begin{cases} \frac{dX_s}{dt} = Q_1 (X_s - DFE) + Q_2 X_i \\ \frac{dX_i}{dt} = Q_3 X_i \end{cases} \quad (18)$$

Where X_s is the vector for non-transmitting individuals(susceptible) compartments, X_i is the vector for transmitting individuals (Exposed and infected), DFE is the CMD free equilibrium point, and Q_1, Q_2 and Q_3 are matrices we need to find. Therefore, $X_s = (S_c, S_w, S_h)^T$, $X_i =$

$$(E_c, I_c, I_w, I_h)^T \text{ and DFE} = \left(\frac{(r_c - \psi) \kappa_c}{r_c}, 0, 0, \frac{(r_w - \omega) \kappa_w}{r_w}, 0, \frac{(r_h - \eta) \kappa_h}{r_h}, 0 \right).$$

In order to verify the DFE point of the CMD Model system (1) is globally asymptotic stable when $\mathcal{R}_0 < 1$, we showed that, the matrix Q_1 has real and negative eigenvalues and Q_3 is a Metzler matrix (i.e., the out-diagonal elements of Q_3 are non-negative). Now, if we write the CMD Model system (1) to the form stipulated by equation (18) we get:

$$\begin{pmatrix} r_c \left(1 - \frac{N_c}{\kappa_c} \right) S_c + \phi I_c - a S_c I_w - \psi S_c \\ \left(1 - \frac{N_w}{\kappa_w} \right) r_w N_w - (b(E_c + I_c) + c I_h) S_w - \omega S_w \\ r_h \left(1 - \frac{N_h}{\kappa_h} \right) S_h - d S_h I_w - \eta S_h \end{pmatrix} = Q_1 \begin{pmatrix} S_c - \frac{(r_c - \psi) \kappa_c}{r_c} \\ S_w - \frac{(r_w - \omega) \kappa_w}{r_w} \\ S_h - \frac{(r_h - \eta) \kappa_h}{r_h} \end{pmatrix} + Q_2 \begin{pmatrix} E_c \\ I_c \\ I_w \\ I_h \end{pmatrix} \quad (19)$$

and

$$\begin{pmatrix} r_c \left(1 - \frac{N_c}{\kappa_c} \right) \rho E_c + a S_c I_w - (\psi + \varepsilon) E_c \\ \varepsilon E_c - (\psi + \phi) I_c \\ (b(E_c + I_c) + c I_h) S_w - \omega I_w \\ d S_h I_w - \eta I_h \end{pmatrix} = Q_3 \begin{pmatrix} E_c \\ I_c \\ I_w \\ I_h \end{pmatrix} \quad (20)$$

If we solve for Q_1, Q_2 and Q_3 , we find:

$$Q_1 = \begin{pmatrix} -\frac{S_c r_c}{\kappa_c} & 0 & 0 \\ 0 & -\frac{N_w r_w}{\kappa_w} & 0 \\ 0 & 0 & -\frac{S_h r_h}{\kappa_h} \end{pmatrix} \quad (21)$$

$$Q_2 = \begin{pmatrix} -\frac{S_c r_c}{\kappa_c} & -\frac{S_c r_c}{\kappa_c} + \phi & -a S_c & 0 \\ -b S_w & -b S_w & -\frac{N_w r_w}{\kappa_w} + \omega & -c S_w \\ 0 & 0 & -d S_h & -\frac{S_h r_h}{\kappa_h} \end{pmatrix} \quad (22)$$

and

$$Q_3 = \begin{pmatrix} -\left(-r_c \left(1 - \frac{N_c}{\kappa_c}\right) \rho + (\varepsilon + \psi)\right) & 0 & aS_c & 0 \\ \varepsilon & -(\psi + \phi) & 0 & 0 \\ bS_w & bS_w & -\omega & cS_w \\ 0 & 0 & dS_h & -\eta \end{pmatrix} \quad (23)$$

From the obtained results, we can see the eigenvalues of the Q_1 are $-\frac{S_c r_c}{\kappa_c}$, $-\frac{N_w r_w}{\kappa_w}$ and $-\frac{S_h r_h}{\kappa_h}$ which are real and negative. Also, from Equation (5) it is evident that $-r_c \left(1 - \frac{N_c}{\kappa_c}\right) \rho + (\varepsilon + \psi) > 0$, hence, the matrix Q_3 is the Metzler matrix. Thus, the DFE point is globally and asymptotic stable when $\mathcal{R}_0 < 1$.

Theorem 3.2

The DFE point of the CMD Model system (1) is globally asymptotically stable when $\mathcal{R}_0 < 1$ and unstable otherwise.

3.6 Control model formulation

In this section, the formulated control model includes two-time dependant control parameters $u_1(t) \in [0, 1]$ and $u_2(t) \in [0, 1]$ to the basic model (1) as disease management efforts made on roguing activities and insecticide spraying respectively. Therefore, the control $u_1(t)\tau$ intends to reduce the whitefly virus acquisition from the infected cassava and non-cassava host plants through roguing activities, while control $u_2(t)\varsigma$ increases the death rate of whitefly through insecticide spraying. This implies that τ and ς represent the number of harvested cassava and non-cassava plants due to roguing activities and the death rate of whiteflies due to insecticide spraying respectively. When $u_1(t)$ and $u_2(t)$ equals zero it implies that no controlling measures are taken to mitigate the disease and when set to one, it means that the control strategy is fully implemented.

The definitions of variables and parameters remain the same as in the model system (1) except for model assumptions. For the control model, the assumptions are; $r_c - (\psi + u_1\tau) > 0$, $r_w - (\omega + u_2\varsigma) > 0$, and $r_h - (\eta + u_1\tau) > 0$. Figure 4 and the system of equations (24) summarize the formulated control model.

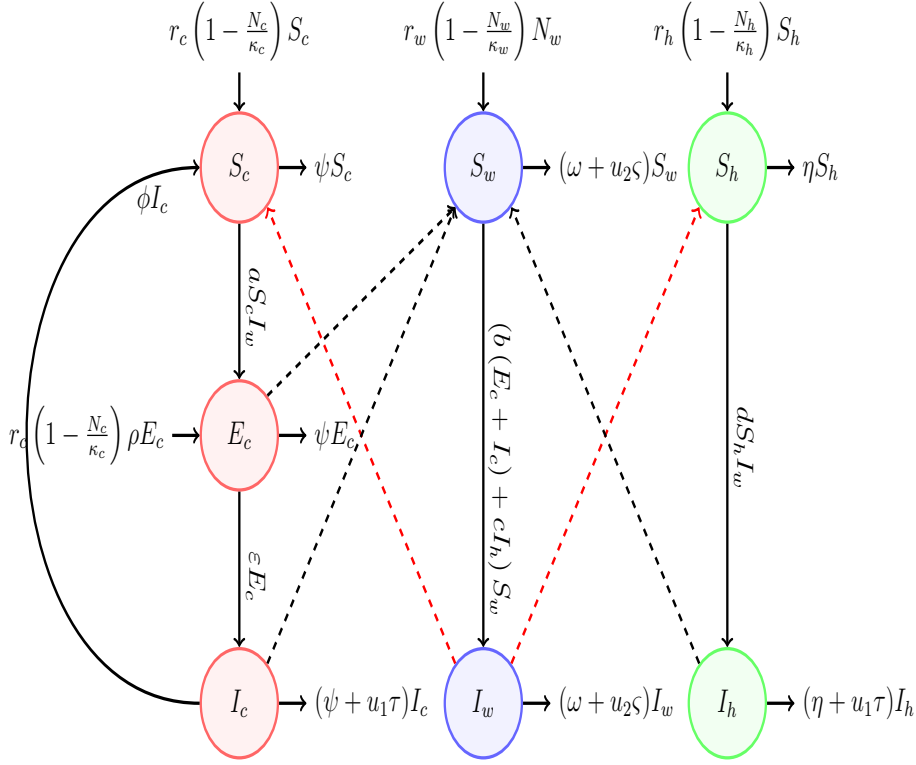


Figure 4: Cassava mosaic disease flow diagram with control measure

$$\begin{cases}
 \frac{dS_c}{dt} = r_c \left(1 - \frac{N_c}{\kappa_c}\right) S_c + \phi I_c - a S_c I_w - \psi S_c \\
 \frac{dE_c}{dt} = r_c \left(1 - \frac{N_c}{\kappa_c}\right) \rho E_c + a S_c I_w - (\psi + \varepsilon) E_c \\
 \frac{dI_c}{dt} = \varepsilon E_c - (\psi + \phi + u_1 \tau) I_c \\
 \frac{dS_w}{dt} = \left(1 - \frac{N_w}{\kappa_w}\right) r_w N_w - (b(E_c + I_c) + c I_h) S_w - (\omega + u_2 \zeta) S_w \\
 \frac{dI_w}{dt} = (b(E_c + I_c) + c I_h) S_w - (\omega + u_2 \zeta) I_w \\
 \frac{dS_h}{dt} = r_h \left(1 - \frac{N_h}{\kappa_h}\right) S_h - d S_h I_w - \eta S_h \\
 \frac{dI_h}{dt} = d S_h I_w - (\eta + u_1 \tau) I_h
 \end{cases} \quad (24)$$

provided, $S_c(0) > 0$, $E_c(0) \geq 0$, $I_c(0) \geq 0$, $S_w(0) > 0$, $I_w(0) \geq 0$, $S_h(0) > 0$, $I_h(0) \geq 0$.

3.7 Basic model properties for the control model

3.7.1 Invariant region

Lemma 3.2

With the initial conditions $S_c(0) > 0$, $E_c(0) \geq 0$, $I_c(0) \geq 0$, $S_w(0) > 0$, $I_w(0) \geq 0$, $S_h(0) > 0$, $I_h(0) \geq 0$.

0, $I_h(0) \geq 0$, the solution of the model system (24) in \mathbb{R}_+^7 enters the invariant region $\Omega = (S_c, E_c, I_c, S_w, I_w, S_h, I_h) \geq 0$ in \mathbb{R}_+^7 .

Proof: As in the Subsection 3.3.1 we utilize the box invariant approach to examine the feasibility of the CMD control model. We write the model system (24) as:

$$\frac{dX}{dt} = \mathcal{A}X + Z$$

Where, column vector $X = (S_c, E_c, I_c, S_w, I_w, S_h, I_h)^T$ and

$$Z = \left(r_c \left(1 - \frac{N_c}{\kappa_c} \right) S_c, r_c \left(1 - \frac{N_c}{\kappa_c} \right) \rho E_c, 0, r_w \left(1 - \frac{N_w}{\kappa_w} \right) N_w, 0, r_h \left(1 - \frac{N_h}{\kappa_h} \right) S_h, 0 \right)^T$$

and the Metzler matrix $\mathcal{A} \forall X \in \mathbb{R}_+^7$ is expressed as:

$$\mathcal{A} = \begin{pmatrix} -(\psi + aI_w) & 0 & \phi & 0 & 0 & 0 & 0 \\ 0 & (\psi + \varepsilon) & 0 & 0 & aS_c & 0 & 0 \\ 0 & \varepsilon & P_6 & 0 & 0 & 0 & 0 \\ 0 & 0 & 0 & -P_7 & 0 & 0 & 0 \\ 0 & 0 & 0 & P_8 & -(\omega + u_2\varsigma) & 0 & 0 \\ 0 & 0 & 0 & 0 & 0 & -(dI_w + \eta) & 0 \\ 0 & 0 & 0 & 0 & 0 & dI_w & -(\eta + u_1\tau) \end{pmatrix} \quad (25)$$

Where, $P_6 = -(\psi + \phi + u_1\tau)$, $P_7 = b(E_c + I_c) + cI_h + \omega + u_2\varsigma$, and $P_8 = b(E_c + I_c) + cI_h$.

Since we have negative values in the major diagonal of the matrix \mathcal{A} in equation (25) and the rest are non-negative values we can conclude that all variable solutions will enter and remain in the feasible area Ω . This indicates that the developed control model system (24) is properly posed and epidemiologically meaningful in the invariant region Ω .

3.7.2 Positivity of the model solution

As in Subsection 27, using the first equation of the control model equation (24) we obtain:

$$\frac{dS_c}{dt} = r_c \left(1 - \frac{N_c}{\kappa_c} \right) S_c + \phi I_c - a S_c I_w - \psi S_c \quad (26)$$

$$\frac{dS_c}{dt} \geq - (a I_w + \psi) S_c$$

through separating the variables, we integrate both sides to obtain:

$$\int \frac{dS_c}{S_c} \geq \int - (a I_w + \psi) dt$$

$$\ln S_c \geq - (a I_w + \psi) t + \mathcal{C}$$

$$S_c(t) \geq \mathcal{B} e^{-(a I_w + \psi) t}$$

At the point $t = 0$, we obtain:

$$S_c(0) \geq \mathcal{B}$$

Hence:

$$S_c(t) \geq S_c(0) e^{-(a I_w + \psi) t} \geq 0 \quad \forall t \geq 0$$

Following the same procedure for $t \geq 0$, we establish:

$$\begin{aligned} E_c(t) &\geq E_c(0) e^{-(\psi + \varepsilon) t} \geq 0 \\ I_c(t) &\geq I_c(0) e^{-(\psi + \phi + u_1 \tau) t} \geq 0 \\ S_w(t) &\geq S_w(0) e^{-(b(E_c + I_c) + c I_h + \omega + u_2 \varsigma) t} \geq 0 \\ I_w(t) &\geq I_w(0) e^{-(\omega + u_2 \varsigma) t} \geq 0 \\ S_h(t) &\geq S_h(0) e^{-(d I_w + \eta) t} \geq 0 \\ I_h(t) &\geq I_h(0) e^{-(\eta + u_1 \tau) t} \geq 0 \end{aligned} \quad (27)$$

The results infer that for all $t \geq 0$ the formulated control model (24) has the positive solution.

3.7.3 Disease-free equilibrium

As in Subsection 3.3.3, we equate the rate of change of model variables of the formulated control model (24) equal to zero and solve the model system simultaneously to obtain:

$$DFE = \left(\frac{\kappa_c (r_c - \psi)}{r_c}, 0, 0, \frac{\kappa_w (r_w - (\omega + u_2 \varsigma))}{r_w}, 0, \frac{\kappa_h (r_h - \eta)}{r_h}, 0 \right) \quad (28)$$

3.7.4 The effective reproduction number

Here, the same concept of the next generation matrix as used in the previous Subsection 3.3.4 of the basic model (1) was employed to obtain the effective reproduction number (\mathcal{R}_e) for the control model (24). The concept of \mathcal{R}_e refers the same as \mathcal{R}_0 except \mathcal{R}_e is computed when control measures are applied to the basic model (Nyerere *et al.*, 2020b). It helps in examining the potentiality of control parameters in the dynamics of the disease. If we assign:

$$\begin{aligned} g_{11} &= \frac{\psi \rho}{\psi + \varepsilon}, g_{13} = a \frac{(r_c - \psi) \kappa_c}{(\omega + u_2 \varsigma) r_c}, g_{31} = b \kappa_w \frac{(r_w - (\omega + u_2 \varsigma)) (u_1 \tau + \psi + \phi + \varepsilon)}{(\psi + \varepsilon) (u_1 \tau + \phi + \psi) r_w}, \\ g_{32} &= b \frac{(r_w - (\omega + u_2 \varsigma)) \kappa_w}{(u_1 \tau + \psi + \phi) r_w}, g_{34} = c \frac{(r_w - (\omega + u_2 \varsigma)) \kappa_w}{(\eta + u_1 \tau) r_w} \text{ and } g_{43} = d \frac{(r_h - \eta) \kappa_h}{(\omega + u_2 \varsigma) r_h} \end{aligned}$$

we find:

$$\mathcal{R}_e = \max \left\{ \frac{Y}{6} + \frac{2X}{Y} + \frac{1}{3} g_{11}, -\frac{Y}{12} - \frac{X}{Y} + \frac{1}{3} g_{11} \pm \frac{\sqrt{3}}{2} i \left(\frac{Y}{6} - \frac{2X}{Y} \right) \right\} \quad (29)$$

where, $Y = (Y_0 + 12\sqrt{Y_1})^{\frac{1}{3}}$, $Y_0 = 4(9g_{31}g_{13} - 18g_{43}g_{34} + 2(g_{11})^2)g_{11}$,

$$\begin{aligned} Y_1 &= -3(g_{11})^2(4g_{34}g_{43}(1 - 2g_{34}g_{43}) + g_{13}g_{31}(g_{13}g_{31} + 20g_{34}g_{43})) \\ &\quad - 12(g_{13}g_{31})^2(g_{13}g_{31} + 3g_{34}g_{43}) - 12(g_{34}g_{43})^2(3g_{13}g_{31} + g_{34}g_{43}) \end{aligned}$$

$$\text{and } X = g_{13}g_{31} + g_{43}g_{34} + \frac{(g_{11})^2}{3}$$

3.8 Optimal control

In this section, we develop the objective function to minimize the costs of applying our time-dependent controls $u_1(t)$ and $u_2(t)$. Our objective function is defined as:

$$\mathcal{J} = \int_0^t \left(A_1 (I_c(t) + I_h(t)) + A_2 I_w(t) + A_3 \frac{u_1(t)^2}{2} + A_4 \frac{u_2(t)^2}{2} \right) dt \quad (30)$$

where parameters A_1 and A_2 describe the positive weight constant associated with the application of roguing to the infected population of cassava and non-cassava hosts plants and insecticides to the whitefly population. Parameters A_3 and A_4 represent the application costs for roguing and insecticides control strategies respectively. The estimate $A_3 \frac{u_1(t)^2}{2}$ and $A_4 \frac{u_2(t)^2}{2}$ for the cost of each control strategy intends to avoid linearity on cost and avoid singular cases for the optimal control solution.

The aim is to minimize $\mathcal{J}(u_1, u_2)$ and obtain optimal control u_1^* and u_2^* in the time interval $[0, t]$, such that:

$$\mathcal{J}(u_1^*, u_2^*) = \min(\mathcal{J}(u_1, u_2)) : (u_1, u_2 \in U), \text{ subject to model (24)}$$

$$\text{where } U = U_1 \times U_2 \text{ and } u_1 \in [0, 1], u_2 \in [0, 1]$$

Theorem 3.3

There exists an optimal control set $u_1^*, u_2^* \in U$ and the state solutions of the model system (24), $(S_c^*, E_c^*, I_c^*, S_w^*, I_w^*, S_h^*, I_h^*)$ that minimizes the objective function $\mathcal{J}(u_1, u_2)$.

The condition stated by Heimann (1979) as cited by Kinene *et al.* (2015) verifies Theorem 3.3. Since by definition U is convex and closed, and the set of controls and the corresponding state variables are non-negative, then the integrand $\mathcal{K}(u_1, u_2)$ of $\mathcal{J}(u_1, u_2)$ with respect to U is convex if there exist $a_1, a_2 > 0$ and $w > 1$ such that, the integrand $\mathcal{K}(u_1, u_2) \geq a_2 + a_1 (|u_1| + |u_2|)^{\frac{w}{2}}$.

Theorem 3.4

For an optimal control $u_1, u_2 \in U$, there exist an adjoint function $\lambda : \mathbb{R} \rightarrow \mathbb{R}^n$ such that $x(t, u_i^*), u_i^*, \lambda$ satisfy the model (24) with initial conditions and the adjoint system for $i = 1, 2$

$$\begin{cases} \lambda'(t) = \frac{\partial H}{\partial X} \\ \lambda(t) = 0 \end{cases}$$

where H is a Hamiltonian function defined as $H(t, X, u_i) = f(t, X, u_i) + \lambda g(t, X, u_i)$, f is the integrand of equation (30), g is the state system (24) and $X = (S_c, E_c, I_c, S_w, I_w, S_h, I_h)$.

Proof

Suppose u_1^* and $u_2^* \in U$ are the optimal control, given $X = (S_c, E_c, I_c, S_w, I_w, S_h, I_h)$, then the

Hamiltonian function is described as:

$$\begin{aligned}
H = & A_1(I_c + I_h) + A_2I_w + A_3\frac{u_1^2}{2} + A_4\frac{u_2^2}{2} \\
& + \lambda_1 \left(r_c \left(1 - \frac{N_c}{\kappa_c} \right) S_c + \phi I_c - aS_cI_w - \psi S_c \right) \\
& + \lambda_2 \left(r_c \left(1 - \frac{N_c}{\kappa_c} \right) \rho E_c + aS_cI_w - (\psi + \varepsilon) E_c \right) \\
& + \lambda_3 (\varepsilon E_c - (\psi + \phi + u_1\tau)I_c) \\
& + \lambda_4 \left(\left(1 - \frac{N_w}{\kappa_w} \right) r_w N_w - (b(E_c + I_c) + cI_h) S_w - (\omega + u_2\varsigma) S_w \right) \\
& + \lambda_5 ((b(E_c + I_c) + cI_h) S_w - (\omega + u_2\varsigma) I_w) \\
& + \lambda_6 \left(r_h \left(1 - \frac{N_h}{\kappa_h} \right) S_h - dS_hI_w - \eta S_h \right) \\
& + \lambda_7 (dS_hI_w - (\eta + u_1\tau)I_h)
\end{aligned}$$

for, $\lambda'_1 = -\frac{\partial H}{\partial S_c}, \lambda'_2 = -\frac{\partial H}{\partial E_c}, \lambda'_3 = -\frac{\partial H}{\partial I_c}, \lambda'_4 = -\frac{\partial H}{\partial S_w}, \lambda'_5 = -\frac{\partial H}{\partial I_w}, \lambda'_6 = -\frac{\partial H}{\partial S_h}, \lambda'_7 = -\frac{\partial H}{\partial I_h}$,
there exist adjoint variables $\lambda_i, i = 1, 2, 3, 4, 5, 6, 7$, that assures:

$$\begin{cases}
\lambda'_1 = \lambda_1 \left(r_c \left(1 - \frac{S_c + N_c}{\kappa_c} \right) - aI_w - \psi \right) + \lambda_2 \left(aI_w - \frac{r_c \rho E_c}{\kappa_c} \right) \\
\lambda'_2 = -\frac{\lambda_1 r_c S_c}{\kappa_c} + \lambda_2 \left(r_c \rho \left(1 - \frac{E_c + N_c}{\kappa_c} \right) - \psi - \varepsilon \right) + \lambda_3 \varepsilon - (\lambda_4 - \lambda_5) b S_w \\
\lambda'_3 = A_1 + \lambda_1 \left(\phi - \frac{r_c S_c}{\kappa_c} \right) - \frac{\lambda_2 r_c \rho E_c}{\kappa_c} - \lambda_3 (u_1 \tau + \phi + \psi) - (\lambda_4 - \lambda_5) b S_w \\
\lambda'_4 = \lambda_4 \left(r_w \left(1 - \frac{2N_w}{\kappa_w} \right) - b(E_c + I_c) - cI_h - u_2 \varsigma - \omega \right) + \lambda_5 (b(E_c + I_c) + cI_h) \\
\lambda'_5 = A_2 - (\lambda_1 - \lambda_2) a S_c + \lambda_4 \left(r_w \left(1 - \frac{2N_w}{\kappa_w} \right) \right) - \lambda_5 (u_2 \varsigma + \omega) - (\lambda_6 - \lambda_7) d S_h \\
\lambda'_6 = \lambda_6 \left(r_h \left(1 - \frac{S_h + N_h}{\kappa_h} \right) - dI_w - \eta \right) + \lambda_7 d I_w \\
\lambda'_7 = A_1 - (\lambda_4 - \lambda_5) c S_w - \lambda_7 (\eta + u_1 \tau) - \frac{\lambda_6 r_h S_h}{\kappa_h}
\end{cases} \quad (31)$$

given transversality conditions: $\lambda_1(t) = \lambda_2(t) = \lambda_3(t) = \lambda_4(t) = \lambda_5(t) = \lambda_6(t) = \lambda_7(t) = 0$

To obtain the optimality equation (32), we compute the partial derivatives of the Hamiltonian equation (31) with respect u_1 and u_2 and obtain:

$$\begin{cases}
\frac{\partial H}{\partial u_1} = A_3 u_1 - \lambda_3 I_c \tau - \lambda_7 I_h \tau \\
\frac{\partial H}{\partial u_2} = A_4 u_2 - \lambda_4 S_w \varsigma - \lambda_5 I_w \varsigma
\end{cases} \quad (32)$$

Solving for u_1 and u_2 from (32) when $\frac{\partial H}{\partial u_1}$ and $\frac{\partial H}{\partial u_2} = 0$, we obtain:

$$\begin{cases} u_1^* = \frac{\lambda_3 I_c + \lambda_7 I_h}{A_3} * \tau \\ u_2^* = \frac{\lambda_4 S_w + \lambda_5 I_w}{A_4} * \varsigma \end{cases} \quad (33)$$

hence, we can characterize the optimal control u_1 and u_2 as:

$$u_1^* = \min \left\{ \max \left(0, \frac{\lambda_3 I_c + \lambda_7 I_h}{A_3} * \tau \right), 1 \right\} \quad (34)$$

$$u_2^* = \min \left\{ \max \left(0, \frac{\lambda_4 S_w + \lambda_5 I_w}{A_4} * \varsigma \right), 1 \right\} \quad (35)$$

Equations (34) and (35) give the optimal solution for the objective function (30). Since system equation (24) and adjoint equation (31) are bounded and satisfy Lipschitz conditions, the optimality system is unique for some small t . Therefore, the uniqueness of the optimal solution is guaranteed by the restriction on the length of the time interval $[0, t]$ (Kinene *et al.*, 2015).

CHAPTER FOUR

RESULTS AND DISCUSSION

4.1 Introduction

The numerical simulation results for the basic model (1), optimal control model (24) and time series plots to depict the global stability of DFE and EEP are presented in this chapter. Further, the chapter presents the Incremental Cost-Effectiveness Ratio (ICER) results for the CMD management strategies as used on the optimal control model (24).

4.2 Numerical simulation and results

The fourth-order Runge-Kutta method was used to simulate the formulated model (1) and observe the trajectories of the population over time, the effects of varying the whitefly mortality rate (ω) and whitefly carrying capacity (κ_w). We use $S_c(0) = 0.35, E_c(0) = 0.05, I_c(0) = 0.05, S_w(0) = 40, I_w(0) = 10, S_h(0) = 0.2, I_h(0) = 0.1$ as our initial state values for model system variables and parameter baseline values as highlighted in Table 1 to simulate the formulated model system (1).

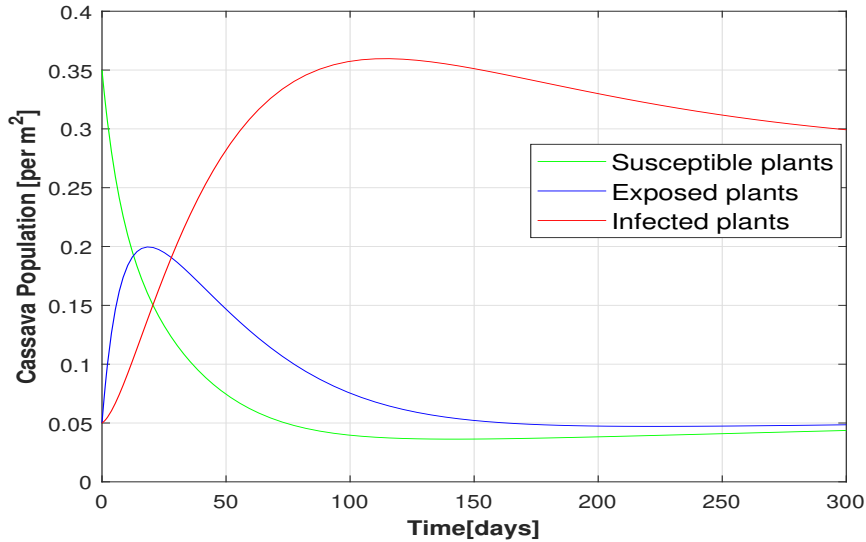


Figure 5: Cassava population dynamics

In Fig. 5 it was clearly observed that during the first 100 days, infected cassava plants per m^2 increased from 0.05 per m^2 to 0.35 per m^2 and drop slightly up to 0.3 per m^2 after 300 days. Conversely, the susceptible cassava plant population per m^2 decreases exponentially from 0.35

per m^2 to 0.05 per m^2 during the first 300 days. Further, it was noticed that during the first 25 days the exposed cassava per m^2 increases from 0.05 plants per m^2 and reaches the top value of 0.2 plants per m^2 prior to exponential decrease to 0.05 per m^2 . This result implies that in 300 days, infected cassava plants per m^2 will be greater than the exposed and susceptible cassava plants when the outbreak occurs with the same variable and parameter values as used in the simulation.

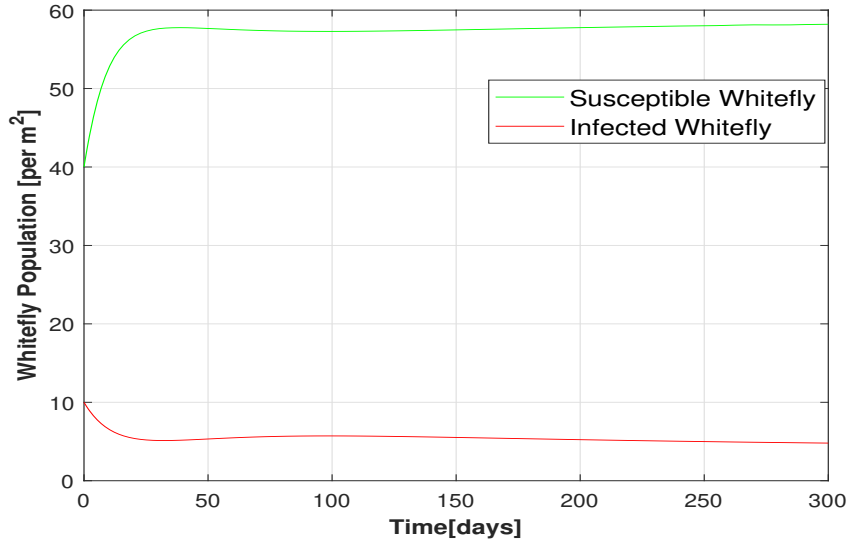


Figure 6: Whitefly population dynamics

For the case of the whitefly population, it was witnessed in Fig. 6 that, there is a slight decrease in the number of infected whiteflies per m^2 from 10 whiteflies per m^2 to the constant rate of five infected whiteflies per m^2 in less than 50 days. Contrarily, the increase in the number of susceptible whitefly populations per m^2 from 40 to around 58 per m^2 in less than 50 days before it maintained for the rest of 300 days was observed.

Fig. 7 presents the dynamics in non-cassava host plants. It was observed that during the first 100 days, the number of susceptible non-cassava host plants drops to zero while the infected plants increase to approximately 0.33 per m^2 . Further, after 300 days the number of infected non-cassava plants per m^2 is anticipated to be 0.27 per m^2 .

In Fig. 8 the impacts of altering the whitefly mortality rate (ω) on the infected population of the model system (1) is portrayed. In all infected populations, it was evident that when (ω) increases, the number of infected individuals per m^2 decreases and vice versa. This result reveals that control strategies that increase the whitefly mortality rate are vital in combating the

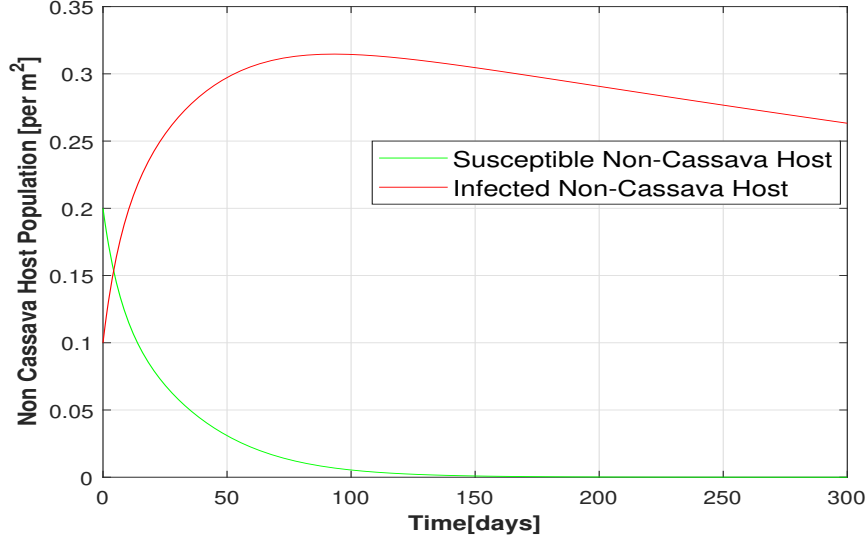


Figure 7: Non-cassava hosts population dynamics

spread of CMD.

Similarly, Fig. 9 depicts the impacts of altering the whitefly carrying capacity (κ_w) on infected populations of the model system (1). Contrary to what was observed when changing the whitefly mortality rate (ω), an increase in the density of whiteflies (κ_w) speeds up the spread of infection in the population. This scenario highlights that the stakeholders can mitigate the intensity of the CMD by reducing the number of infected or unnecessary plants that helps to accommodate whitefly in farms and surrounding areas.

4.3 Numerical simulation for the global stability analysis

Table 2 was used as used in Erick and Mayengo (2022) to illustrate the numerical stability of DFE and EEP of the model system (1) by using time series plots. The parameter values were twisted within their respective range to obtain values that give $\mathcal{R}_0 \leq 1$ and $\mathcal{R}_0 > 1$. For DFE we select $a = 0.002, b = 0.002, c = 0.002, d = 0.002, \varepsilon = 0.033, \eta = 0.002, \rho = 0.001, \phi = 0.004, \psi = 0.004, r_c = 0.5e - 1, r_w = 0.2, r_h = 0.01, k_c = 0.5, k_h = 0.3, k_w = 70, \omega = 0.06$ with $\mathcal{R}_0 = 0.7747$, whilst in EEP the selected values were $a = 0.01, b = 0.01, c = 0.01, d = 0.01, \varepsilon = 0.033, \eta = 0.001, \rho = 0.1, \phi = 0.003, \psi = 0.003, \omega = 0.06, r_c = 0.05, r_w = 0.2, r_h = 0.07, k_c = 0.7, k_h = 0.7, k_w = 160$ with $\mathcal{R}_0 = 12.2879$. Fig. 10 and 11 present the simulated global stability for DFE and EEP respectively for the model (1).

From Fig. 10 it can be noticed that using different initial conditions the trajectories for all

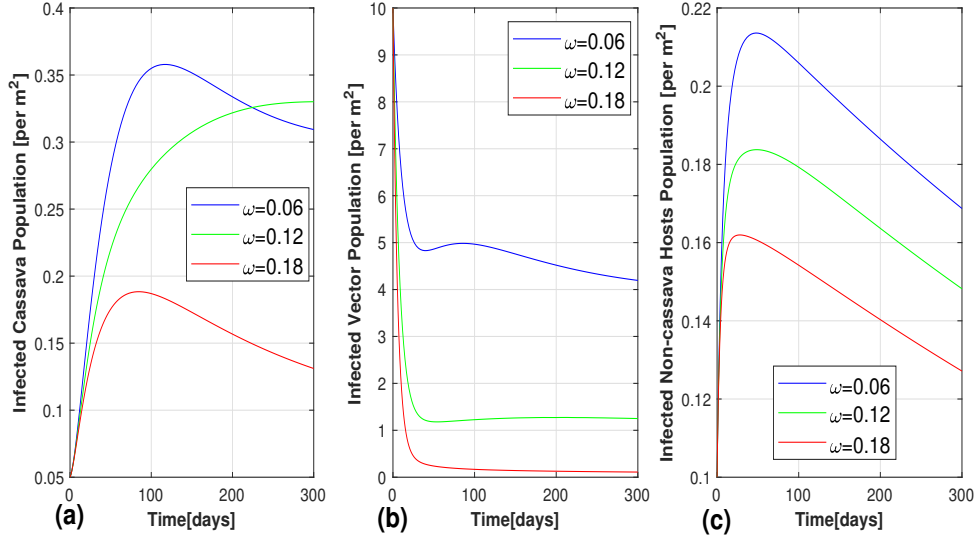


Figure 8: The impact of altering the whitefly mortality rate (ω) on the infected population. Subplots (a), (b) and (c) represent the simulation of the infectious cassava plants, whiteflies and non-cassava host plants respectively

infected population (E_c), (I_c), (I_w) and (I_h) converges at a given fixed point on the time axis. This indicates that the disease can distinct from the population when sufficient control strategies are applied and hence proves the existence and global stability of DFE whenever $\mathcal{R}_0 \leq 1$.

Moreover, the trajectories in the Fig. 11 presents the number of infected population E_c , I_c , I_w and I_h when $\mathcal{R}_0 > 1$. It was observed that with different initial conditions, the trajectories converge at a given point above the time axis. This implies that the disease will prevail in the environment when significant control strategies are not implemented. The Figure also confirms the existence and global stability of EEP whenever $\mathcal{R}_0 > 1$.

4.4 Numerical simulation for optimal control model

This section presents the numerical simulation results of suggested control measures in the model system (24). The roguing ($u_1\tau$) (uprooting and burning of infected cassava and non-cassava host plants), insecticides application ($u_2\varsigma$), and the combination of roguing ($u_1\tau$) and insecticides application ($u_2\varsigma$) were considered as control strategies for eradicating CMD. The forward and backward fourth-order Runge-Kutta iterative scheme was employed to solve the system model equation (1) and adjoint equation (31) respectively. Firstly, the forward Runge-Kutta method was used to compute the state solution then the obtained state solution and the transversality conditions were used to solve the adjoint equations through the backward fourth-

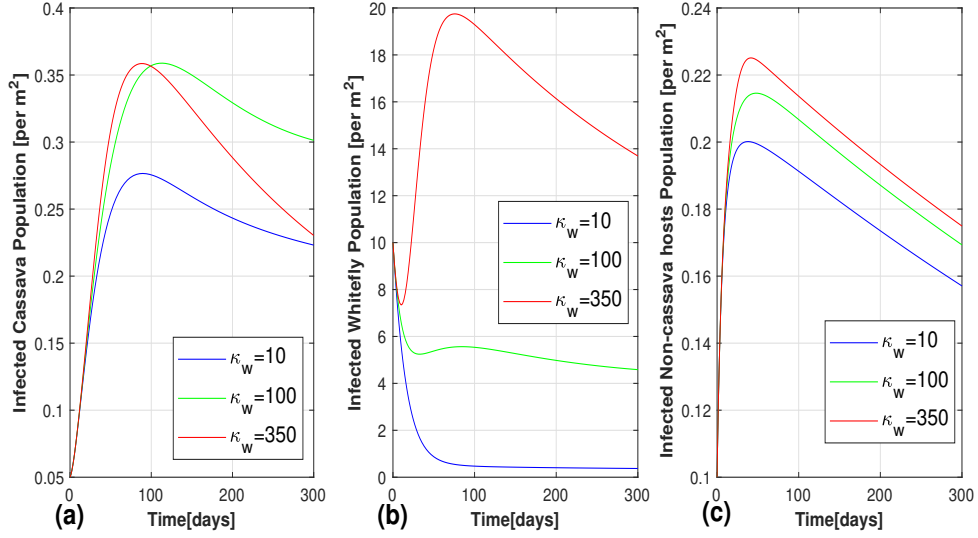


Figure 9: The impact of altering the whitefly carrying capacity (κ_w) on the infected population. Subplots (a), (b) and (c) represent the simulation of the infectious cassava plants, whiteflies and non-cassava host plants respectively

order Runge-Kutta method. Furthermore, the convex combination of the previous controls and the value from the characterizations values was used to update controls. This process repeats whenever the unknown values from the previous iteration are not noticeably closer to the unknown values from the current iteration.

The collection of weight factors was theoretically selected for simulation purposes as follows: $A_1 = 10$, $A_2 = 5$, $A_3 = 50$ and $A_4 = 100$ and initial state variables $S_c = 0.35$, $E_c = 0.05$, $I_c = 0.05$, $S_w = 40$, $I_w = 10$, $S_h = 0.2$ and $I_h = 0.1$. The roguing rate and whitefly death rate due to insecticide spraying was set to 0.1 day^{-1} and 0.18 day^{-1} respectively as used by Bokil *et al.* (2019) and Jittamai *et al.* (2021). Other parameters are as shown in baseline values in Table 1.

4.4.1 Strategy 1: Roguing

Under this strategy, the insecticides application effort (u_2) was set to zero while roguing of infected cassava and non-cassava host plants (u_1) alone was used to optimize the objective function (30). The results in Fig. 12 portray that, in the first 200 days, the number of infected whiteflies (I_w), cassava (I_c) and non-cassava host plants (I_h) drop significantly to less than 0.1 m^{-2} , 2 m^{-2} and approximately zero respectively. The Figure also reveals a significant difference between the implementation of roguing activities and the case of no applied control measure. Furthermore, in Fig. 13 it was witnessed that, during the first 120 days roguing

Table 2: The range and baseline values for the model parameter

Parameter	Range	Baseline Value
r_c	0.025-0.1	0.05 day^{-1}
r_w	0.1-0.3	0.2 day^{-1}
r_h	-	0.02 day^{-1}
ρ	0-1	0.1
a	0.002-0.032	$0.008 \text{ plant}^{-1} \text{ day}^{-1}$
b	0.002-0.032	$0.008 \text{ whitefly}^{-1} \text{ day}^{-1}$
c	-	$0.008 \text{ whitefly}^{-1} \text{ day}^{-1}$
d	-	$0.008 \text{ plant}^{-1} \text{ day}^{-1}$
ε	-	0.033 day^{-1}
ω	0.06-0.18	0.06 day^{-1}
η	-	0.001 day^{-1}
ψ	0.002-0.004	0.003 day^{-1}
κ_c	0.01-1	0.7 m^{-2}
κ_w	0-350	90 m^{-2}
κ_h	0.01-1	0.1 m^{-2}
ϕ	0.002-0.004	0.003 day^{-1}

activities were fully implemented before it stops and dropped to zero. Then, after 230 days the roguing activities resume to full implementation for 40 days before it sharply decreases to zero after 300 days. The results also reveal that strategy 1 does not affect the number of exposed cassava plants in the first 100 days. This implies that for significant results, roguing needs to be implemented at its full scale in the first 120 days and the last 70 days if it is used as the only control strategy.

4.4.2 Strategy 2: Insecticides application

In strategy 2, only insecticide application was employed to optimize the objective function (30). From Fig. 14 it was witnessed that the application of insecticides alone reduces the number of infected populations of cassava, whitefly, and non-cassava host plants, and exposed cassava compared to the case of no control. When compared to strategy 1(roguing activities) it was evident that the number of infected cassava and non-cassava host populations is higher but

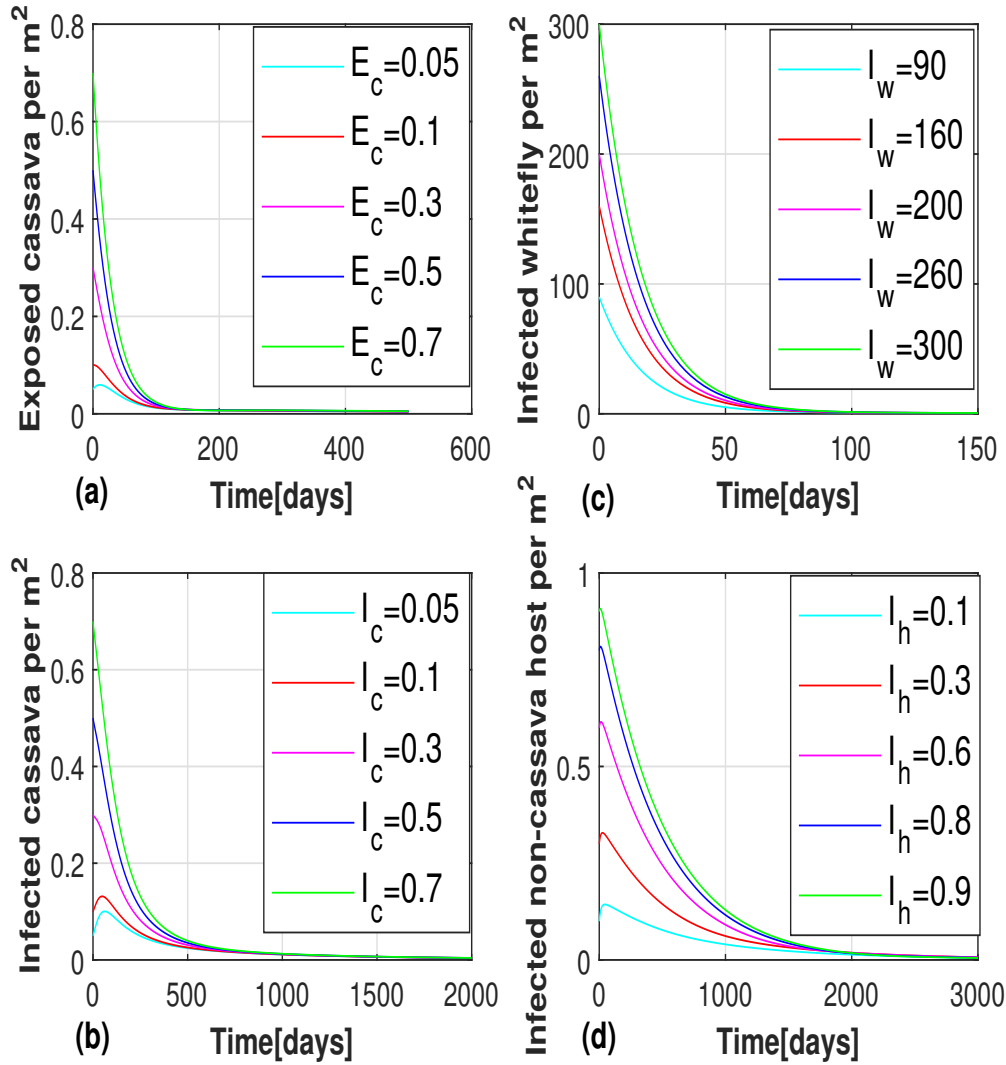


Figure 10: A graphical depiction of global stability for DFE

whitefly and exposed cassava plants population attain their disease-free equilibrium points in less than 200 days. Moreover, the control profile Fig. 15 portrays that, insecticides application was fully implemented in the first 100 days only then drops to zero for the remaining 200 days.

4.4.3 Strategy 3: Roguing and insecticides application

Here considerations were made on the combination of roguing activities and insecticides application in optimizing the objective function (30). The outcomes portrayed in Fig. 16 tell that the combination of strategy 1 and strategy 2 was able to reduce the disease in all infected populations significantly compared to the previous strategies. In Fig. 17 we observed that roguing was

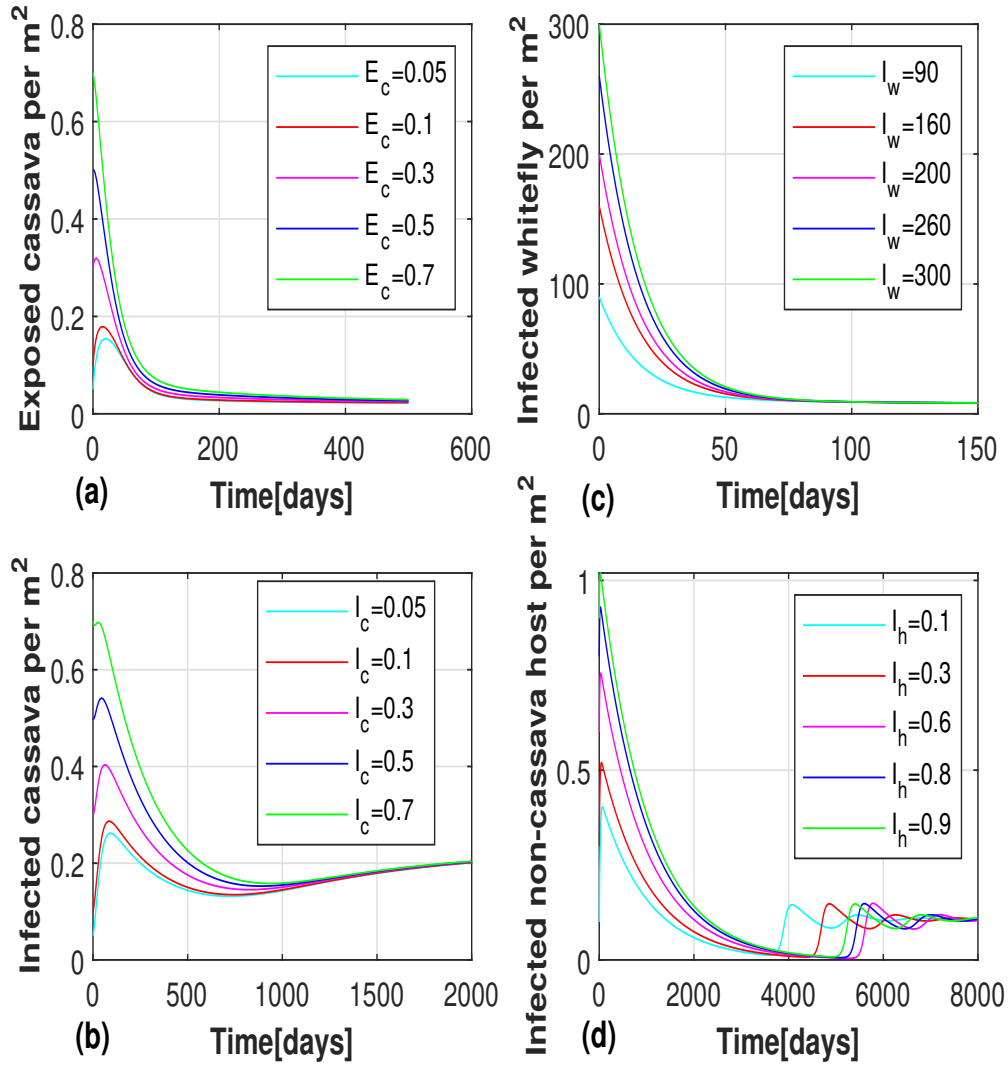


Figure 11: A graphical depiction of global stability for EEP

fully implemented in the first 50 days and approximately 70% implementation in the last 50 days. On the other hand, the application of the insecticide was fully implemented for 50 days after the first 25 days before it drops to zero and starts again after 240 days for approximately 25 days before it drops sharply to zero. As witnessed in the control profile Fig. 17 roguing activities and insecticides application were not fully implemented throughout the year.

4.5 Cost-effectiveness analysis

In this part, the Incremental Cost-Effectiveness Ratio (ICER) as expressed by Mwasunda *et al.* (2022) and Nyerere *et al.* (2020b) and Alemneh *et al.* (2020) was employed to rank the implemented strategies in mitigating CMD. The ICER results provide useful information to

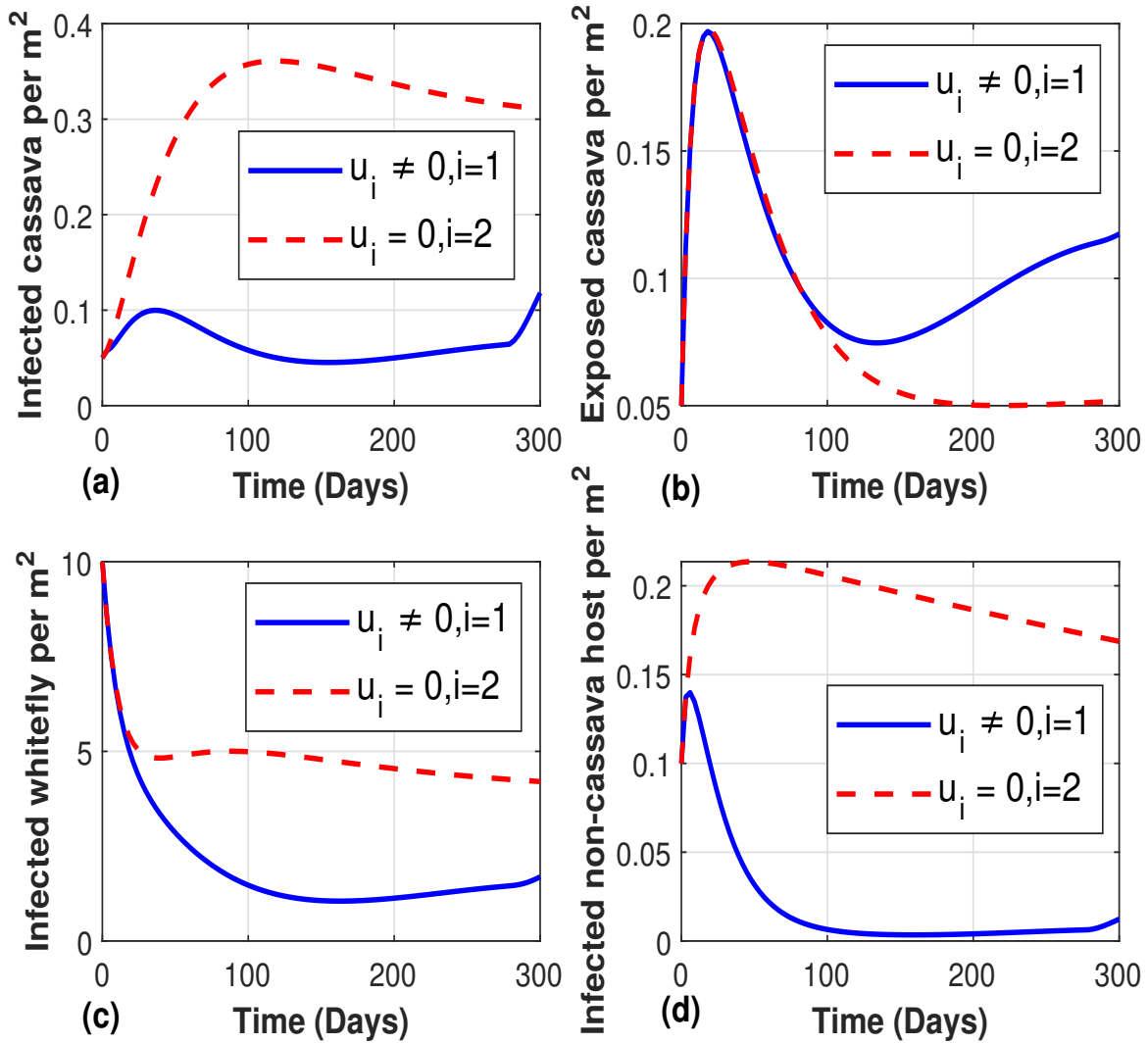


Figure 12: Infected population dynamics when roguing activities are implemented

stakeholders and policymakers on how to mitigate the disease with limited resource allocation.

As in the study by Kinene *et al.* (2015) and Nyerere *et al.* (2020b) ICER was defined as;

$$\text{ICER} = \frac{\text{The costs difference between two control methods}}{\text{The difference of the total number of their infections averted}} \quad (1)$$

The optimality simulation results were arranged in increasing order of effectiveness based on cases of infection averted as shown in Table 3. In Table 3, it was observed that strategy 2 has the highest ICER value compared to the results of strategies 3 and 1. This signifies that strategy 2 is strongly dominated, with more running costs and less effective than other implemented strategies. Therefore, strategy 2 was removed from the set of control strategies since it does not

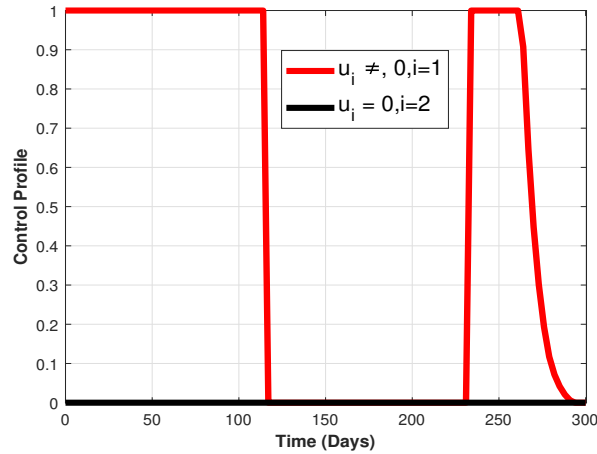


Figure 13: The control profile for roguing activities

Table 3: Total infection averted with their respective ICER in ascending order

Strategy	Infections Averted	Total Cost	ICER
No control	0	0	-
Strategy 3	534.0185351	2114.501713	3.959603599
Strategy 2	534.1025494	2455.927458	4063.896286
Strategy 1	534.1233924	2376.048165	-3832.440744

consume limited resources. Then, ICERs were recalculated by using strategies 3 and 1 only and the results were presented in Table 4.

Table 4: Recalculated ICER for strategy 3 and 1

Strategy	Infections Averted	Total Cost	ICER
No control	0	0	-
Strategy 3	534.0185351	2114.501713	3.959603599
Strategy 1	534.1233924	2376.048165	2494.308129

Again, the observed recalculated ICER value in Table 4 reveals that strategy 1 has a greater ICER value than strategy 3. The results imply that strategy 3 is cheaper and more effective than strategy 1. Therefore, the implementation of strategy 3 (roguing and insecticide application) is regarded as the less expensive and most effective strategy in combating CMD compared to insecticide application or roguing activities when implemented alone.

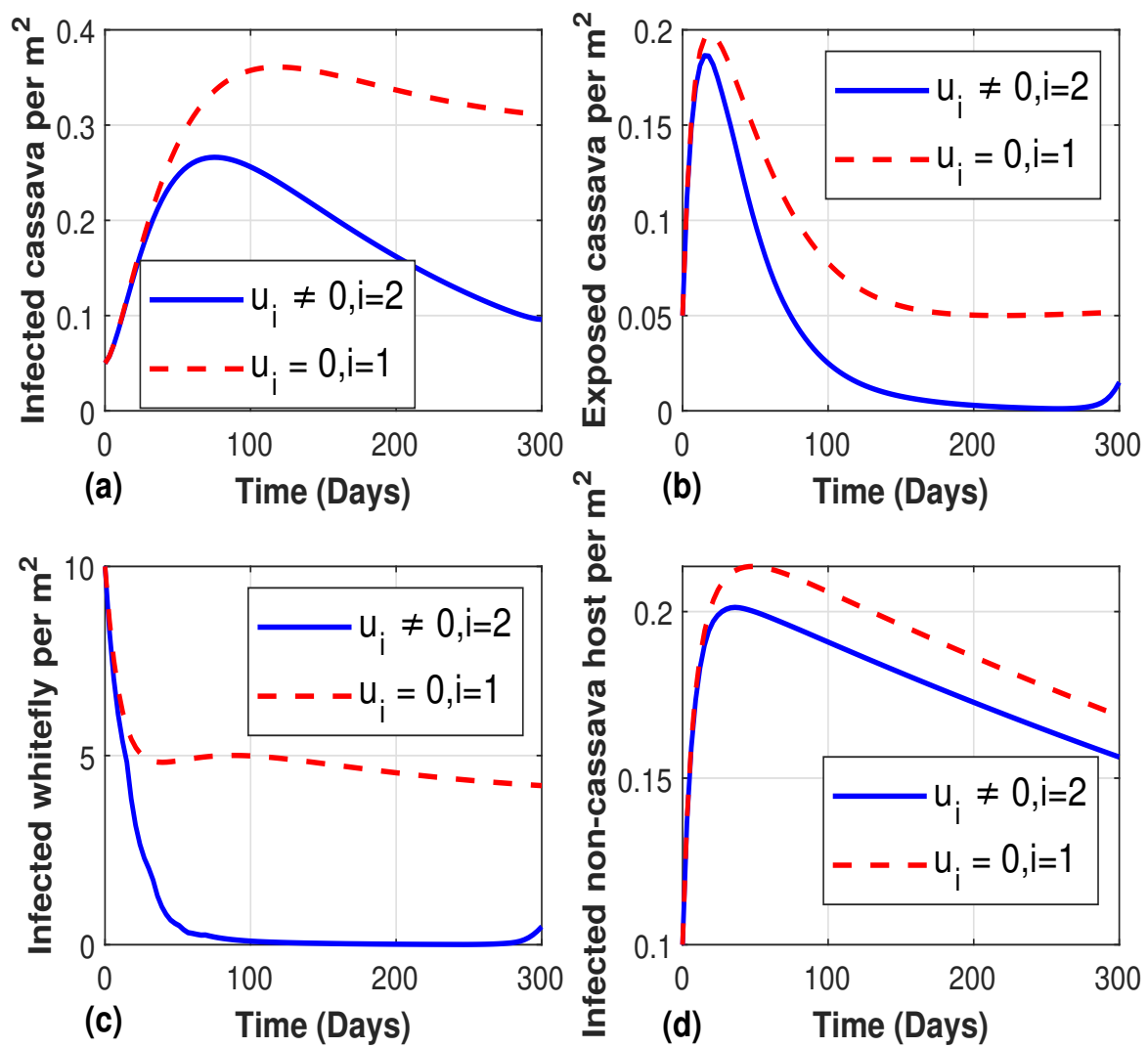


Figure 14: Infected population dynamics for optimal insecticides application

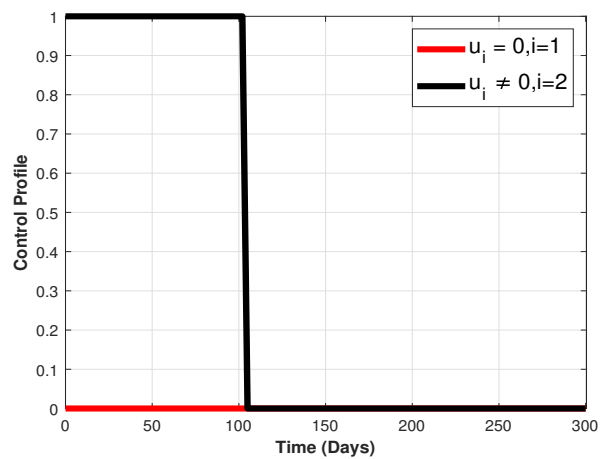


Figure 15: The control profile for insecticides application

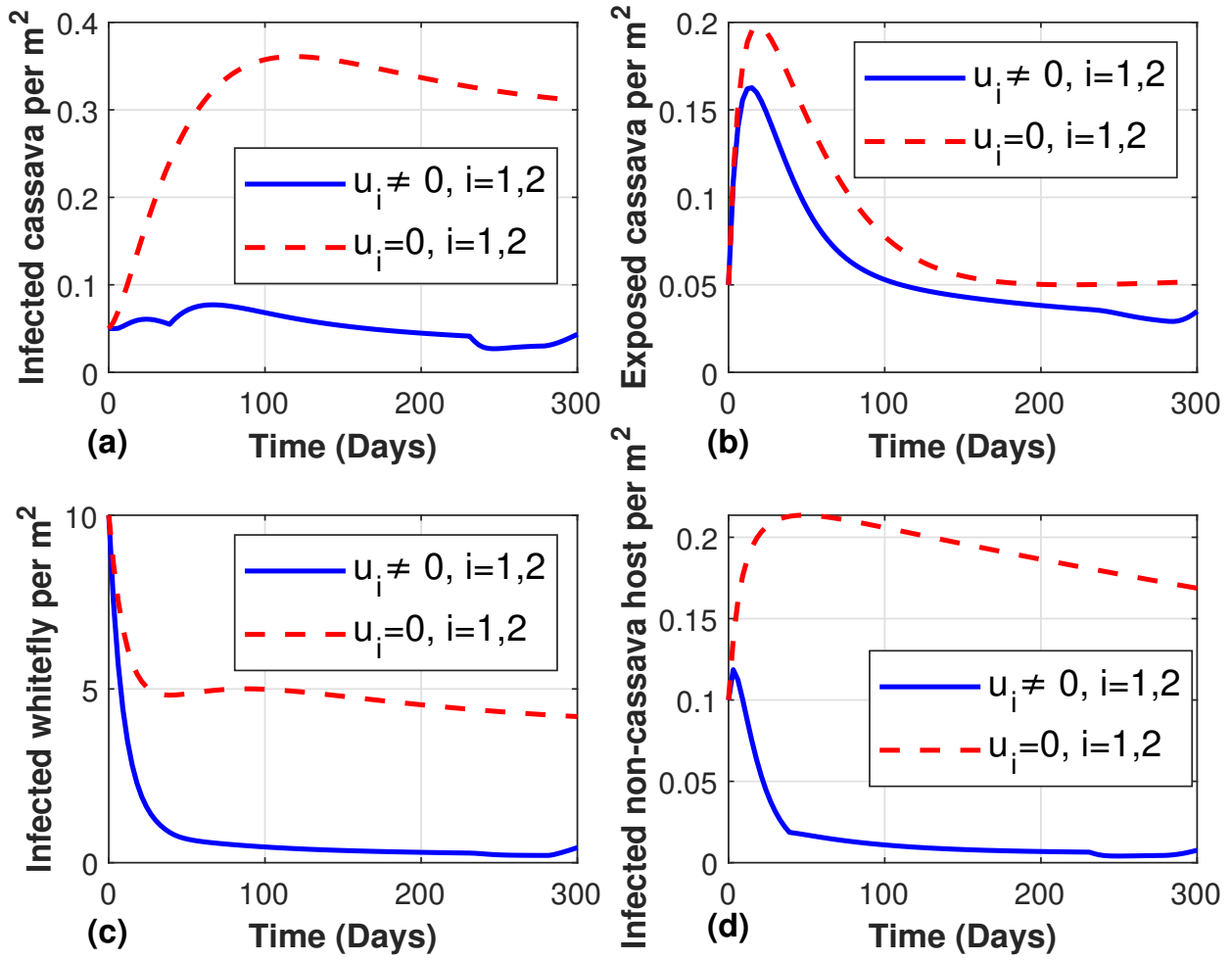


Figure 16: The dynamics of the infected population when roguing and insecticides application was implemented

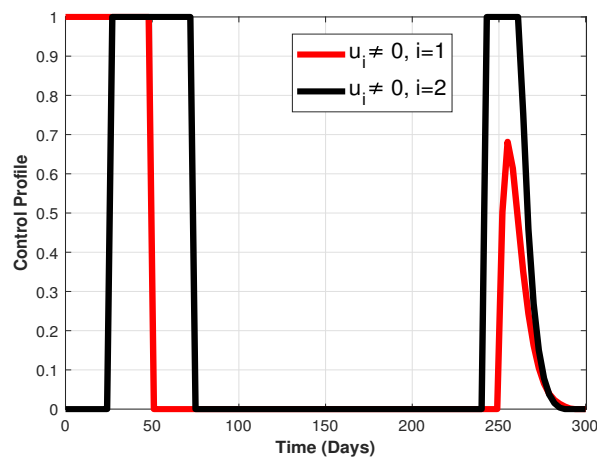


Figure 17: The control profile for roguing implementation and insecticides application

CHAPTER FIVE

CONCLUSION AND RECOMMENDATIONS

5.1 Conclusion

Cassava mosaic disease (CMD) has affected cassava production in Africa for many years. This study develops and examines a deterministic model by incorporating the non-cassava host plant population. The study particularly: develops a mathematical dynamics model for CMD that takes non-cassava host plants into account; analyses the model theoretically to look at things like the solutions' positivity, the stability of model equilibrium points, and sensitivity analysis; estimates the control parameters and their importance by simulating the model numerically; and finally, determine the most economical disease control method.

In this work, the non-cassava host population were incorporated in the formulation and analysis of the ordinary differential equation (ODE) model for the transmission dynamics and optimal control strategies of CMD. The basic model properties analysis results ensure the positivity and boundedness of the model solution for all time $t \geq 0$. The analysis of the local stability of the formulated model confirms that the DFE is asymptotic stable when $\mathcal{R}_0 \leq 1$ and unstable when $\mathcal{R}_0 > 1$. These stability results imply that CMD can persist and spread in the environment when $\mathcal{R}_0 > 1$, and can perish when $\mathcal{R}_0 \leq 1$. Furthermore, the sensitivity analysis and simulation of the model (1) highlighted that the whitefly death rate (ω) and whitefly carrying capacity per m^2 (κ_w) as the most sensitive parameter compared to other parameters. These findings portray that the control strategies such as using insecticides to increase (ω) and removing the infected population of cassava and non-cassava to decrease (κ_w) could have promising impacts in fighting CMD compared to other model parameters.

Furthermore, the concept by Castillo-Chavez *et al.* (2002) and numerical simulation were employed to explore the existence and global stability of DFE and EEP on the model (1). The findings reveal that the DFE is globally stable when $\mathcal{R}_0 < 1$ and unstable otherwise. The performed numerical simulations using time series plots to confirm the global asymptotical stability of DFE and EEP reveal that for DFE when $\mathcal{R}_0 < 1$ as the infected population converges to zero, the susceptible population converges to a distinct point above the time axis regardless of the initial condition used. This assures that the disease can perish when significant control strategies are applied. Further, the simulation for EEP shows that irrespective of the initial state

of the model variables, the infected compartments converge to a distinct point above the time axis, indicating that the disease will eventually spread across the population.

Additionally, the optimality system for CMD was developed by using roguing of infected cassava and non-cassava host plants ($u_1\tau$), and insecticides application ($u_2\varsigma$) as our disease management strategies. The concepts of Pontryagin's Maximum Principle were used for the analysis of the control model (24). Further, the cost-effectiveness analysis to find the most appropriate control strategies for combating CMD was performed by using ICER. Moreover, the numerical simulation was performed after solving the state equation (24) and adjoint equation (31) by utilizing forward and backward fourth-order Runge-Kutta iteration schemes respectively. Numerical simulation results reveal that strategy 3 (combination of roguing and insecticides application) performs better in reducing the number of infected populations compared to strategy 2 (insecticide application) and strategy 1 (roguing activities).

Lastly, the cost-effectiveness analysis reveals that strategy 3 has a high impact and a reduced cost of disease control compared to others. These results concur with the study of Bokil *et al.* (2019) and Fahad and Roy (2018) which also suggests integrating roguing activities and insecticide application in combating CMD against the single control approach. Therefore, we recommend strategy 3 for effective and efficient mitigation of CMD.

5.2 Recommendations

Research findings on the global stability of equilibrium points assure that the CMD can be controlled when appropriate and sufficient control strategies are applied. Therefore, the study recommends the following:

- (i) The use of the combined strategy of roguing and insecticides application during the outbreak of CMD as suggested by results on numerical simulation and ICER analysis.
- (ii) Based on sensitivity analysis, the whitefly carrying capacity influences the spread of CMD. Therefore, we recommend the removal of all non-potential host plants in the farm and the surrounding area. This will help to reduce the spread of the disease.
- (iii) The education programs to raise awareness on the symptoms of infected cassava and non-cassava host plants should be provided to farmers and other stockholders for effective roguing programs.

- (iv) Biological control strategies, such as using whitefly predators should be studied and implemented to reduce the effects of insecticides in the control of the CMD.
- (v) The influence of seasonal weather variation on the whitefly population should be investigated.
- (vi) The formulation of a stochastic model to incorporate uncertainty in the dynamics of CMD.
- (vii) Incorporation of weather seasonality variation in the CMD Model.
- (viii) To include the predators of whitefly vectors such as Phytoseiidae and spiders in the control strategies of CMD.

REFERENCES

- Alabi, O. J., Ogbe, F. O., Bandyopadhyay, R., Lava Kumar, P., Dixon, A. G. O., Hughes, J. d., & Naidu, R. A. (2008). Alternate hosts of African cassava mosaic virus and East African cassava mosaic Cameroon virus in Nigeria. *Archives of Virology*, 153(9), 1743–1747. <https://doi.org/10.1007/s00705-008-0169-8>
- Alaux, J., & Fauquet, C. (1990). *African cassava mosaic disease: From knowledge to control*. Technical Centre for Agricultural; Rural Cooperation (CTA).
- Al-Basir, F., Roy, P. K., & Ray, S. (2017). Impact of roguing and insecticide spraying on mosaic disease in jatropha curcas. *Control and Cybernetics*, 46(4), 325–344.
- Alemneh, H. T., Makinde, O. D., & Theuri, D. M. (2020). Optimal control model and cost effectiveness analysis of maize streak virus pathogen interaction with pest invasion in maize plant. *Egyptian Journal of Basic and Applied Sciences*, 7(1), 180–193.
- Alves, A. C. (2002). Cassava botany and physiology [Publisher: CABI Publishing: Oxon, UK]. *Cassava: Biology, Production and Utilization*, 1, 67–89.
- Anitha, J., Makesh Kumar, T., & Edison, S. (2020). Potential hosts of Sri Lankan cassava mosaic virus evaluated through whitefly inoculation [Number: 2]. *Journal of Root Crops*, 45(2), 55–61. Retrieved August 23, 2021, from <https://isrc.in/ojs/index.php/jrc/article/view/564>
- Badamasi, H., Alegbejo, M. D., Kashina, B. D., & Banwo, O. O. (2020). Alternative hosts of cassava viruses in Kaduna and Sokoto states, Nigeria [ISBN: 1597-6343]. *Science World Journal*, 15(2), 51–55.
- Bokil, V. A., Allen, L. J. S., Jeger, M. J., & Lenhart, S. (2019). Optimal control of a vectored plant disease model for a crop with continuous replanting [Publisher: Taylor & Francis _eprint: <https://doi.org/10.1080/17513758.2019.1622808>]. *Journal of Biological Dynamics*, 13(sup1), 325–353. <https://doi.org/10.1080/17513758.2019.1622808>
- Castillo-Chavez, C., Blower, S., Van den Driessche, P., Kirschner, D., & Yakubu, A. (2002). *Mathematical approaches for emerging and reemerging infectious diseases: Models, methods, and theory* (Vol. 126). Springer Science & Business Media.

- Chapwanya, M., & Dumont, Y. (2021). Application of mathematical epidemiology to crop vector-borne diseases: The cassava mosaic virus disease case. In M. I. Teboh-Ewungkem & G. A. Ngwa (Eds.), *Infectious Diseases and Our Planet* (pp. 57–95). Springer International Publishing. https://doi.org/10.1007/978-3-030-50826-5_4
- Chikoti, P. C., Mulenga, R. M., Tembo, M., & Sseruwagi, P. (2019). Cassava mosaic disease: A review of a threat to cassava production in Zambia. *Journal of Plant Pathology*, 101(3), 467–477. <https://doi.org/10.1007/s42161-019-00255-0>
- Chuma, F. (2019). *Modeling the dynamics, control and economic loss of newcastle disease in village chicken: A case of Pwani region in Tanzania* (Doctoral dissertation).
- Chuma, F., & Mwanga, G. (2019). Stability analysis of equilibrium points of Newcastle disease model of village chicken in the presence of wild birds reservoir. *International Journal of Mathematical Sciences and Computing*, 5(2), 1–18. <https://doi.org/10.5815/ijmsc.2019.02.01>
- Daudi, S., Luboobi, L., Kgosimore, M., & Kuznetsov, D. (2021). Modelling the control of the impact of fall armyworm (*Spodoptera frugiperda*) infestations on maize production (J. Yu, Ed.). *International Journal of Differential Equations*, 2021, 1–16. <https://doi.org/10.1155/2021/8838089>
- Driessche, V., & Watmough, J. (2002). Reproduction numbers and sub-threshold endemic equilibria for compartmental models of disease transmission. *Mathematical Biosciences*, 180(1), 29–48. [https://doi.org/10.1016/S0025-5564\(02\)00108-6](https://doi.org/10.1016/S0025-5564(02)00108-6)
- Driessche, V., & Watmough, J. (2008). Further notes on the basic reproduction number. In *Mathematical Epidemiology* (pp. 159–178). Springer.
- Erick, B., & Mayengo, M. (2022). Modelling the dynamics of cassava mosaic disease with non-cassava host plants. *Informatics in Medicine Unlocked*, 101086. <https://doi.org/10.1016/j.imu.2022.101086>
- Fahad, A. B., Kyrychko, Y. N., Blyuss, K. B., & Ray, S. (2021). Effects of vector maturation time on the dynamics of cassava mosaic disease. *Bulletin of Mathematical Biology*, 83(8), 87. <https://doi.org/10.1007/s11538-021-00921-4>

- Fahad, A. B., & Roy, P. K. (2018). Dynamics of mosaic disease with roguing and delay in *Jatropha curcas* plantations. *Journal of Applied Mathematics and Computing*, 58(1), 1–31. <https://doi.org/10.1007/s12190-017-1131-2>
- Fargette, D., Jeger, M., Fauquet, C., & Fishpool, L. D. C. (1994). Analysis of temporal disease progress of African cassava mosaic virus [ISBN: 0031-949X Publisher: [St. Paul, Minn., etc.: American Phytopathological Society]]. *Phytopathology*, 84(1), 91–98.
- Fasuyi, A. O. (2005). Nutrient composition and processing effects on cassava leaf (*Manihot esculenta*, Crantz) antinutrients [ISBN: 1680-5194 Publisher: Citeseer]. *Pakistan Journal of Nutrition*, 4(1), 37–42.
- Gao, S., Xia, L., Liu, Y., & Xie, D. (2016). A plant virus disease model with periodic environment and pulse roguing. *Studies in Applied Mathematics*, 136(4), 357–381.
- Heffernan, J., Smith, R., & Wahl, L. (2005). Perspectives on the basic reproductive ratio. *Journal of The Royal Society Interface*, 2(4), 281–293. <https://doi.org/10.1098/rsif.2005.0042>
- Heimann, B. (1979). Deterministic and stochastic optimal control. *ZAMM - Journal of Applied Mathematics and Mechanics / Zeitschrift für Angewandte Mathematik und Mechanik*, 59(9), 494–494. <https://doi.org/10.1002/zamm.19790590940>
- Hillocks, R. (1997). Cassava virus diseases and their control with special reference to southern Tanzania. *Integrated Pest Management Reviews*, 2(3), 125–138. <https://doi.org/10.1023/A:1018449017411>
- Holt, J., Jeger, M. J., Thresh, J. M., & Otim-Nape, G. W. (1997). An epidemiological model incorporating vector population dynamics applied to African cassava mosaic virus disease [Publisher: [British Ecological Society, Wiley]]. *Journal of Applied Ecology*, 34(3), 793–806. <https://doi.org/10.2307/2404924>
- Howeler, R. H. (2002). Cassava mineral nutrition and fertilization [Publisher: CAB. International, CIAT: Chatuchak, Bangkok Thailand]. *Cassava: Biology, Production and Utilization*, 115–147.

- James, L., Kumar, P. L., Makesh Kumar, T., Tripathi, L., Ferguson, M., Kanju, E., Ntawurunga, P., & Cuellar, W. (2015). Cassava virus diseases: Biology, epidemiology, and management [ISBN: 0065-3527 Publisher: Elsevier]. *Advances in Virus Research*, 91, 85–142.
- James, L., Owor, B., Sseruwagi, P., & Ndunguru, J. (2006). Cassava mosaic virus disease in east and central Africa: Epidemiology and management of a regional pandemic. In *Advances in Virus Research* (pp. 355–418). Elsevier. [https://doi.org/10.1016/S0065-3527\(06\)67010-3](https://doi.org/10.1016/S0065-3527(06)67010-3)
- James, L., & Thresh, J. M. (2000). Cassava mosaic virus disease in East Africa: A dynamic disease in a changing environment [ISBN: 0168-1702 Publisher: Elsevier]. *Virus Research*, 71(1-2), 135–149.
- Jeger, M. J., Holt, J., Bosch, F. V. D., & Madden, L. V. (2004). Epidemiology of insect-transmitted plant viruses: modelling disease dynamics and control interventions [eprint: <https://onlinelibrary.wiley.com/doi/pdf/10.1111/j.0307-6962.2004.00394.x>]. *Physiological Entomology*, 29(3), 291–304. <https://doi.org/10.1111/j.0307-6962.2004.00394.x>
- Jittamai, P., Chanlawong, N., Atisattapong, W., Anlamlert, W., & Buensanteai, N. (2021). Reproduction number and sensitivity analysis of cassava mosaic disease spread for policy design [ISBN: 1551-0018]. *Mathematical Biosciences and Engineering*, 18(5), 5069–5093.
- Kinene, T., Luboobi, L. S., Nannyonga, B., & Mwanga, G. G. (2015). A mathematical model for the dynamics and cost effectiveness of the current controls of cassava brown streak disease in Uganda. *Journal of Mathematical and Computational Science*, 5(4), 567–600. Retrieved August 14, 2021, from <http://scik.org/index.php/jmcs/article/view/2185>
- Korobeinikov, A., & Maini, P. K. (2004). A lyapunov function and global properties for SIR and SEIR epidemiological models with nonlinear incidence. *Mathematical Biosciences & Engineering*, 1(1), 57.

- Korobeinikov, A., & Wake, G. C. (2002). Lyapunov functions and global stability for SIR, SIRS, and SIS epidemiological models. *Applied Mathematics Letters*, 15(8), 955–960.
- Kung'aro, M. (2016). *Mathematical modelling of intra and inter dynamics and control of yellow fever in primate and human populations* (Thesis) [Accepted: 2019-05-14T14:29:12Z]. The Nelson Mandela African Institution of Science and Technology. Retrieved February 3, 2022, from <https://dspace.nm-aist.ac.tz/handle/20.500.12479/57>
- Li, M. Y., & Shuai, Z. (2010). Global-stability problem for coupled systems of differential equations on networks. *Journal of Differential Equations*, 248(1), 1–20.
- Liao, S., & Wang, J. (2012). Global stability analysis of epidemiological models based on Volterra–Lyapunov stable matrices. *Chaos, Solitons & Fractals*, 45(7), 966–977.
- Mabasa, K. G. (2007). *Epidemiology of cassava mosaic disease and molecular characterization of cassava mosaic viruses and their associated whitefly (Bemisia tabaci) vector in South Africa* (Doctoral dissertation). University of the Witwatersrand Johannesburg.
- Macfadyen, S., Paull, C., Boykin, L. M., De Barro, P., Maruthi, M. N., Otim, M., Kalyebi, A., Vassão, D. G., Sseruwagi, P., Tay, W. T., Delatte, H., Seguni, Z., Colvin, J., & Omongo, C. A. (2018). Cassava whitefly, *Bemisia tabaci* (Gennadius) (Hemiptera: Aleyrodidae) in East African farming landscapes: A review of the factors determining abundance. *Bulletin of Entomological Research*, 108(5), 565–582. <https://doi.org/10.1017/S0007485318000032>
- Magoyo, F. D., Irunde, J. I., & Kuznetsov, D. (2019). Modeling the dynamics and transmission of cassava mosaic disease in Tanzania [Number: 0]. *Communications in Mathematical Biology and Neuroscience*, 2019(0), Article ID 4. <https://doi.org/10.28919/cmbn/3819>
- Mayengo, M. M., Kgosimore, M., & Chakraverty, S. (2022). Fuzzy dynamical system in alcohol-related health risk behaviors and beliefs. In *Soft Computing in Interdisciplinary Sciences* (pp. 109–127). Springer.
- Milenovic, M., Wosula, E. N., Rapisarda, C., & Legg, J. P. (2019). Impact of host plant species and whitefly species on feeding behavior of *Bemisia tabaci*. *Frontiers in Plant Science*, 10, 1. <https://doi.org/10.3389/fpls.2019.00001>

- Mtunguja, M. K., Beckles, D. M., Laswai, H. S., Ndunguru, J. C., & Sinha, N. J. (2019). Opportunities to commercialize cassava production for poverty alleviation and improved food security in Tanzania [Number: 1]. *African Journal of Food, Agriculture, Nutrition and Development*, 19(1), 13928–13946. <https://doi.org/10.4314/ajfand.v19i1>
- Mwasunda, J. A., Irunde, J. I., Kajunguri, D., & Kuznetsov, D. (2022). Optimal control analysis of taenia saginata bovine cysticercosis and human taeniasis. *Parasite Epidemiology and Control*, 16, e00236.
- Nyerere, N., Luboobi, L., Mpeshe, S., & Shirima, G. (2020a). Modeling the impact of seasonal weather variations on the infectiology of brucellosis [Accepted: 2021-09-23T12:41:54Z Publisher: Hindawi]. <https://doi.org/10.1155/2020/8972063>
- Nyerere, N., Luboobi, L. S., Mpeshe, S. C., & Shirima, G. M. (2020b). Optimal control strategies for the infectiology of brucellosis. *International Journal of Mathematics and Mathematical Sciences*, 2020.
- Parsaei, M. R., Javidan, R., Shayegh Kargar, N., & Saberi Nik, H. (2017). On the global stability of an epidemic model of computer viruses. *Theory in Biosciences*, 136(3), 169–178.
- Rakshit, N., Al Basir, F., Banerjee, A., & Ray, S. (2019). Dynamics of plant mosaic disease propagation and the usefulness of roguing as an alternative biological control [ISBN: 1476-945X Publisher: Elsevier]. *Ecological Complexity*, 38, 15–23.
- Renald, E. K. (2020). *A mathematical model to inform on desirable dog-rabies control methods in an urban setting: A case study of Arusha - Tanzania* (Master's thesis). NM-AIST.
- Sseruwagi, P., Maruthi, M. N., Colvin, J., Rey, M. E. C., Brown, J. K., & Legg, J. P. (2006). Colonization of non-cassava plant species by cassava whiteflies (*Bemisia tabaci*) in Uganda [ISBN: 0013-8703 Publisher: Wiley Online Library]. *Entomologia Experimentalis et Applicata*, 119(2), 145–153.
- Tadesse, D., & Regessa, D. (2017). Cassava Integrated Pest Management: Review on Cassava Mosaic Disease and Mealybug. <https://doi.org/10.13140/RG.2.2.12481.66404>
Publisher: Unpublished

- Tairo, F., Mbewe, W., Mark, D., Lupembe, M., Sseruwagi, P., & Ndunguru, J. (2017). Phylogenetic characterization of East African cassava mosaic begomovirus (Geminiviridae) isolated from *Manihot carthagenensis* subsp. *glaziovii* (Mill.Arg.) Allem., from a non-cassava growing region in Tanzania. *African Journal of Biotechnology*, 16(36), 1826–1831. <https://doi.org/10.5897/AJB2017.16130>
- Technical Centre for Agricultural and Rural Cooperation. (1990). *African cassava mosaic disease: From knowledge to control; Yamoussoukro, Ivory Coast, 4-8 May 1987* (J. P. Alaux & C. Fauquet, Eds.). CTA.
- Tiendrebeogo, F., Lefeuvre, P., Hoareau, M., Harimalala, M., De Bruyn, A., Villemot Brachet, J., Traoré, V., Konaté, G., Traore, A., Barro, N., Reynaud, B., Traore, O., & Lett, J.-M. (2012). Evolution of African cassava mosaic virus by recombination between bipartite and monopartite begomoviruses. *Virology Journal*, 9, 67. <https://doi.org/10.1186/1743-422X-9-67>
- Wangari, I. M. (2020). Condition for global stability for a SEIR model incorporating exogenous reinfection and primary infection mechanisms (M. G. Tsipouras, Ed.) [Publisher: Hindawi]. *Computational and Mathematical Methods in Medicine*, 2020, 9435819. <https://doi.org/10.1155/2020/9435819>
- Zahedi, M. S., & Kargar, N. S. (2017). The Volterra–Lyapunov matrix theory for global stability analysis of a model of the HIV/AIDS. *International Journal of Biomathematics*, 10(01), 1750002.

APPENDICES

Appendix 1: Code for the basic model simulation

```
% Your MATLAB code here
\begin{verbatim}
clc
clear
close all
tspan=[0 300];
% initial condition for model variable
y0=[0.35 0.05 0.05 40 10 0.2 0.1];
[t,y]=ode45(@population,tspan,y0);
%plotting cassava population
figure (1)
plot(t,y(:,1),'g', t,y(:,2),'b', t,y(:,3),'r');
l=legend('Susceptible plants','Exposed plants','Infected plants'
    );
xl=xlabel('Time[days]');
yl=ylabel('Cassava Population [per m^2]');
set(yl,'FontWeight', 'bold');
set(xl,'FontWeight', 'bold');
set(l,'FontSize',12);
grid on
%plotting Whitefly population
figure (2)
plot(t,y(:,4),'g', t,y(:,5),'r');
l=legend('Susceptible Whitefly','Infected Whitefly');
xl=xlabel('Time[days]');
yl=ylabel('Whitefly Population [per m^2]');
set(yl,'FontWeight', 'bold');
set(xl,'FontWeight', 'bold');
set(l,'FontSize',12);
grid on
```

```

%plotting Non-cassava host plant population
figure (3)
plot(t,y(:,6),'g', t,y(:,7),'r');
l=legend('Susceptible Non-Cassava Host','Infected Non-Cassava
        Host');
xl=xlabel('Time[days]');
yl=ylabel('Non Cassava Host Population [per m^2]');
set(yl,'FontWeight', 'bold');
set(xl,'FontWeight', 'bold');
set(l,'FontSize',12);
grid on
\end{verbatim}

+++++
\begin{verbatim}
function dy=population(t ,y)
dy=zeros(size(y));
Sc=y(1);Ec=y(2);Ic=y(3);Sw=y(4);Iw=y(5);Sh=y(6);Ih=y(7);
Nc=Sc+Ec+Ic;
Nw=Sw+Iw;
Nh=Sh+Ih;
a = 0.008; b = 0.008; c = 0.008; d = 0.008; varepsilon = 0.033;
eta = 0.1e-2; rho = .1; phi = 0.003; psi = 0.003; omega = 0.06;
rc = 0.5e-1; rw = .2; rh = 0.02; kc = 0.7; kh = 0.7; kw=90;

dy(1)=rc*(1-Nc/kc)*Sc+phi*Ic-a*Sc*Iw-psi*Sc;
dy(2)=rc*(1-Nc/kc)*rho*Sc+a*Sc*Iw-(psi+varepsilon)*Ec;
dy(3)=varepsilon*Ec-(psi+phi)*Ic;
dy(4)=rw*(1-Nw/kw)*Nw-(b*(Ec+Ic)+c*Ih)*Sw-omega*Sw;
dy(5)=(b*(Ec+Ic)+c*Ih)*Sw-omega*Iw;
dy(6)=rh*(1-Nh/kh)*Sh-d*Sh*Iw-eta*Sh;
dy(7)=d*Sh*Iw-eta*Ih;
end
\end{verbatim}
+++++

```

```

\begin{verbatim}
clc
clear
close all
tspan=[0 300];
% initial condition for model variable
y0=[0.35 0.05 0.05 40 10 0.2 0.1];
[t,y]=ode45(@omeg1,tspan,y0);
[t1,y1]=ode45(@omeg2,tspan,y0);
[t2,y2]=ode45(@omeg3,tspan,y0);
% omega
%Plotting Infected Cassava plant with different values of omega
subplot(1,3,1)
plot(t,y(:,3),'b', t1,y1(:,3),'g', t2,y2(:,3),'r');
legend('\omega=0.06','\omega=0.12','\omega=0.18')
xlabel('Time[days]')
ylabel('Infected Cassava Population [per m^2]')
title('(a)', 'FontSize', 15);
grid on
%Plotting Infected vector with different values of omega
subplot(1,3,2)
plot(t,y(:,5),'b', t1,y1(:,5),'g', t2,y2(:,5),'r');
legend('\omega=0.06','\omega=0.12','\omega=0.18')
xlabel('Time[days]')
ylabel('Infected Vector Population [per m^2]')
title('(b)', 'FontSize', 15);
grid on
%Plotting Infected Non-cassava plant with different values of
    omega
subplot(1,3,3)
plot(t,y(:,7),'b', t1,y1(:,7),'g', t2,y2(:,7),'r');
legend('\omega=0.06','\omega=0.12','\omega=0.18')
xlabel('Time[days]')
ylabel('Infected Non-cassava Hosts Population [per m^2]')

```

```

title(' (c)', 'FontSize', 15);
grid on
% extending figure space
fig = gcf;
fig.Position(3) = fig.Position(3) + 400;
\end{verbatim}
+++++
\begin{verbatim}
clc
clear
close all
tspan=[0 300];
% initial condition for model variables
y0=[0.35 0.05 0.05 40 10 0.2 0.1];
[t,y]=ode45(@vector,tspan,y0);
[t1,y1]=ode45(@vector1,tspan,y0);
[t2,y2]=ode45(@vector2,tspan,y0);
% Carring capacity of white fly vector k[w]
%Plotting Infected Cassava plant with different values of k[w]
subplot(1,3,1)
plot(t,y(:,3),'b', t1,y1(:,3),'g', t2,y2(:,3),'r');
legend('\kappa_w=10', '\kappa_w=100', '\kappa_w=350')
xlabel('Time[days]')
ylabel('Infected Cassava plan Population [per m^2]')
title(' (a)', 'FontSize', 15);
grid on
%Plotting Infected vector with different values of k[w]
subplot(1,3,2)
plot(t,y(:,5),'b', t1,y1(:,5),'g', t2,y2(:,5),'r');
legend('\kappa_w=10', '\kappa_w=100', '\kappa_w=350')
xlabel('Time[days]')
ylabel('Infected vector Population [per m^2]')
title(' (b)', 'FontSize', 15);
grid on

```

```

%Plotting Infected Non-cassava plant with different values of k[
    w]
subplot(1,3,3)
plot(t,y(:,7),'b', t1,y1(:,7),'g', t2,y2(:,7),'r');
legend('\kappa_w=10','\kappa_w=100','\kappa_w=350')
xlabel('Time[days]')
ylabel(' Infected Non-cassava hosts Population [per m^2]')
title('(c)', 'FontSize', 15);
grid on
% increasing figure space
fig = gcf;
fig.Position(3) = fig.Position(3) + 400;
\end{verbatim}

```

Appendix 2: Main file for global stability simulation

```
\begin{verbatim}
clc
clear
close all
tspan=[0 60];
% initializing model variables
y0=[0.2 0.05 0.05 40 10 0.2 0.1];
[t,y]=ode45(@population_stab,tspan,y0);
%plotting cassava population
figure (1)
plot(t,y(:,1),'c');
grid on
hold on
% initial condition for model variables
y0=[0.4 0.05 0.05 40 10 0.2 0.1];
[t,y]=ode45(@population_stab,tspan,y0);
%plotting cassava population
figure (1)
plot(t,y(:,1),'r');
grid on
hold on
% initial condition for model variables
y0=[0.6 0.05 0.05 40 10 0.2 0.1];
[t,y]=ode45(@population_stab,tspan,y0);
%plotting cassava population
figure (1)
plot(t,y(:,1),'m');
grid on
hold on
% initial condition for model variables
y0=[0.8 0.05 0.05 40 10 0.2 0.1];
[t,y]=ode45(@population_stab,tspan,y0);
```

```

%plotting cassava population
figure (1)
plot(t,y(:,1),'b');
hold on
%initial condition for model variables
y0=[1 0.05 0.05 40 10 0.2 0.1];
[t,y]=ode45(@population_stab,tspan,y0);
%plotting cassava population
figure (1)
plot(t,y(:,1),'g')
legend('Sc=0.2','Sc=0.4','Sc=0.6','Sc=0.8','Sc=1')
xlabel('Time[days]')
ylabel('Susceptible cassava plants [per m^2]')
grid on
hold off
%-----
tspan=[0 1000];
% initial condition for model variables
y0=[0.2 0.05 0.05 40 10 0.2 0.1];
[t,y]=ode45(@population_stab,tspan,y0);
%plotting cassava population
figure (2)
plot(t,y(:,2),'c');
grid on
hold on
% initial condition for model variables
y0=[0.2 0.1 0.05 40 10 0.2 0.1];
[t,y]=ode45(@population_stab,tspan,y0);
%plotting cassava population
figure (2)
plot(t,y(:,2),'r');
grid on
hold on
% initial condition for model variables

```

```

y0=[0.2 0.3 0.05 40 10 0.2 0.1];
[t,y]=ode45(@population_stab,tspan,y0);
%plotting cassava population
figure (2)
plot(t,y(:,2),'m');
grid on
hold on
% initial condition for model variables
y0=[0.2 0.5 0.05 40 10 0.2 0.1];
[t,y]=ode45(@population_stab,tspan,y0);
%plotting cassava population
figure (2)
plot(t,y(:,2),'b');
grid on
hold on
% initial condition for model variables
y0=[0.2 0.7 0.05 40 10 0.2 0.1];
[t,y]=ode45(@population_stab,tspan,y0);
%plotting cassava population
figure (2)
plot(t,y(:,2),'g');
legend('Ec=0.05','Ec=0.1','Ec=0.3','Ec=0.5','Ec=0.7')
xlabel('Time[days]')
ylabel('Exposed cassava plants [per m^2]')
grid on
hold off
%-----
tspan=[0 3000];
% initial condition for model variables
y0=[0.2 0.05 0.05 40 10 0.2 0.1];
[t,y]=ode45(@population_stab,tspan,y0);
%plotting cassava population
figure (3)
plot(t,y(:,3),'c');

```



```

grid on
hold on
% initial condition for model variables
y0=[0.2 0.05 0.1 40 10 0.2 0.1];
[t,y]=ode45(@population_stab,tspan,y0);
%plotting cassava population
figure (3)
plot(t,y(:,3),'r');
grid on
hold on
% initial condition for model variables
y0=[0.2 0.05 0.3 40 10 0.2 0.1];
[t,y]=ode45(@population_stab,tspan,y0);
%plotting cassava population
figure (3)
plot(t,y(:,3),'m');
grid on
hold on
% initial condition for model variables
y0=[0.2 0.05 0.5 40 10 0.2 0.1];
[t,y]=ode45(@population_stab,tspan,y0);
%plotting cassava population
figure (3)
plot(t,y(:,3),'b');
grid on
hold on
% initial condition for model variables
y0=[0.2 0.05 0.7 40 10 0.2 0.1];
[t,y]=ode45(@population_stab,tspan,y0);
%plotting cassava population
figure (3)
plot(t,y(:,3),'g');
legend('Ic=0.05','Ic=0.1','Ic=0.3','Ic=0.5','Ic=0.7')
xlabel('Time[days]')

```

```

ylabel('Infected cassava plants [per m^2]')
grid on
hold off

%-----
tspan=[0 30];
% initial condition for model variables
y0=[0.2 0.05 0.05 40 10 0.2 0.1];
[t,y]=ode45(@population_stab,tspan,y0);
%plotting cassava population
figure (4)
plot(t,y(:,4),'c');
grid on
hold on
% initial condition for model variables
y0=[0.2 0.05 0.05 160 10 0.2 0.1];
[t,y]=ode45(@population_stab,tspan,y0);
%plotting cassava population
figure (4)
plot(t,y(:,4),'r');
grid on
hold on
% initial condition for model variables
y0=[0.2 0.05 0.05 200 10 0.2 0.1];
[t,y]=ode45(@population_stab,tspan,y0);
%plotting cassava population
figure (4)
plot(t,y(:,4),'m');
grid on
hold on
% initial condition for model variables
y0=[0.2 0.05 0.05 260 10 0.2 0.1];
[t,y]=ode45(@population_stab,tspan,y0);
%plotting cassava population
figure (4)

```

```

plot(t,y(:,4),'b');
grid on
hold on
% initial condition for model variables
y0=[0.2 0.05 0.05 300 10 0.2 0.1];
[t,y]=ode45(@population_stab,tspan,y0);
%plotting cassava population
figure (4)
plot(t,y(:,4),'g');
legend('Sw=90','Sw=160','Sw=200','Sw=260','Sw=300')
xlabel('Time[days]')
ylabel('Susceptible whitefly [per m^2]')
grid on
hold off
%-----
tspan=[0 150];
% initial condition for model variables
y0=[0.2 0.05 0.05 40 90 0.2 0.1];
[t,y]=ode45(@population_stab,tspan,y0);
%plotting cassava population
figure (5)
plot(t,y(:,5),'c');
grid on
hold on
% initial condition for model variables
y0=[0.2 0.05 0.05 40 160 0.2 0.1];
[t,y]=ode45(@population_stab,tspan,y0);
%plotting cassava population
figure (5)
plot(t,y(:,5),'r');
grid on
hold on
% initial condition for model variables
y0=[0.2 0.05 0.05 40 200 0.2 0.1];

```

```

[t,y]=ode45(@population_stab,tspan,y0);
%plotting cassava population
figure (5)
plot(t,y(:,5),'m');
grid on
hold on
% initial condition for model variables
y0=[0.2 0.05 0.05 40 260 0.2 0.1];
[t,y]=ode45(@population_stab,tspan,y0);
%plotting cassava population
figure (5)
plot(t,y(:,5),'b');
grid on
hold on
% initial condition for model variables
y0=[0.2 0.05 0.05 40 300 0.2 0.1];
[t,y]=ode45(@population_stab,tspan,y0);
%plotting cassava population
figure (5)
plot(t,y(:,5),'g');
legend('Iw=90','Iw=160','Iw=200','Iw=260','Iw=300')
xlabel('Time[days]')
ylabel('Infected whitefly [per m^2]')
grid on
hold off
%-----
tspan=[0 60];
% initial condition for model variables
y0=[0.2 0.05 0.05 40 10 0.5 0.1];
[t,y]=ode45(@population_stab,tspan,y0);
%plotting cassava population
figure (6)
plot(t,y(:,6),'c');
grid on

```

```

hold on
% initial condition for model variables
y0=[0.2 0.05 0.05 40 10 0.4 0.1];
[t,y]=ode45(@population_stab,tspan,y0);
%plotting cassava population
figure (6)
plot(t,y(:,6),'r');
grid on
hold on
% initial condition for model variables
y0=[0.2 0.05 0.05 40 10 0.6 0.1];
[t,y]=ode45(@population_stab,tspan,y0);
%plotting cassava population
figure (6)
plot(t,y(:,6),'m');
grid on
hold on
% initial condition for model variables
y0=[0.2 0.05 0.05 40 10 0.8 0.1];
[t,y]=ode45(@population_stab,tspan,y0);
%plotting cassava population
figure (6)
plot(t,y(:,6),'b');
grid on
hold on
% initial condition for model variables
y0=[0.2 0.05 0.05 40 10 0.9 0.1];
[t,y]=ode45(@population_stab,tspan,y0);
%plotting cassava population
figure (6)
plot(t,y(:,6),'g');
legend('Sh=0.2','Sh=0.4','Sh=0.6','Sh=0.8','Sh=0.9')
xlabel('Time[days]')
ylabel('Susceptible non-cassava host plants [per m^2]')

```

```

grid on
hold off
%-----
tspan=[0 10000];
% initial condition for model variables
y0=[0.2 0.05 0.05 40 10 0.2 0.1];
[t,y]=ode45(@population_stab,tspan,y0);
%plotting cassava population
figure (7)
plot(t,y(:,7),'c');
grid on
hold on
% initial condition for model variables
y0=[0.2 0.05 0.05 40 10 0.2 0.3];
[t,y]=ode45(@population_stab,tspan,y0);
%plotting cassava population
figure (7)
plot(t,y(:,7),'r');
grid on
hold on
% initial condition for model variables
y0=[0.2 0.05 0.05 40 10 0.2 0.6];
[t,y]=ode45(@population_stab,tspan,y0);
%plotting cassava population
figure (7)
plot(t,y(:,7),'m');
grid on
hold on
% initial condition for model variables
y0=[0.2 0.05 0.05 40 10 0.2 0.8];
[t,y]=ode45(@population_stab,tspan,y0);
%plotting cassava population
figure (7)
plot(t,y(:,7),'b');

```

```

grid on
hold on
% initial condition for model variables
y0=[0.2 0.05 0.05 40 10 0.2 0.9];
[t,y]=ode45(@population_stab,tspan,y0);
%plotting cassava population
figure (7)
plot(t,y(:,7),'g');
legend('Ih=0.1','Ih=0.3','Ih=0.6','Ih=0.8','Ih=0.9')
xlabel('Time[days]')
ylabel('Infected non-cassava host plants [per m^2]')
grid on
hold off
%+++++
figure (8)
tspan=[0 1000];
% initial condition for model variables
y0=[0.2 0.05 0.05 40 10 0.2 0.1];
[t,y]=ode45(@population_stab,tspan,y0);
%plotting cassava population
subplot(2,2,1)
title('(a)')
plot(t,y(:,2),'c');
grid on
hold on
% initial condition for model variables
y0=[0.2 0.1 0.05 40 10 0.2 0.1];
[t,y]=ode45(@population_stab,tspan,y0);
%plotting cassava population
plot(t,y(:,2),'r');
grid on
hold on
% initial condition for model variables
y0=[0.2 0.3 0.05 40 10 0.2 0.1];

```

```

[t,y]=ode45(@population_stab,tspan,y0);
%plotting cassava population
plot(t,y(:,2),'m');
grid on
hold on
% initial condition for model variables
y0=[0.2 0.5 0.05 40 10 0.2 0.1];
[t,y]=ode45(@population_stab,tspan,y0);
%plotting cassava population
plot(t,y(:,2),'b');
grid on
hold on
% initial condition for model variables
y0=[0.2 0.7 0.05 40 10 0.2 0.1];
[t,y]=ode45(@population_stab,tspan,y0);
%plotting cassava population
plot(t,y(:,2),'g');
m=legend('Ec=0.05','Ec=0.1','Ec=0.3','Ec=0.5','Ec=0.7');
set(m,'FontSize',11);
pp=xlabel('Time[days]');
mm=ylabel('Exposed cassava plants [per m^2]');
set(pp,'FontWeight','bold');
set(mm,'FontWeight','bold');
grid on
title('(a)')
hold off
%-----
tspan=[0 3000];
% initial condition for model variables
y0=[0.2 0.05 0.05 40 10 0.2 0.1];
[t,y]=ode45(@population_stab,tspan,y0);
%plotting cassava population
subplot(2,2,3)
plot(t,y(:,3),'c');

```



```

grid on
hold on
% initial condition for model variables
y0=[0.2 0.05 0.1 40 10 0.2 0.1];
[t,y]=ode45(@population_stab,tspan,y0);
%plotting cassava population
plot(t,y(:,3),'r');
grid on
hold on
% initial condition for model variables
y0=[0.2 0.05 0.3 40 10 0.2 0.1];
[t,y]=ode45(@population_stab,tspan,y0);
%plotting cassava population
plot(t,y(:,3),'m');
grid on
hold on
% initial condition for model variables
y0=[0.2 0.05 0.5 40 10 0.2 0.1];
[t,y]=ode45(@population_stab,tspan,y0);
%plotting cassava population
plot(t,y(:,3),'b');
grid on
hold on
% initial condition for model variables
y0=[0.2 0.05 0.7 40 10 0.2 0.1];
[t,y]=ode45(@population_stab,tspan,y0);
%plotting cassava population
plot(t,y(:,3),'g');
q=legend('Ic=0.05','Ic=0.1','Ic=0.3','Ic=0.5','Ic=0.7');
set(q,'FontSize',11);
pp=xlabel('Time[days]');
mm=ylabel('Infected cassava plants [per m^2]');
set(pp,'FontWeight','bold');
set(mm,'FontWeight','bold');

```

```

grid on
title('(b)')
hold off

%+++++
tspan=[0 150];
% initial condition for model variables
y0=[0.2 0.05 0.05 40 90 0.2 0.1];
[t,y]=ode45(@population_stab,tspan,y0);
%plotting cassava population
subplot(2,2,2)
plot(t,y(:,5),'c');
grid on
hold on
% initial condition for model variables
y0=[0.2 0.05 0.05 40 160 0.2 0.1];
[t,y]=ode45(@population_stab,tspan,y0);
%plotting cassava population
plot(t,y(:,5),'r');
grid on
hold on
% initial condition for model variables
y0=[0.2 0.05 0.05 40 200 0.2 0.1];
[t,y]=ode45(@population_stab,tspan,y0);
%plotting cassava population
plot(t,y(:,5),'m');
grid on
hold on
% initial condition for model variables
y0=[0.2 0.05 0.05 40 260 0.2 0.1];
[t,y]=ode45(@population_stab,tspan,y0);
%plotting cassava population
plot(t,y(:,5),'b');
grid on
hold on

```

```

% initial condition for model variables
y0=[0.2 0.05 0.05 40 300 0.2 0.1];
[t,y]=ode45(@population_stab,tspan,y0);
%plotting cassava population
plot(t,y(:,5),'g');
p=legend('Iw=90','Iw=160','Iw=200','Iw=260','Iw=300');
set(p,'FontSize',11);
pp=xlabel('Time[days]');
mm=ylabel('Infected whitefly [per m^2]');
set(pp,'FontWeight','bold');
set(mm,'FontWeight','bold');
grid on
title('(c)')
hold off
%+++++
tspan=[0 10000];
% Initial condition for model variables
y0=[0.2 0.05 0.05 40 10 0.2 0.1];
[t,y]=ode45(@population_stab,tspan,y0);
%plotting cassava population
subplot(2,2,4)
plot(t,y(:,7),'c');
grid on
hold on
% initial condition for model variables
y0=[0.2 0.05 0.05 40 10 0.2 0.3];
[t,y]=ode45(@population_stab,tspan,y0);
%plotting cassava population
plot(t,y(:,7),'r');
grid on
hold on
% initial condition for model variables
y0=[0.2 0.05 0.05 40 10 0.2 0.6];
[t,y]=ode45(@population_stab,tspan,y0);

```

```

%plotting cassava population
plot(t,y(:,7),'m');
grid on
hold on
% initial condition for model variables
y0=[0.2 0.05 0.05 40 10 0.2 0.8];
[t,y]=ode45(@population_stab,tspan,y0);
%plotting cassava population
plot(t,y(:,7),'b');
grid on
hold on
% initial condition for model variables
y0=[0.2 0.05 0.05 40 10 0.2 0.9];
[t,y]=ode45(@population_stab,tspan,y0);
%plotting cassava population
plot(t,y(:,7),'g');
l=legend('Ih=0.1','Ih=0.3','Ih=0.6','Ih=0.8','Ih=0.9');
set(l,'FontSize',11);
xl=xlabel('Time[days]');
mm=ylabel('Infected non-cassava host plants [per m^2]');
set(xl,'FontWeight','bold');
set(mm,'FontWeight','bold');
grid on
title('(d)')
hold off
\end{verbatim}

```

Appendix 3: Main file for optimal control model

```
%main file for optimal control
\begin{verbatim}
clc;
clear;
close all;
format long
t0 = 0; tf=300; N=100;
time =linspace(t0,tf,N);
%initializing state variable
y0 = [0.35 0.05 0.05 40 10 0.2 0.1];% initial conditions
%+++++
par_val=[0.008 0.008 0.008 0.008 0.033 0.1e-2 .1 0.003 0.003
         0.06 0.5e-1 .2 0.02 0.7 90 0.3 10 5 50 100 0.1 0.18];
%-----
%=====
a=par_val(1);b = par_val(2);c= par_val(3);d = par_val(4);
    varepsilon = par_val(5);eta = par_val(6);rho = par_val(7);phi
    = par_val(8);psi =par_val(9);omega= par_val(10);rc= par_val
    (11);rw = par_val(12);rh = par_val(13);kc = par_val(14);kw=
    par_val(15); kh =par_val(16);A1 =par_val(17);A2 = par_val(18)
    ;A3 = par_val(19); A4 =par_val(20);tau= par_val(21);varsigma=
    par_val(22);
%+++++
lf = [0 0 0 0 0 0 0];
% TEST SECTION
init =y0;
init2 =lf;
h = (tf-t0)/N;
u = linspace(0,0,N+1);
u1=u'; u2=u';
U = [u1 u2];
% algorithm implementation
```

```

%Test 1
delta = 0.5;
X=init;
i=0; % iteration_c initialization
mm=size(X);
NumXX =10e10;
Xnew = rand(N+1,mm(2)).*(repmat(X,N+1,1));
DenXnew=norm(Xnew);
while NumXX/DenXnew>delta
Xold = Xnew;
oldu = U;
%%%%%%%%%%%%%%%%%%%%%%%%%%%%%%%%%%%%%%%%%%%%%%%%%%%%%%%%%%%%%%%%%%%%%%%%
% RK_4WD FOR STATES
[Tx, X]=rk4foward(@kims,t0, tf,N, init,U,par_val);
%%%%%%%%%%%%%%%%%%%%%%%%%%%%%%%%%%%%%%%%%%%%%%%%%%%%%%%%%%%%%%%%%%%%%%%%
% RK_BACK FOR CO-STATES
[Tp, P]=rk4back(@kims_costate,t0,tf,N,init2,U,X,par_val);
%%%%%%%%%%%%%%%%%%%%%%%%%%%%%%%%%%%%%%%%%%%%%%%%%%%%%%%%%%%%%%%%%%%%%%%%
%Updating control parameter
f1 = X(1,:);g = X(2,:);r = X(3,:);s = X(4,:);
v= X(5,:);x = X(6,:);z = X(7,:);
%%%%%%%%%%%%%%%%%%%%%%%%%%%%%%%%%%%%%%%%%%%%%%%%%%%%%%%%%%%%%%%%%%%%%%%%
L1 = P(1,:); L2 = P(2,:); L3 = P(3,:); L4 = P(4,:); L5 = P(5,:);
L6 = P(6,:); L7 = P(7,:);
%%%%%%%%%%%%%%%%%%%%%%%%%%%%%%%%%%%%%%%%%%%%%%%%%%%%%%%%%%%%%%%%%%%%%%%%
% Case0: No control,
% u1 = zeros(1,N+1);
% u2 = zeros(1,N+1);
%%%%%%%%%%%%%%%%%%%%%%%%%%%%%%%%%%%%%%%%%%%%%%%%%%%%%%%%%%%%%%%%%%%%%%%%
%Implementation of all controls
% Case1:u1\neq 0, u2\neq 0, u3\neq 0, u4\neq 0,
% u1 =min(max(0,((L3.*r+L7.*z)./A3)*tau),1);
% u2 =min(max(0,((L4.*s+L5.*v)./A4)*varsigma),1);
%%%%%%%%%%%%%%%%%%%%%%%%%%%%%%%%%%%%%%%%%%%%%%%%%%%%%%%%%%%%%%%%%%%%%%%%

```

```

%Implementation of roughing only
% Case3:u1\neq 0, u2\neq 0, u3\neq 0, u4= 0,
% u1 =min(max(0, ((L3.*r+L7.*z)./A3)*tau),1);
% u2 =zeros(1,N+1);
%+++++
%Implementation of Insecticides alone
% Case2:u1\neq 0, u2\neq 0, u3\neq 0, u4\neq 0,
u1 =zeros(1,N+1);
u2 =min(max(0, ((L4.*s+L5.*v)./A4)*varsigma),1);
%+++++
Uu=[u1' u2'];
U = 0.5*Uu + 0.5*oldu; % control conv_combination
%+++++
Xnew = X';
NumXX =abs(norm(Xnew-Xold));
DenXnew =norm(Xnew);
i=i+1; %Updating counter
end
% simulating
X=X';
Tx =Tx';
XX=X(:,1); YY=X(:,2); VV=X(:,3); ZZ=X(:,4); LL=X(:,5);
AA=X(:,6); BB=X(:,7);
%+++++
Up = [0 0];
[T,Y] = ode45(@kims,time,y0,[],Up, par_val);
%+++++
%Objective Function
J =sum((A1.*(VV(1:end)+BB(1:end))+A2.*+LL(1:end))+((A3/2).*Uu
(:,1).*Uu(:,1)+(A4/2).*Uu(:,2).*Uu(:,2))));
%+++++
S=[Tx,X];
%+++++
figure(1)

```

```

subplot(2,2,1)
plot(Tx,X(:,3),'-b',T, Y(:,3),'--r','LineWidth',1.5);
yl=ylabel('Infected cassava per m^2');
xl=xlabel('Time (Days)');
title('(a)')
% legend('u_i=0, i=1,2','u_i=0, i=1,2')
% legend('u_i \neq 0,i=1','u_i = 0,i=1,2')
%legend( u_i \neq 0,i=2 , u_i = 0,i=1,2 )
% legend('u_i\neq0, i=1,2', 'u_i=0, i=1,2')
set(yl,'FontWeight', 'bold');
set(xl,'FontWeight', 'bold');
%+++++
subplot(2,2,2)
plot(Tx,X(:,2),'-b',T, Y(:,2),'--r','LineWidth',1.5);
yl=ylabel('Exposed cassava per m^2');
xl=xlabel('Time (Days)');
title('(b)')
% legend('u_i=0, i=1,2','u_i=0, i=1,2')
% legend('u_i \neq 0,i=1','u_i = 0,i=1,2')
%legend( u_i \neq 0,i=2 , u_i = 0,i=1,2 )
% legend('u_i\neq0, i=1,2', 'u_i=0, i=1,2')
set(yl,'FontWeight', 'bold');
set(xl,'FontWeight', 'bold');
%+++++
subplot(2,2,3)
plot(Tx,X(:,5),'-b',T, Y(:,5),'--r','LineWidth',1.5);
yl=ylabel('Infected whitefly per m^2');
xl=xlabel('Time (Days)');
title('(c)')
% legend('u_i=0, i=1,2','u_i=0, i=1,2')
% legend('u_i \neq 0,i=1','u_i = 0,i=1,2')
%legend( u_i \neq 0,i=2 , u_i = 0,i=1,2 )
% legend('u_i\neq0, i=1,2', 'u_i=0, i=1,2')
set(yl,'FontWeight', 'bold');

```



```

set(xl,'FontWeight', 'bold');
%+++++
subplot(2,2,4)
plot(Tx,X(:,7),'-b',T, Y(:,7),'--r','LineWidth',1.5);
yl=ylabel('Infected non-cassava host per m^2');
xl=xlabel('Time (Days)');
title('(d)')
% l=legend('u_i=0, i=1,2','u_i=0, i=1,2');
l=legend('u_i \neq 0,i=1','u_i = 0,i=2');
% l=legend('u_i \neq 0,i=2','u_i = 0,i=1');
% l=legend('u_i\neq 0, i=1,2', 'u_i=0, i=1,2');
set(yl,'FontWeight', 'bold');
set(xl,'FontWeight', 'bold');
set(l,'FontSize',12);
%+++++
figure(2)
plot(Tx,Uu(:,1),'-r',Tx,Uu(:,2),'-k',Tx,2.0,'linewidth',1.5);
ylim([0 0.05])
xlim([0 300.5])
yl=ylabel('Control Profile');
set(yl,'FontWeight', 'bold');
xl=xlabel('Time (Days)');
set(xl,'FontWeight', 'bold');
% title('(d)')
% l=legend('u_i=0, i=1','u_i=0, i=2');
l=legend('u_i \neq, 0,i=1','u_i = 0,i=2');
% l=legend('u_i = 0,i=1','u_i \neq 0,i=2');
% l=legend('u_i\neq 0, i=1', 'u_i\neq 0, i=2');
set(l,'FontSize',12);
%+++++
X=XX'; % solution of the optimal control
U =[0 0]; % when no control
[Tx,Y] = ode45(@kims,time,y0,[],U, par_val);
Y=(Y);

```

```

%+++++
% Infection Averted
Inew=sum(Y(:,3))-sum(X(:,3))+sum(Y(:,5))-sum(X(:,5))+sum(Y(:,7))
    -sum(X(:,7));
%+++++
Output=[J Inew]
%=====
\end{verbatim}
+++++
\begin{verbatim}
%=====
% state eqn solving function definition
%File Name: kims
%=====
function ydot = kims(t,yy,U,par_val)
f1=yy(1); g=yy(2); r=yy(3);s=yy(4);
v=yy(5);x=yy(6); z=yy(7);
Nc=f1+g+r;
Nw=s+v;
Nh=x+z;
%+++++
a=par_val(1);b = par_val(2);c= par_val(3);d = par_val(4);
varepsilon = par_val(5);eta = par_val(6);rho = par_val(7);phi =
    par_val(8);psi =par_val(9);omega= par_val(10);rc= par_val(11)
    ;rw = par_val(12);rh= par_val(13);kc = par_val(14);kw=
    par_val(15); kh =par_val(16);A1 =par_val(17);A2 = par_val(18)
    ;A3 = par_val(19); A4 =par_val(20);tau= par_val(21);varsigma=
    par_val(22);
%+++++
u1 = U(1); u2=U(2);
%+++++
ydot1=rc.*(1-Nc./kc).*f1+phi.*r-a.*f1.*v-psi.*f1;
ydot2=rc.*(1-Nc./kc).*rho.*g+a.*f1.*v-(psi+varepsilon).*g;
ydot3=varepsilon.*g-(psi+phi+u1.*tau).*r;

```

```

ydot4=(1-Nw./kw).*rw.*Nw-(b.*(g+r)+c.*z).*s-(omega+u2.*varsigma)
    .*s;
ydot5=(b.*(g+r)+c.*z).*s-(omega+u2.*varsigma).*v;
ydot6=rh.*(1-Nh./kh).*x-d.*x.*v-eta.*x;
ydot7=d.*x.*v-(eta+u1.*tau).*z;
ydot = [ydot1; ydot2; ydot3; ydot4; ydot5; ydot6; ydot7];
%=====
\end{verbatim}
+++++
\begin{verbatim}
%=====
%co-state(adjoint) eqn solving function definition
%File Name: kims_costate
%=====
function ydot = kims_costate(t,y,U,X,par_val);
L1=y(1); L2=y(2); L3=y(3);L4=y(4);L5=y(5);L6=y(6);
L7=y(7);
%=====
a=par_val(1);b = par_val(2);c= par_val(3);d = par_val(4);
varepsilon = par_val(5);eta = par_val(6);rho = par_val(7);phi =
    par_val(8);psi =par_val(9);omega= par_val(10);rc= par_val(11)
    ;rw = par_val(12);rh = par_val(13);kc = par_val(14);kw=
    par_val(15); kh =par_val(16);A1 =par_val(17);A2 = par_val(18)
    ;A3 = par_val(19); A4 =par_val(20);tau= par_val(21);varsigma=
    par_val(22);
%+++++
u1 = U(1); u2=U(2);
% Variables
% Sc=f1;Ec=g;Ic=r;Sw=s,Iw=v;Sh=x;Ih=z;
f1 = X(1,:);g = X(2,:);r = X(3,:);s = X(4,:);
v= X(5,:);x = X(6,:);z = X(7,:);
Nc=f1+g+r;
Nw=s+v;
Nh=x+z;

```

```

ydot1=L1.*(-rc.*f1./kh+rc.*(1-(Nc)./kc)-a.*v-psi)+L2.*(-rc.*rho
.*g./kc+a.*v);
ydot2=-L1.*rc.*f1./kc+L2.*(-rc.*rho.*g./kc+rc.*(1-(Nc)./kc).*rho
-psi-varepsilon)+L3.*varepsilon-L4.*b.*s+L5.*b.*s;
ydot3=A1+L1.*(-rc.*f1./kc+phi)-L2.*rc.*rho.*g./kc+L3.*(-tau.*u1-
phi-psi)-L4.*b.*s+L5.*b.*s;
ydot4=L4.*(-rw.*(s+v)./kw+(1-(s+v)/kw).*rw-b.*(g+r)-c.*z-u2.*
varsigma-omega)+L5.*(b.*(g+r)+c.*z);
ydot5=A2-L1.*a.*f1+L2.*a.*f1+L4.*(-rw.*(s+v)./kw+(1-(s+v)./kw).*
rw)+L5.*(-u2.*varsigma-omega)-L6.*d.*x+L7.*d.*x;
ydot6= L6.*(-rh.*x./kh+rh.*(1-(x+z)./kh)-d.*v-eta)+L7.*d.*v;
ydot7=A1-L4.*c.*s+L5.*c.*s-L6.*rh.*x./kh+L7.*(-tau.*u1-eta);
ydot = [ydot1; ydot2; ydot3; ydot4; ydot5; ydot6; ydot7];
%=====
\end{verbatim}

```

Appendix 4: Maple code for sensitivity indices

```
> restart;
> #Computing sensitivity indices
# Set up numerical values for all problem parameters
#
params:= {a=0.008, b=0.008, c=0.008, d=0.008, varepsilon=0.033, eta=0.1e-2, rho=.1, phi=0.003, psi=0.003,
r[c]=0.5e-1, r[w]=.2, r[n]=0.02, k[c]=0.7, k[n]=0.1, k[w]=90, omega=0.06};
params := { a=0.008, b=0.008, c=0.008, d=0.008, η=0.001, ω=0.06, ϕ=0.003, ψ=0.003, ρ=0.1, ε
=0.033, kc=0.7, kn=0.1, kw=90, rc=0.05, rn=0.02, rw=0.2} (1)
```

```
> # Define main function
R := (1/6) * (8 * psi^3 * rho^3 / (psi + varepsilon)^3 + 36 * b * (r[w]-omega) * k[w] * (1 + varepsilon / (psi
+ phi)) * psi * rho * a * (r[c]-psi) * k[c] / (r[w] * (psi + varepsilon)^2 * r[c] * omega) - 72 * d * (r[n]-eta)
* k[n] * c * (r[w]-omega) * k[w] * psi * rho / (r[n] * omega * r[w] * eta * (psi + varepsilon)) + 12 * sqrt(
-12 * psi^4 * rho^4 * c * (r[w]-omega) * k[w] * d * (r[n]-eta) * k[n] / ((psi + varepsilon)^4 * r[w] * eta
* r[n] * omega) - 3 * psi^2 * rho^2 * a^2 * (r[c]-psi)^2 * k[c]^2 * b^2 * (r[w]-omega)^2 * k[w]^2 * (1
+ varepsilon / (psi + phi))^2 / ((psi + varepsilon)^4 * r[c]^2 * omega^2 * r[w]^2) - 60 * psi^2 * rho^2 * a
* (r[c]-psi) * k[c] * b * (r[w]-omega)^2 * k[w]^2 * (1 + varepsilon / (psi + phi)) * c * d * (r[n]-eta)
* k[n] / ((psi + varepsilon)^3 * r[c] * omega^2 * r[w]^2 * eta * r[n]) + 24 * psi^2 * rho^2 * c^2 * (r[w]
-omega)^2 * k[w]^2 * d^2 * (r[n]-eta)^2 * k[n]^2 / ((psi + varepsilon)^2 * r[w]^2 * eta^2 * r[n]^2
* omega^2) - 12 * a^3 * (r[c]-psi)^3 * k[c]^3 * b^3 * (r[w]-omega)^3 * k[w]^3 * (1 + varepsilon / (psi
+ phi))^3 / (r[c]^3 * omega^3 * r[w]^3 * (psi + varepsilon)^3) - 36 * a^2 * (r[c]-psi)^2 * k[c]^2 * b^2
* (r[w]-omega)^3 * k[w]^3 * (1 + varepsilon / (psi + phi))^2 * c * d * (r[n]-eta) * k[n] / (r[c]^2 * omega
^3 * r[w]^3 * (psi + varepsilon)^2 * eta * r[n]) - 36 * a * (r[c]-psi) * k[c] * b * (r[w]-omega)^3 * k[w]^3
* (1 + varepsilon / (psi + phi)) * c^2 * d^2 * (r[n]-eta)^2 * k[n]^2 / (r[c] * omega^3 * r[w]^3 * (psi
+ varepsilon) * eta^2 * r[n]^2) - 12 * c^3 * (r[w]-omega)^3 * k[w]^3 * d^3 * (r[n]-eta)^3 * k[n]^3
/ (r[w]^3 * eta^3 * r[n]^3 * omega^3))^(1/3) - (6 * (-1/3) * a * (r[c]-psi) * k[c] * b * (r[w]
-omega) * k[w] * (1 + varepsilon / (psi + phi)) / (r[c] * omega * r[w] * (psi + varepsilon)) - (1/3) * d
* (r[n]-eta) * k[n] * c * (r[w]-omega) * k[w] / (r[n] * omega * r[w] * eta) - (1/9) * psi^2 * rho^2 / (psi
+ varepsilon)^2)) / (8 * psi^3 * rho^3 / (psi + varepsilon)^3 + 36 * b * (r[w]-omega) * k[w] * (1
+ varepsilon / (psi + phi)) * psi * rho * a * (r[c]-psi) * k[c] / (r[w] * (psi + varepsilon)^2 * r[c] * omega)
- 72 * d * (r[n]-eta) * k[n] * c * (r[w]-omega) * k[w] * psi * rho / (r[n] * omega * r[w] * eta * (psi
+ varepsilon)) + 12 * sqrt(-12 * psi^4 * rho^4 * c * (r[w]-omega) * k[w] * d * (r[n]-eta) * k[n] / ((psi
+ varepsilon)^4 * r[w] * eta * r[n] * omega) - 3 * psi^2 * rho^2 * a^2 * (r[c]-psi)^2 * k[c]^2 * b^2 * (r[w]
-omega)^2 * k[w]^2 * (1 + varepsilon / (psi + phi))^2 / ((psi + varepsilon)^4 * r[c]^2 * omega^2 * r[w]
^2) - 60 * psi^2 * rho^2 * a * (r[c]-psi) * k[c] * b * (r[w]-omega)^2 * k[w]^2 * (1 + varepsilon / (psi
+ phi)) * c * d * (r[n]-eta) * k[n] / ((psi + varepsilon)^3 * r[c] * omega^2 * r[w]^2 * eta * r[n]) + 24 * psi
^2 * rho^2 * c^2 * (r[w]-omega)^2 * k[w]^2 * d^2 * (r[n]-eta)^2 * k[n]^2 / ((psi + varepsilon)^2 * r[w]
^2 * eta^2 * r[n]^2 * omega^2) - 12 * a^3 * (r[c]-psi)^3 * k[c]^3 * b^3 * (r[w]-omega)^3 * k[w]^3 * (1
+ varepsilon / (psi + phi))^3 / (r[c]^3 * omega^3 * r[w]^3 * (psi + varepsilon)^3) - 36 * a^2 * (r[c]-psi)^2
* k[c]^2 * b^2 * (r[w]-omega)^3 * k[w]^3 * (1 + varepsilon / (psi + phi))^2 * c * d * (r[n]-eta) * k[n]
/ (r[c]^2 * omega^3 * r[w]^3 * (psi + varepsilon)^2 * eta * r[n]) - 36 * a * (r[c]-psi) * k[c] * b * (r[w]
-omega)^3 * k[w]^3 * (1 + varepsilon / (psi + phi)) * c^2 * d^2 * (r[n]-eta)^2 * k[n]^2 / (r[c] * omega^3
* r[w]^3 * (psi + varepsilon) * eta^2 * r[n]^2) - 12 * c^3 * (r[w]-omega)^3 * k[w]^3 * d^3 * (r[n]-eta)
^3 * k[n]^3 / (r[w]^3 * eta^3 * r[n]^3 * omega^3))^(1/3) + (1/3) * psi * rho / (psi + varepsilon);
```

$$R := \frac{1}{6} \left(\frac{8 \psi^3 \rho^3}{(\psi + \varepsilon)^3} + \frac{36 b (r_w - \omega) k_w \left(1 + \frac{\varepsilon}{\psi + \phi}\right) \psi \rho a (r_c - \psi) k_c}{r_w (\psi + \varepsilon)^2 r_c \omega} \right. \\ \left. - \frac{72 d (r_n - \eta) k_n c (r_w - \omega) k_w \psi \rho}{r_n \omega r_w \eta (\psi + \varepsilon)} \right. \\ \left. + 12 \left(- \frac{12 \psi^4 \rho^4 c (r_w - \omega) k_w d (r_n - \eta) k_n}{(\psi + \varepsilon)^4 r_w \eta r_n \omega} \right. \right. \quad (2)$$

$$\begin{aligned}
& - \frac{3 \psi^2 \rho^2 a^2 (r_c - \psi)^2 k_c^2 b^2 (r_w - \omega)^2 k_w^2 \left(1 + \frac{\varepsilon}{\psi + \phi}\right)^2}{(\psi + \varepsilon)^4 r_c^2 \omega^2 r_w^2} \\
& - \frac{60 \psi^2 \rho^2 a (r_c - \psi) k_c b (r_w - \omega)^2 k_w^2 \left(1 + \frac{\varepsilon}{\psi + \phi}\right) c d (r_n - \eta) k_n}{(\psi + \varepsilon)^3 r_c \omega^2 r_w^2 \eta r_n} \\
& + \frac{24 \psi^2 \rho^2 c^2 (r_w - \omega)^2 k_w^2 d^2 (r_n - \eta)^2 k_n^2}{(\psi + \varepsilon)^2 r_w^2 \eta^2 r_n^2 \omega^2} - \frac{12 a^3 (r_c - \psi)^3 k_c^3 b^3 (r_w - \omega)^3 k_w^3 \left(1 + \frac{\varepsilon}{\psi + \phi}\right)^3}{r_c^3 \omega^3 r_w^3 (\psi + \varepsilon)^3} \\
& - \frac{36 a^2 (r_c - \psi)^2 k_c^2 b^2 (r_w - \omega)^3 k_w^3 \left(1 + \frac{\varepsilon}{\psi + \phi}\right)^2 c d (r_n - \eta) k_n}{r_c^2 \omega^3 r_w^3 (\psi + \varepsilon)^2 \eta r_n} \\
& - \frac{36 a (r_c - \psi) k_c b (r_w - \omega)^3 k_w^3 \left(1 + \frac{\varepsilon}{\psi + \phi}\right) c^2 d^2 (r_n - \eta)^2 k_n^2}{r_c \omega^3 r_w^3 (\psi + \varepsilon) \eta^2 r_n^2} \\
& - \frac{12 c^3 (r_w - \omega)^3 k_w^3 d^3 (r_n - \eta)^3 k_n^3}{r_w^3 \eta^3 r_n^3 \omega^3} \Bigg)^{1/2} \Bigg)^{1/3} - \left(6 \left(\right. \right. \\
& - \frac{1}{3} \frac{a (r_c - \psi) k_c b (r_w - \omega) k_w \left(1 + \frac{\varepsilon}{\psi + \phi}\right)}{r_c \omega r_w (\psi + \varepsilon)} - \frac{1}{3} \frac{d (r_n - \eta) k_n c (r_w - \omega) k_w}{r_n \omega r_w \eta} - \frac{1}{9} \frac{\psi^2 \rho^2}{(\psi + \varepsilon)^2} \Bigg) \Bigg) \\
& \Bigg/ \left(\frac{8 \psi^3 \rho^3}{(\psi + \varepsilon)^3} + \frac{36 b (r_w - \omega) k_w \left(1 + \frac{\varepsilon}{\psi + \phi}\right) \psi \rho a (r_c - \psi) k_c}{r_w (\psi + \varepsilon)^2 r_c \omega} \right. \\
& - \frac{72 d (r_n - \eta) k_n c (r_w - \omega) k_w \psi \rho}{r_n \omega r_w \eta (\psi + \varepsilon)} \\
& + 12 \left(- \frac{12 \psi^4 \rho^4 c (r_w - \omega) k_w d (r_n - \eta) k_n}{(\psi + \varepsilon)^4 r_w \eta r_n \omega} \right. \\
& - \frac{3 \psi^2 \rho^2 a^2 (r_c - \psi)^2 k_c^2 b^2 (r_w - \omega)^2 k_w^2 \left(1 + \frac{\varepsilon}{\psi + \phi}\right)^2}{(\psi + \varepsilon)^4 r_c^2 \omega^2 r_w^2}
\end{aligned}$$

$$\begin{aligned}
& - \frac{60 \psi^2 \rho^2 a (r_c - \psi) k_c b (r_w - \omega)^2 k_w^2 \left(1 + \frac{\varepsilon}{\psi + \phi}\right) c d (r_n - \eta) k_n}{(\psi + \varepsilon)^3 r_c \omega^2 r_w^2 \eta r_n} \\
& + \frac{24 \psi^2 \rho^2 c^2 (r_w - \omega)^2 k_w^2 d^2 (r_n - \eta)^2 k_n^2}{(\psi + \varepsilon)^2 r_w^2 \eta^2 r_n^2 \omega^2} - \frac{12 a^3 (r_c - \psi)^3 k_c^3 b^3 (r_w - \omega)^3 k_w^3 \left(1 + \frac{\varepsilon}{\psi + \phi}\right)^3}{r_c^3 \omega^3 r_w^3 (\psi + \varepsilon)^3} \\
& - \frac{36 a^2 (r_c - \psi)^2 k_c^2 b^2 (r_w - \omega)^3 k_w^3 \left(1 + \frac{\varepsilon}{\psi + \phi}\right)^2 c d (r_n - \eta) k_n}{r_c^2 \omega^3 r_w^3 (\psi + \varepsilon)^2 \eta r_n} \\
& - \frac{36 a (r_c - \psi) k_c b (r_w - \omega)^3 k_w^3 \left(1 + \frac{\varepsilon}{\psi + \phi}\right) c^2 d^2 (r_n - \eta)^2 k_n^2}{r_c \omega^3 r_w^3 (\psi + \varepsilon) \eta^2 r_n^2} \\
& - \left. \frac{12 c^3 (r_w - \omega)^3 k_w^3 d^3 (r_n - \eta)^3 k_n^3}{r_w^3 \eta^3 r_n^3 \omega^3} \right)^{1/2} \Bigg)^{1/3} + \frac{1}{3} \frac{\psi \rho}{\psi + \varepsilon}
\end{aligned}$$

> # Evaluating the eigenvalue for the first expression basing on baseline values

> eval(R, params)

3.792797569 + 0.1

(3)

> abs((3))

3.792797569

(4)

> # The second eigenvalue function

> R := -(1/12) * (8 * psi^3 * rho^3 / (psi + varepsilon)^3 + 36 * b * (r[w]-omega) * k[w] * (1 + varepsilon / (psi + phi)) * psi * rho * a * (r[c]-psi) * k[c] / (r[w] * (psi + varepsilon)^2 * r[c] * omega) - 72 * d * (r[n]-eta) * k[n] * c * (r[w]-omega) * k[w] * psi * rho / (r[n] * omega * r[w] * eta * (psi + varepsilon))) + 12 * sqrt(-12 * psi^4 * rho^4 * c * (r[w]-omega) * k[w] * d * (r[n]-eta) * k[n] / ((psi + varepsilon)^4 * r[w] * eta * r[n] * omega) - 3 * psi^2 * rho^2 * a^2 * (r[c]-psi)^2 * k[c]^2 * b^2 * (r[w]-omega)^2 * k[w]^2 * (1 + varepsilon / (psi + phi))^2 / ((psi + varepsilon)^4 * r[c]^2 * omega^2 * r[w]^2) - 60 * psi^2 * rho^2 * a * (r[c]-psi) * k[c] * b * (r[w]-omega)^2 * k[w]^2 * (1 + varepsilon / (psi + phi)) * c * d * (r[n]-eta) * k[n] / ((psi + varepsilon)^3 * r[c] * omega^2 * r[w]^2 * eta * r[n])) + 24 * psi^2 * rho^2 * c^2 * (r[w]-omega)^2 * k[w]^2 * d^2 * (r[n]-eta)^2 * k[n]^2 / ((psi + varepsilon)^2 * r[w]^2 * eta^2 * r[n]^2 * omega^2) - 12 * a^3 * (r[c]-psi)^3 * k[c]^3 * b^3 * (r[w]-omega)^3 * k[w]^3 * (1 + varepsilon / (psi + phi))^3 / (r[c]^3 * omega^3 * r[w]^3 * (psi + varepsilon)^3) - 36 * a^2 * (r[c]-psi)^2 * k[c]^2 * b^2 * (r[w]-omega)^3 * k[w]^3 * (1 + varepsilon / (psi + phi))^2 * c * d * (r[n]-eta) * k[n] / (r[c]^2 * omega^3 * r[w]^3 * (psi + varepsilon)^2 * eta * r[n]) - 36 * a * (r[c]-psi) * k[c] * b * (r[w]-omega)^3 * k[w]^3 * (1 + varepsilon / (psi + phi)) * c^2 * d^2 * (r[n]-eta)^2 * k[n]^2 / (r[c] * omega^3 * r[w]^3 * (psi + varepsilon) * eta^2 * r[n]^2) - 12 * c^3 * (r[w]-omega)^3 * k[w]^3 * d^3 * (r[n]-eta)^3 * k[n]^3 / (r[w]^3 * eta^3 * r[n]^3 * omega^3)))^(1/3) + (3 * (-1/3) * a * (r[c]-psi) * k[c] * b * (r[w]-omega) * k[w] * (1 + varepsilon / (psi + phi)) / (r[c] * omega * r[w] * (psi + varepsilon)) - (1/3) * d * (r[n]-eta) * k[n] * c * (r[w]-omega) * k[w] / (r[n] * omega * r[w] * eta) - (1/9) * psi^2 * rho^2 / (psi + varepsilon)^2)) / (8 * psi^3 * rho^3 / (psi + varepsilon)^3 + 36 * b * (r[w]-omega) * k[w] * (1 + varepsilon / (psi + phi)) * psi * rho * a * (r[c]-psi) * k[c] / (r[w] * (psi + varepsilon)^2 * r[c] * omega) - 72 * d * (r[n]-eta) * k[n] * c * (r[w]-omega) * k[w] * psi * rho / (r[n] * omega * r[w] * eta * (psi + varepsilon))) + 12 * sqrt(-12 * psi^4 * rho^4 * c * (r[w]-omega) * k[w] * d * (r[n]-eta) * k[n] / ((psi + varepsilon)^4 * r[w] * eta * r[n] * omega) - 3 * psi^2 * rho^2 * a^2 * (r[c]-psi)^2 * k[c]^2 * b^2 * (r[w]-omega)^2 * k[w]^2 * (1 + varepsilon / (psi + phi))^2 / ((psi + varepsilon)^4 * r[c]^2 * omega^2 * r[w]^2) - 60 * psi^2 * rho^2 * a * (r[c]-psi) * k[c] * b * (r[w]-omega)^2 * k[w]^2 * (1 + varepsilon / (psi + phi)) * c * d * (r[n]-eta) * k[n] / ((psi + varepsilon)^3 * r[c] * omega^2 * r[w]^2 * eta * r[n])) + 24 * psi^2 * rho^2 * c^2 * (r[w]-omega)^2 * k[w]^2 * d^2 * (r[n]-eta)^2 * k[n]^2 / ((psi + varepsilon)^2 * r[w]^2 * eta^2 * r[n]^2 * omega^2))

$$\begin{aligned}
& \wedge^2 * \eta^2 * r[n]^2 * \omega^2) - 12 * a^3 * (r[c] - \psi)^3 * k[c]^3 * b^3 * (r[w] - \omega)^3 * k[w]^3 * (1 \\
& + \text{varepsilon}) / (\psi + \phi))^3 / (r[c]^3 * \omega^3 * r[w]^3 * (\psi + \text{varepsilon})^3) - 36 * a^2 * (r[c] - \psi)^2 \\
& * k[c]^2 * b^2 * (r[w] - \omega)^2 * k[w]^2 * (1 + \text{varepsilon}) / (\psi + \phi))^2 * c * d * (r[n] - \eta) * k[n] \\
& / (r[c]^2 * \omega^2 * r[w]^2 * (\psi + \text{varepsilon})^2 * \eta^2 * r[n]^2) - 36 * a * (r[c] - \psi) * k[c] * b * (r[w] \\
& - \omega)^2 * k[w]^2 * (1 + \text{varepsilon}) / (\psi + \phi)) * c^2 * d^2 * (r[n] - \eta)^2 * k[n]^2 / (r[c] * \omega^3 \\
& * r[w]^3 * (\psi + \text{varepsilon}) * \eta^2 * r[n]^2) - 12 * c^3 * (r[w] - \omega)^3 * k[w]^3 * d^3 * (r[n] - \eta)^3 \\
& * k[n]^3 / (r[w]^3 * \eta^3 * r[n]^3 * \omega^3)))^{(1/3)} + (1/3) * \psi * \rho / (\psi + \text{varepsilon}) + (1/2 \\
& * I) * \sqrt{3} * ((1/6) * (8 * \psi^3 * \rho^3 / (\psi + \text{varepsilon})^3 + 36 * b * (r[w] - \omega) * k[w] * (1 \\
& + \text{varepsilon}) / (\psi + \phi)) * \psi * \rho * a * (r[c] - \psi) * k[c] / (r[w] * (\psi + \text{varepsilon})^2 * r[c] * \omega) \\
& - 72 * d * (r[n] - \eta) * k[n] * c * (r[w] - \omega) * k[w] * \psi * \rho / (r[n] * \omega * r[w] * \eta * (\psi \\
& + \text{varepsilon})) + 12 * \sqrt{-12 * \psi^4 * \rho^4 * c * (r[w] - \omega) * k[w] * d * (r[n] - \eta) * k[n] / ((\psi \\
& + \text{varepsilon})^4 * r[w] * \eta * r[n] * \omega) - 3 * \psi^2 * \rho^2 * a^2 * (r[c] - \psi)^2 * k[c]^2 * b^2 * (r[w] \\
& - \omega)^2 * k[w]^2 * (1 + \text{varepsilon}) / (\psi + \phi))^2 / ((\psi + \text{varepsilon})^4 * r[c]^2 * \omega^2 * r[w] \\
& ^2) - 60 * \psi^2 * \rho^2 * a * (r[c] - \psi) * k[c] * b * (r[w] - \omega)^2 * k[w]^2 * (1 + \text{varepsilon}) / (\psi \\
& + \phi)) * c * d * (r[n] - \eta) * k[n] / ((\psi + \text{varepsilon})^3 * r[c] * \omega^2 * r[w]^2 * \eta^2 * r[n]^2) + 24 * \psi \\
& ^2 * \rho^2 * c^2 * (r[w] - \omega)^2 * k[w]^2 * d^2 * (r[n] - \eta)^2 * k[n]^2 / ((\psi + \text{varepsilon})^2 * r[w] \\
& ^2 * \eta^2 * r[n]^2 * \omega^2) - 12 * a^3 * (r[c] - \psi)^3 * k[c]^3 * b^3 * (r[w] - \omega)^3 * k[w]^3 * (1 \\
& + \text{varepsilon}) / (\psi + \phi))^3 / (r[c]^3 * \omega^3 * r[w]^3 * (\psi + \text{varepsilon})^3) - 36 * a^2 * (r[c] - \psi)^2 \\
& * k[c]^2 * b^2 * (r[w] - \omega)^2 * k[w]^2 * (1 + \text{varepsilon}) / (\psi + \phi))^2 * c * d * (r[n] - \eta) * k[n] \\
& / (r[c]^2 * \omega^2 * r[w]^2 * (\psi + \text{varepsilon})^2 * \eta^2 * r[n]^2) - 36 * a * (r[c] - \psi) * k[c] * b * (r[w] \\
& - \omega)^2 * k[w]^2 * (1 + \text{varepsilon}) / (\psi + \phi)) * c^2 * d^2 * (r[n] - \eta)^2 * k[n]^2 / (r[c] * \omega^3 \\
& * r[w]^3 * (\psi + \text{varepsilon}) * \eta^2 * r[n]^2) - 12 * c^3 * (r[w] - \omega)^3 * k[w]^3 * d^3 * (r[n] - \eta)^3 \\
& * k[n]^3 / (r[w]^3 * \eta^3 * r[n]^3 * \omega^3)))^{(1/3)} + (6 * (-1/3) * a * (r[c] - \psi) * k[c] * b \\
& * (r[w] - \omega) * k[w] * (1 + \text{varepsilon}) / (\psi + \phi)) / (r[c] * \omega * r[w] * (\psi + \text{varepsilon})) - (1/3) \\
& * d * (r[n] - \eta) * k[n] * c * (r[w] - \omega) * k[w] / (r[n] * \omega * r[w] * \eta) - (1/9) * \psi^2 * \rho^2 / (\psi \\
& + \text{varepsilon})^2) / (8 * \psi^3 * \rho^3 / (\psi + \text{varepsilon})^3 + 36 * b * (r[w] - \omega) * k[w] * (1 \\
& + \text{varepsilon}) / (\psi + \phi)) * \psi * \rho * a * (r[c] - \psi) * k[c] / (r[w] * (\psi + \text{varepsilon})^2 * r[c] * \omega) \\
& - 72 * d * (r[n] - \eta) * k[n] * c * (r[w] - \omega) * k[w] * \psi * \rho / (r[n] * \omega * r[w] * \eta * (\psi \\
& + \text{varepsilon})) + 12 * \sqrt{-12 * \psi^4 * \rho^4 * c * (r[w] - \omega) * k[w] * d * (r[n] - \eta) * k[n] / ((\psi \\
& + \text{varepsilon})^4 * r[w] * \eta * r[n] * \omega) - 3 * \psi^2 * \rho^2 * a^2 * (r[c] - \psi)^2 * k[c]^2 * b^2 * (r[w] \\
& - \omega)^2 * k[w]^2 * (1 + \text{varepsilon}) / (\psi + \phi))^2 / ((\psi + \text{varepsilon})^4 * r[c]^2 * \omega^2 * r[w] \\
& ^2) - 60 * \psi^2 * \rho^2 * a * (r[c] - \psi) * k[c] * b * (r[w] - \omega)^2 * k[w]^2 * (1 + \text{varepsilon}) / (\psi \\
& + \phi)) * c * d * (r[n] - \eta) * k[n] / ((\psi + \text{varepsilon})^3 * r[c] * \omega^2 * r[w]^2 * \eta^2 * r[n]^2) + 24 * \psi \\
& ^2 * \rho^2 * c^2 * (r[w] - \omega)^2 * k[w]^2 * d^2 * (r[n] - \eta)^2 * k[n]^2 / ((\psi + \text{varepsilon})^2 * r[w] \\
& ^2 * \eta^2 * r[n]^2 * \omega^2) - 12 * a^3 * (r[c] - \psi)^3 * k[c]^3 * b^3 * (r[w] - \omega)^3 * k[w]^3 * (1 \\
& + \text{varepsilon}) / (\psi + \phi))^3 / (r[c]^3 * \omega^3 * r[w]^3 * (\psi + \text{varepsilon})^3) - 36 * a^2 * (r[c] - \psi)^2 \\
& * k[c]^2 * b^2 * (r[w] - \omega)^2 * k[w]^2 * (1 + \text{varepsilon}) / (\psi + \phi))^2 * c * d * (r[n] - \eta) * k[n] \\
& / (r[c]^2 * \omega^2 * r[w]^2 * (\psi + \text{varepsilon})^2 * \eta^2 * r[n]^2) - 36 * a * (r[c] - \psi) * k[c] * b * (r[w] \\
& - \omega)^2 * k[w]^2 * (1 + \text{varepsilon}) / (\psi + \phi)) * c^2 * d^2 * (r[n] - \eta)^2 * k[n]^2 / (r[c] * \omega^3 \\
& * r[w]^3 * (\psi + \text{varepsilon}) * \eta^2 * r[n]^2) - 12 * c^3 * (r[w] - \omega)^3 * k[w]^3 * d^3 * (r[n] - \eta)^3 \\
& * k[n]^3 / (r[w]^3 * \eta^3 * r[n]^3 * \omega^3)))^{(1/3)})
\end{aligned}$$

$$\begin{aligned}
R := & -\frac{1}{12} \left[\frac{8 \psi^3 \rho^3}{(\psi + \varepsilon)^3} + \frac{36 b (r_w - \omega) k_w \left(1 + \frac{\varepsilon}{\psi + \phi} \right) \psi \rho a (r_c - \psi) k_c}{r_w (\psi + \varepsilon)^2 r_c \omega} \right. \\
& - \frac{72 d (r_n - \eta) k_n c (r_w - \omega) k_w \psi \rho}{r_n \omega r_w \eta (\psi + \varepsilon)} \\
& + 12 \left[-\frac{12 \psi^4 \rho^4 c (r_w - \omega) k_w d (r_n - \eta) k_n}{(\psi + \varepsilon)^4 r_w \eta r_n \omega} \right. \\
& \left. \left. - \frac{3 \psi^2 \rho^2 a^2 (r_c - \psi)^2 k_c^2 b^2 (r_w - \omega)^2 k_w^2 \left(1 + \frac{\varepsilon}{\psi + \phi} \right)^2}{(\psi + \varepsilon)^4 r_c^2 \omega^2 r_w^2} \right] \right] \quad (5)
\end{aligned}$$

$$\begin{aligned}
& - \frac{60 \psi^2 \rho^2 a (r_c - \psi) k_c b (r_w - \omega)^2 k_w^2 \left(1 + \frac{\varepsilon}{\psi + \phi}\right) c d (r_n - \eta) k_n}{(\psi + \varepsilon)^3 r_c \omega^2 r_w^2 \eta r_n} \\
& + \frac{24 \psi^2 \rho^2 c^2 (r_w - \omega)^2 k_w^2 d^2 (r_n - \eta)^2 k_n^2}{(\psi + \varepsilon)^2 r_w^2 \eta^2 r_n^2 \omega^2} - \frac{12 a^3 (r_c - \psi)^3 k_c^3 b^3 (r_w - \omega)^3 k_w^3 \left(1 + \frac{\varepsilon}{\psi + \phi}\right)^3}{r_c^3 \omega^3 r_w^3 (\psi + \varepsilon)^3} \\
& - \frac{36 a^2 (r_c - \psi)^2 k_c^2 b^2 (r_w - \omega)^3 k_w^3 \left(1 + \frac{\varepsilon}{\psi + \phi}\right)^2 c d (r_n - \eta) k_n}{r_c^2 \omega^3 r_w^3 (\psi + \varepsilon)^2 \eta r_n} \\
& - \frac{36 a (r_c - \psi) k_c b (r_w - \omega)^3 k_w^3 \left(1 + \frac{\varepsilon}{\psi + \phi}\right) c^2 d^2 (r_n - \eta)^2 k_n^2}{r_c \omega^3 r_w^3 (\psi + \varepsilon) \eta^2 r_n^2} \\
& - \frac{12 c^3 (r_w - \omega)^3 k_w^3 d^3 (r_n - \eta)^3 k_n^3}{r_w^3 \eta^3 r_n^3 \omega^3} \Bigg)^{1/2} \Bigg)^{1/3} + \left(3 \left(\right. \right. \\
& \left. \left. - \frac{1}{3} \frac{a (r_c - \psi) k_c b (r_w - \omega) k_w \left(1 + \frac{\varepsilon}{\psi + \phi}\right)}{r_c \omega r_w (\psi + \varepsilon)} - \frac{1}{3} \frac{d (r_n - \eta) k_n c (r_w - \omega) k_w}{r_n \omega r_w \eta} - \frac{1}{9} \frac{\psi^2 \rho^2}{(\psi + \varepsilon)^2} \right) \right) \\
& \Bigg/ \left(\frac{8 \psi^3 \rho^3}{(\psi + \varepsilon)^3} + \frac{36 b (r_w - \omega) k_w \left(1 + \frac{\varepsilon}{\psi + \phi}\right) \psi \rho a (r_c - \psi) k_c}{r_w (\psi + \varepsilon)^2 r_c \omega} \right. \\
& - \frac{72 d (r_n - \eta) k_n c (r_w - \omega) k_w \psi \rho}{r_n \omega r_w \eta (\psi + \varepsilon)} \\
& + 12 \left(- \frac{12 \psi^4 \rho^4 c (r_w - \omega) k_w d (r_n - \eta) k_n}{(\psi + \varepsilon)^4 r_w \eta r_n \omega} \right. \\
& - \frac{3 \psi^2 \rho^2 a^2 (r_c - \psi)^2 k_c^2 b^2 (r_w - \omega)^2 k_w^2 \left(1 + \frac{\varepsilon}{\psi + \phi}\right)^2}{(\psi + \varepsilon)^4 r_c^2 \omega^2 r_w^2} \\
& \left. \left. - \frac{60 \psi^2 \rho^2 a (r_c - \psi) k_c b (r_w - \omega)^2 k_w^2 \left(1 + \frac{\varepsilon}{\psi + \phi}\right) c d (r_n - \eta) k_n}{(\psi + \varepsilon)^3 r_c \omega^2 r_w^2 \eta r_n} \right) \right)
\end{aligned}$$

$$\begin{aligned}
& + \frac{24 \psi^2 \rho^2 c^2 (r_w - \omega)^2 k_w^2 d^2 (r_n - \eta)^2 k_n^2}{(\psi + \varepsilon)^2 r_w^2 \eta^2 r_n^2 \omega^2} - \frac{12 a^3 (r_c - \psi)^3 k_c^3 b^3 (r_w - \omega)^3 k_w^3 \left(1 + \frac{\varepsilon}{\psi + \phi}\right)^3}{r_c^3 \omega^3 r_w^3 (\psi + \varepsilon)^3} \\
& - \frac{36 a^2 (r_c - \psi)^2 k_c^2 b^2 (r_w - \omega)^3 k_w^3 \left(1 + \frac{\varepsilon}{\psi + \phi}\right)^2 c d (r_n - \eta) k_n}{r_c^2 \omega^3 r_w^3 (\psi + \varepsilon)^2 \eta r_n} \\
& - \frac{36 a (r_c - \psi) k_c b (r_w - \omega)^3 k_w^3 \left(1 + \frac{\varepsilon}{\psi + \phi}\right) c^2 d^2 (r_n - \eta)^2 k_n^2}{r_c \omega^3 r_w^3 (\psi + \varepsilon) \eta^2 r_n^2} \\
& - \frac{12 c^3 (r_w - \omega)^3 k_w^3 d^3 (r_n - \eta)^3 k_n^3}{r_w^3 \eta^3 r_n^3 \omega^3} \Bigg)^{1/2} \Bigg)^{1/3} + \frac{1}{3} \frac{\psi \rho}{\psi + \varepsilon} + \frac{1}{2} \text{I}\sqrt{3} \left[\frac{1}{6} \left(\frac{8 \psi^3 \rho^3}{(\psi + \varepsilon)^3} \right. \right. \\
& + \frac{36 b (r_w - \omega) k_w \left(1 + \frac{\varepsilon}{\psi + \phi}\right) \psi \rho a (r_c - \psi) k_c}{r_w (\psi + \varepsilon)^2 r_c \omega} - \frac{72 d (r_n - \eta) k_n c (r_w - \omega) k_w \psi \rho}{r_n \omega r_w \eta (\psi + \varepsilon)} \\
& + 12 \left(- \frac{12 \psi^4 \rho^4 c (r_w - \omega) k_w d (r_n - \eta) k_n}{(\psi + \varepsilon)^4 r_w \eta r_n \omega} \right. \\
& \left. - \frac{3 \psi^2 \rho^2 a^2 (r_c - \psi)^2 k_c^2 b^2 (r_w - \omega)^2 k_w^2 \left(1 + \frac{\varepsilon}{\psi + \phi}\right)^2}{(\psi + \varepsilon)^4 r_c^2 \omega^2 r_w^2} \right)
\end{aligned}$$

$$\begin{aligned}
& - \frac{60 \psi^2 \rho^2 a (r_c - \psi) k_c b (r_w - \omega)^2 k_w^2 \left(1 + \frac{\varepsilon}{\psi + \phi}\right) c d (r_n - \eta) k_n}{(\psi + \varepsilon)^3 r_c \omega^2 r_w^2 \eta r_n} \\
& + \frac{24 \psi^2 \rho^2 c^2 (r_w - \omega)^2 k_w^2 d^2 (r_n - \eta)^2 k_n^2}{(\psi + \varepsilon)^2 r_w^2 \eta^2 r_n^2 \omega^2} - \frac{12 a^3 (r_c - \psi)^3 k_c^3 b^3 (r_w - \omega)^3 k_w^3 \left(1 + \frac{\varepsilon}{\psi + \phi}\right)^3}{r_c^3 \omega^3 r_w^3 (\psi + \varepsilon)^3} \\
& - \frac{36 a^2 (r_c - \psi)^2 k_c^2 b^2 (r_w - \omega)^3 k_w^3 \left(1 + \frac{\varepsilon}{\psi + \phi}\right)^2 c d (r_n - \eta) k_n}{r_c^2 \omega^3 r_w^3 (\psi + \varepsilon)^2 \eta r_n} \\
& - \frac{36 a (r_c - \psi) k_c b (r_w - \omega)^3 k_w^3 \left(1 + \frac{\varepsilon}{\psi + \phi}\right) c^2 d^2 (r_n - \eta)^2 k_n^2}{r_c \omega^3 r_w^3 (\psi + \varepsilon) \eta^2 r_n^2} \\
& - \left(\frac{12 c^3 (r_w - \omega)^3 k_w^3 d^3 (r_n - \eta)^3 k_n^3}{r_w^3 \eta^3 r_n^3 \omega^3} \right)^{1/2} \Bigg)^{1/3} + \left(6 \left(\right. \right. \\
& - \frac{1}{3} \frac{a (r_c - \psi) k_c b (r_w - \omega) k_w \left(1 + \frac{\varepsilon}{\psi + \phi}\right)}{r_c \omega r_w (\psi + \varepsilon)} - \frac{1}{3} \frac{d (r_n - \eta) k_n c (r_w - \omega) k_w}{r_n \omega r_w \eta} - \frac{1}{9} \frac{\psi^2 \rho^2}{(\psi + \varepsilon)^2} \Bigg) \Bigg) \\
& \Bigg/ \left(\frac{8 \psi^3 \rho^3}{(\psi + \varepsilon)^3} + \frac{36 b (r_w - \omega) k_w \left(1 + \frac{\varepsilon}{\psi + \phi}\right) \psi \rho a (r_c - \psi) k_c}{r_w (\psi + \varepsilon)^2 r_c \omega} \right. \\
& - \frac{72 d (r_n - \eta) k_n c (r_w - \omega) k_w \psi \rho}{r_n \omega r_w \eta (\psi + \varepsilon)}
\end{aligned}$$

$$\begin{aligned}
& + 12 \left(- \frac{12 \psi^4 \rho^4 c (r_w - \omega) k_w d (r_n - \eta) k_n}{(\psi + \varepsilon)^4 r_w \eta r_n \omega} \right. \\
& - \frac{3 \psi^2 \rho^2 a^2 (r_c - \psi)^2 k_c^2 b^2 (r_w - \omega)^2 k_w^2 \left(1 + \frac{\varepsilon}{\psi + \phi} \right)^2}{(\psi + \varepsilon)^4 r_c^2 \omega^2 r_w^2} \\
& - \frac{60 \psi^2 \rho^2 a (r_c - \psi) k_c b (r_w - \omega)^2 k_w^2 \left(1 + \frac{\varepsilon}{\psi + \phi} \right) c d (r_n - \eta) k_n}{(\psi + \varepsilon)^3 r_c \omega^2 r_w^2 \eta r_n} \\
& + \frac{24 \psi^2 \rho^2 c^2 (r_w - \omega)^2 k_w^2 d^2 (r_n - \eta)^2 k_n^2}{(\psi + \varepsilon)^2 r_w^2 \eta^2 r_n^2 \omega^2} - \frac{12 a^3 (r_c - \psi)^3 k_c^3 b^3 (r_w - \omega)^3 k_w^3 \left(1 + \frac{\varepsilon}{\psi + \phi} \right)^3}{r_c^3 \omega^3 r_w^3 (\psi + \varepsilon)^3} \\
& - \frac{36 a^2 (r_c - \psi)^2 k_c^2 b^2 (r_w - \omega)^3 k_w^3 \left(1 + \frac{\varepsilon}{\psi + \phi} \right)^2 c d (r_n - \eta) k_n}{r_c^2 \omega^3 r_w^3 (\psi + \varepsilon)^2 \eta r_n} \\
& - \frac{36 a (r_c - \psi) k_c b (r_w - \omega)^3 k_w^3 \left(1 + \frac{\varepsilon}{\psi + \phi} \right) c^2 d^2 (r_n - \eta)^2 k_n^2}{r_c \omega^3 r_w^3 (\psi + \varepsilon) \eta^2 r_n^2} \\
& \left. - \frac{12 c^3 (r_w - \omega)^3 k_w^3 d^3 (r_n - \eta)^3 k_n^3}{r_w^3 \eta^3 r_n^3 \omega^3} \right) \left. \right)^{1/2} \left. \right)^{1/3}
\end{aligned}$$

> # Evaluating the value of the second eigenvalue basing on baseline values

> eval(R,params)

$$-1.892232117 + 1.10^{-10}I + (-1.094618498 - 5.0000000000 \cdot 10^{-10}I) \sqrt{3} \quad (6)$$

> abs((6))

$$\sqrt{(-1.892232117 - 1.094618498\sqrt{3})^2 + (1.10^{-10} - 5.0000000000 \cdot 10^{-10}\sqrt{3})^2} \quad (7)$$

> simplify((7))

$$3.788166971 \quad (8)$$

> # The third eigenvalue function

> R := -(1/12) * (8 * psi^3 * rho^3 / (psi + varepsilon)^3 + 36 * b * (r[w]-omega) * k[w] * (1 + varepsilon / (psi + phi)) * psi * rho * a * (r[c]-psi) * k[c] / (r[w] * (psi + varepsilon)^2 * r[c] * omega) - 72 * d * (r[n]-eta) * k[n] * c * (r[w]-omega) * k[w] * psi * rho / (r[n] * omega * r[w] * eta * (psi + varepsilon))) + 12 * sqrt(-12 * psi^4 * rho^4 * c * (r[w]-omega) * k[w] * d * (r[n]-eta) * k[n] / ((psi + varepsilon)^4 * r[w] * eta * r[n] * omega) - 3 * psi^2 * rho^2 * a^2 * (r[c]-psi)^2 * k[c]^2 * b^2 * (r[w]-omega)^2 * k[w]^2 * (1 + varepsilon / (psi + phi))^2 / ((psi + varepsilon)^4 * r[c]^2 * omega^2 * r[w]^2) - 60 * psi^2 * rho^2 * a * (r[c]-psi) * k[c] * b * (r[w]-omega)^2 * k[w]^2 * (1 + varepsilon / (psi + phi)) * c * d * (r[n]-eta) * k[n] / ((psi + varepsilon)^3 * r[c] * omega^2 * r[w]^2 * eta * r[n]) + 24 * psi^2 * rho^2 * c^2 * (r[w]-omega)^2 * k[w]^2 * d^2 * (r[n]-eta)^2 * k[n]^2 / ((psi + varepsilon)^2 * r[w]^2 * eta^2 * r[n]^2 * omega^2) - 12 * a^3 * (r[c]-psi)^3 * k[c]^3 * b^3 * (r[w]-omega)^3 * k[w]^3 * (1 + varepsilon / (psi + phi))^3 / (r[c]^3 * omega^3 * r[w]^3 * (psi + varepsilon)^3) - 36 * a^2 * (r[c]-psi)^2 * k[c]^2 * b^2 * (r[w]-omega)^2 * k[w]^2 * (1 + varepsilon / (psi + phi))^2 * c * d * (r[n]-eta) * k[n] / (r[c]^2 * omega^2 * r[w]^2 * (psi + varepsilon)^2 * eta * r[n]) - 36 * a * (r[c]-psi) * k[c] * b * (r[w]-omega)^3 * k[w]^3

$$\begin{aligned}
& - \frac{72 d (r_n - \eta) k_n c (r_w - \omega) k_w \psi \rho}{r_n \omega r_w \eta (\psi + \varepsilon)} \\
& + 12 \left(- \frac{12 \psi^4 \rho^4 c (r_w - \omega) k_w d (r_n - \eta) k_n}{(\psi + \varepsilon)^4 r_w \eta r_n \omega} \right. \\
& - \frac{3 \psi^2 \rho^2 a^2 (r_c - \psi)^2 k_c^2 b^2 (r_w - \omega)^2 k_w^2 \left(1 + \frac{\varepsilon}{\psi + \phi} \right)^2}{(\psi + \varepsilon)^4 r_c^2 \omega^2 r_w^2} \\
& - \frac{60 \psi^2 \rho^2 a (r_c - \psi) k_c b (r_w - \omega)^2 k_w^2 \left(1 + \frac{\varepsilon}{\psi + \phi} \right) c d (r_n - \eta) k_n}{(\psi + \varepsilon)^3 r_c \omega^2 r_w^2 \eta r_n} \\
& + \frac{24 \psi^2 \rho^2 c^2 (r_w - \omega)^2 k_w^2 d^2 (r_n - \eta)^2 k_n^2}{(\psi + \varepsilon)^2 r_w^2 \eta^2 r_n^2 \omega^2} - \frac{12 a^3 (r_c - \psi)^3 k_c^3 b^3 (r_w - \omega)^3 k_w^3 \left(1 + \frac{\varepsilon}{\psi + \phi} \right)^3}{r_c^3 \omega^3 r_w^3 (\psi + \varepsilon)^3} \\
& - \frac{36 a^2 (r_c - \psi)^2 k_c^2 b^2 (r_w - \omega)^3 k_w^3 \left(1 + \frac{\varepsilon}{\psi + \phi} \right)^2 c d (r_n - \eta) k_n}{r_c^2 \omega^3 r_w^3 (\psi + \varepsilon)^2 \eta r_n} \\
& - \frac{36 a (r_c - \psi) k_c b (r_w - \omega)^3 k_w^3 \left(1 + \frac{\varepsilon}{\psi + \phi} \right) c^2 d^2 (r_n - \eta)^2 k_n^2}{r_c \omega^3 r_w^3 (\psi + \varepsilon) \eta^2 r_n^2} \\
& - \frac{12 c^3 (r_w - \omega)^3 k_w^3 d^3 (r_n - \eta)^3 k_n^3}{r_w^3 \eta^3 r_n^3 \omega^3} \Bigg)^{1/2} \Bigg)^{1/3} + \left(3 \left(\right. \right. \\
& - \frac{1}{3} \frac{a (r_c - \psi) k_c b (r_w - \omega) k_w \left(1 + \frac{\varepsilon}{\psi + \phi} \right)}{r_c \omega r_w (\psi + \varepsilon)} - \frac{1}{3} \frac{d (r_n - \eta) k_n c (r_w - \omega) k_w}{r_n \omega r_w \eta} - \frac{1}{9} \frac{\psi^2 \rho^2}{(\psi + \varepsilon)^2} \Bigg) \Bigg) \\
& \Bigg/ \left(\frac{8 \psi^3 \rho^3}{(\psi + \varepsilon)^3} + \frac{36 b (r_w - \omega) k_w \left(1 + \frac{\varepsilon}{\psi + \phi} \right) \psi \rho a (r_c - \psi) k_c}{r_w (\psi + \varepsilon)^2 r_c \omega} \right) \\
& - \frac{72 d (r_n - \eta) k_n c (r_w - \omega) k_w \psi \rho}{r_n \omega r_w \eta (\psi + \varepsilon)}
\end{aligned}$$

$$\begin{aligned}
& + 12 \left(- \frac{12 \psi^4 \rho^4 c (r_w - \omega) k_w d (r_n - \eta) k_n}{(\psi + \varepsilon)^4 r_w \eta r_n \omega} \right. \\
& - \frac{3 \psi^2 \rho^2 a^2 (r_c - \psi)^2 k_c^2 b^2 (r_w - \omega)^2 k_w^2 \left(1 + \frac{\varepsilon}{\psi + \phi} \right)^2}{(\psi + \varepsilon)^4 r_c^2 \omega^2 r_w^2} \\
& - \frac{60 \psi^2 \rho^2 a (r_c - \psi) k_c b (r_w - \omega)^2 k_w^2 \left(1 + \frac{\varepsilon}{\psi + \phi} \right) c d (r_n - \eta) k_n}{(\psi + \varepsilon)^3 r_c \omega^2 r_w^2 \eta r_n} \\
& + \frac{24 \psi^2 \rho^2 c^2 (r_w - \omega)^2 k_w^2 d^2 (r_n - \eta)^2 k_n^2}{(\psi + \varepsilon)^2 r_w^2 \eta^2 r_n^2 \omega^2} - \frac{12 a^3 (r_c - \psi)^3 k_c^3 b^3 (r_w - \omega)^3 k_w^3 \left(1 + \frac{\varepsilon}{\psi + \phi} \right)^3}{r_c^3 \omega^3 r_w^3 (\psi + \varepsilon)^3} \\
& - \frac{36 a^2 (r_c - \psi)^2 k_c^2 b^2 (r_w - \omega)^3 k_w^3 \left(1 + \frac{\varepsilon}{\psi + \phi} \right)^2 c d (r_n - \eta) k_n}{r_c^2 \omega^3 r_w^3 (\psi + \varepsilon)^2 \eta r_n} \\
& - \frac{36 a (r_c - \psi) k_c b (r_w - \omega)^3 k_w^3 \left(1 + \frac{\varepsilon}{\psi + \phi} \right) c^2 d^2 (r_n - \eta)^2 k_n^2}{r_c \omega^3 r_w^3 (\psi + \varepsilon) \eta^2 r_n^2} \\
& - \left. \frac{12 c^3 (r_w - \omega)^3 k_w^3 d^3 (r_n - \eta)^3 k_n^3}{r_w^3 \eta^3 r_n^3 \omega^3} \right)^{1/2} \Bigg)^{1/3} + \frac{1}{3} \frac{\psi \rho}{\psi + \varepsilon} - \frac{1}{2} \text{I}\sqrt{3} \left[\frac{1}{6} \left(\frac{8 \psi^3 \rho^3}{(\psi + \varepsilon)^3} \right. \right. \\
& + \frac{36 b (r_w - \omega) k_w \left(1 + \frac{\varepsilon}{\psi + \phi} \right) \psi \rho a (r_c - \psi) k_c}{r_w (\psi + \varepsilon)^2 r_c \omega} - \frac{72 d (r_n - \eta) k_n c (r_w - \omega) k_w \psi \rho}{r_n \omega r_w \eta (\psi + \varepsilon)} \\
& \left. \left. + 12 \left(- \frac{12 \psi^4 \rho^4 c (r_w - \omega) k_w d (r_n - \eta) k_n}{(\psi + \varepsilon)^4 r_w \eta r_n \omega} \right. \right. \right.
\end{aligned}$$

$$\begin{aligned}
& - \frac{3 \psi^2 \rho^2 a^2 (r_c - \psi)^2 k_c^2 b^2 (r_w - \omega)^2 k_w^2 \left(1 + \frac{\varepsilon}{\psi + \phi}\right)^2}{(\psi + \varepsilon)^4 r_c^2 \omega^2 r_w^2} \\
& - \frac{60 \psi^2 \rho^2 a (r_c - \psi) k_c b (r_w - \omega)^2 k_w^2 \left(1 + \frac{\varepsilon}{\psi + \phi}\right) c d (r_n - \eta) k_n}{(\psi + \varepsilon)^3 r_c \omega^2 r_w^2 \eta r_n} \\
& + \frac{24 \psi^2 \rho^2 c^2 (r_w - \omega)^2 k_w^2 d^2 (r_n - \eta)^2 k_n^2}{(\psi + \varepsilon)^2 r_w^2 \eta^2 r_n^2 \omega^2} - \frac{12 a^3 (r_c - \psi)^3 k_c^3 b^3 (r_w - \omega)^3 k_w^3 \left(1 + \frac{\varepsilon}{\psi + \phi}\right)^3}{r_c^3 \omega^3 r_w^3 (\psi + \varepsilon)^3} \\
& - \frac{36 a^2 (r_c - \psi)^2 k_c^2 b^2 (r_w - \omega)^3 k_w^3 \left(1 + \frac{\varepsilon}{\psi + \phi}\right)^2 c d (r_n - \eta) k_n}{r_c^2 \omega^3 r_w^3 (\psi + \varepsilon)^2 \eta r_n} \\
& - \frac{36 a (r_c - \psi) k_c b (r_w - \omega)^3 k_w^3 \left(1 + \frac{\varepsilon}{\psi + \phi}\right) c^2 d^2 (r_n - \eta)^2 k_n^2}{r_c \omega^3 r_w^3 (\psi + \varepsilon) \eta^2 r_n^2} \\
& - \frac{12 c^3 (r_w - \omega)^3 k_w^3 d^3 (r_n - \eta)^3 k_n^3}{r_w^3 \eta^3 r_n^3 \omega^3} \Bigg)^{1/2} \Bigg)^{1/3} + \left(6 \left(\right. \right. \\
& \left. \left. - \frac{1}{3} \frac{a (r_c - \psi) k_c b (r_w - \omega) k_w \left(1 + \frac{\varepsilon}{\psi + \phi}\right)}{r_c \omega r_w (\psi + \varepsilon)} - \frac{1}{3} \frac{d (r_n - \eta) k_n c (r_w - \omega) k_w}{r_n \omega r_w \eta} - \frac{1}{9} \frac{\psi^2 \rho^2}{(\psi + \varepsilon)^2} \right) \right)
\end{aligned}$$

$$\begin{aligned}
& \left(\frac{8 \psi^3 \rho^3}{(\psi + \varepsilon)^3} + \frac{36 b (r_w - \omega) k_w \left(1 + \frac{\varepsilon}{\psi + \phi} \right) \psi \rho a (r_c - \psi) k_c}{r_w (\psi + \varepsilon)^2 r_c \omega} \right. \\
& - \frac{72 d (r_n - \eta) k_n c (r_w - \omega) k_w \psi \rho}{r_n \omega r_w \eta (\psi + \varepsilon)} \\
& + 12 \left(- \frac{12 \psi^4 \rho^4 c (r_w - \omega) k_w d (r_n - \eta) k_n}{(\psi + \varepsilon)^4 r_w \eta r_n \omega} \right. \\
& - \frac{3 \psi^2 \rho^2 a^2 (r_c - \psi)^2 k_c^2 b^2 (r_w - \omega)^2 k_w^2 \left(1 + \frac{\varepsilon}{\psi + \phi} \right)^2}{(\psi + \varepsilon)^4 r_c^2 \omega^2 r_w^2} \\
& - \frac{60 \psi^2 \rho^2 a (r_c - \psi) k_c b (r_w - \omega)^2 k_w^2 \left(1 + \frac{\varepsilon}{\psi + \phi} \right) c d (r_n - \eta) k_n}{(\psi + \varepsilon)^3 r_c \omega^2 r_w^2 \eta r_n} \\
& + \frac{24 \psi^2 \rho^2 c^2 (r_w - \omega)^2 k_w^2 d^2 (r_n - \eta)^2 k_n^2}{(\psi + \varepsilon)^2 r_w^2 \eta^2 r_n^2 \omega^2} - \frac{12 a^3 (r_c - \psi)^3 k_c^3 b^3 (r_w - \omega)^3 k_w^3 \left(1 + \frac{\varepsilon}{\psi + \phi} \right)^3}{r_c^3 \omega^3 r_w^3 (\psi + \varepsilon)^3} \\
& - \frac{36 a^2 (r_c - \psi)^2 k_c^2 b^2 (r_w - \omega)^3 k_w^3 \left(1 + \frac{\varepsilon}{\psi + \phi} \right)^2 c d (r_n - \eta) k_n}{r_c^2 \omega^3 r_w^3 (\psi + \varepsilon)^2 \eta r_n} \\
& - \frac{36 a (r_c - \psi) k_c b (r_w - \omega)^3 k_w^3 \left(1 + \frac{\varepsilon}{\psi + \phi} \right) c^2 d^2 (r_n - \eta)^2 k_n^2}{r_c \omega^3 r_w^3 (\psi + \varepsilon) \eta^2 r_n^2} \\
& \left. - \frac{12 c^3 (r_w - \omega)^3 k_w^3 d^3 (r_n - \eta)^3 k_n^3}{r_w^3 \eta^3 r_n^3 \omega^3} \right)^{1/2} \Bigg)^{1/3} \Bigg)
\end{aligned}$$

> # Evaluating value of the third eigenvalue function basing on baseline values

> eval(R, params)

$$-1.892232117 + 1.10^{-10}I + (1.094618498 + 5.000000000 \cdot 10^{-10}I) \sqrt{3}$$

(10)

> abs((10))

$$\sqrt{(-1.892232117 + 1.094618498\sqrt{3})^2 + (1.10^{-10} + 5.000000000 \cdot 10^{-10}\sqrt{3})^2}$$

(11)

> simplify((11))

$$0.003702431633$$

(12)

> # Therefore, the first function is the spectral radiusreproduction number of the system

> # Computing the sensitivity indices for the reproduction number.

> # defining the reproduction number

$$\begin{aligned}
> R := & (1/6) * (8 * \text{psi}^3 * \text{rho}^3 / (\text{psi} + \text{varepsilon})^3 + 36 * b * (r[w] - \text{omega}) * k[w] * (1 + \text{varepsilon} / (\text{psi} \\
& + \text{phi})) * \text{psi} * \text{rho} * a * (r[c] - \text{psi}) * k[c] / (r[w] * (\text{psi} + \text{varepsilon})^2 * r[c] * \text{omega}) - 72 * d * (r[n] - \text{eta}) \\
& * k[n] * c * (r[w] - \text{omega}) * k[w] * \text{psi} * \text{rho} / (r[n] * \text{omega} * r[w] * \text{eta} * (\text{psi} + \text{varepsilon})) + 12 * \text{sqrt}(-12 \\
& * \text{psi}^4 * \text{rho}^4 * c * (r[w] - \text{omega}) * k[w] * d * (r[n] - \text{eta}) * k[n] / ((\text{psi} + \text{varepsilon})^4 * r[w] * \text{eta} * r[n] \\
& * \text{omega}) - 3 * \text{psi}^2 * \text{rho}^2 * a^2 * (r[c] - \text{psi})^2 * k[c]^2 * b^2 * (r[w] - \text{omega})^2 * k[w]^2 * (1 \\
& + \text{varepsilon} / (\text{psi} + \text{phi}))^2 / ((\text{psi} + \text{varepsilon})^4 * r[c]^2 * \text{omega}^2 * r[w]^2) - 60 * \text{psi}^2 * \text{rho}^2 * a \\
& * (r[c] - \text{psi}) * k[c] * b * (r[w] - \text{omega})^2 * k[w]^2 * (1 + \text{varepsilon} / (\text{psi} + \text{phi})) * c * d * (r[n] - \text{eta}) \\
& * k[n] / ((\text{psi} + \text{varepsilon})^3 * r[c] * \text{omega}^2 * r[w]^2 * \text{eta} * r[n]) + 24 * \text{psi}^2 * \text{rho}^2 * c^2 * (r[w] \\
& - \text{omega})^2 * k[w]^2 * d^2 * (r[n] - \text{eta})^2 * k[n]^2 / ((\text{psi} + \text{varepsilon})^2 * r[w]^2 * \text{eta}^2 * r[n]^2 \\
& * \text{omega}^2) - 12 * a^3 * (r[c] - \text{psi})^3 * k[c]^3 * b^3 * (r[w] - \text{omega})^3 * k[w]^3 * (1 + \text{varepsilon} / (\text{psi} \\
& + \text{phi}))^3 / (r[c]^3 * \text{omega}^3 * r[w]^3 * (\text{psi} + \text{varepsilon})^3) - 36 * a^2 * (r[c] - \text{psi})^2 * k[c]^2 * b^2 \\
& * (r[w] - \text{omega})^3 * k[w]^3 * (1 + \text{varepsilon} / (\text{psi} + \text{phi}))^2 * c * d * (r[n] - \text{eta}) * k[n] / (r[c]^2 * \text{omega} \\
& ^3 * r[w]^3 * (\text{psi} + \text{varepsilon})^2 * \text{eta} * r[n]) - 36 * a * (r[c] - \text{psi}) * k[c] * b * (r[w] - \text{omega})^3 * k[w]^3 \\
& * (1 + \text{varepsilon} / (\text{psi} + \text{phi})) * c^2 * d^2 * (r[n] - \text{eta})^2 * k[n]^2 / (r[c] * \text{omega}^3 * r[w]^3 * (\text{psi} \\
& + \text{varepsilon}) * \text{eta}^2 * r[n]^2) - 12 * c^3 * (r[w] - \text{omega})^3 * k[w]^3 * d^3 * (r[n] - \text{eta})^3 * k[n]^3 \\
& / (r[w]^3 * \text{eta}^3 * r[n]^3 * \text{omega}^3)) ^ (1/3) - (6 * (-1/3) * a * (r[c] - \text{psi}) * k[c] * b * (r[w] - \text{omega}) \\
& * k[w] * (1 + \text{varepsilon} / (\text{psi} + \text{phi})) / (r[c] * \text{omega} * r[w] * (\text{psi} + \text{varepsilon})) - (1/3) * d * (r[n] - \text{eta}) \\
& * k[n] * c * (r[w] - \text{omega}) * k[w] / (r[n] * \text{omega} * r[w] * \text{eta}) - (1/9) * \text{psi}^2 * \text{rho}^2 / (\text{psi} + \text{varepsilon}) \\
& ^2) / (8 * \text{psi}^3 * \text{rho}^3 / (\text{psi} + \text{varepsilon})^3 + 36 * b * (r[w] - \text{omega}) * k[w] * (1 + \text{varepsilon} / (\text{psi} \\
& + \text{phi})) * \text{psi} * \text{rho} * a * (r[c] - \text{psi}) * k[c] / (r[w] * (\text{psi} + \text{varepsilon})^2 * r[c] * \text{omega}) - 72 * d * (r[n] - \text{eta}) \\
& * k[n] * c * (r[w] - \text{omega}) * k[w] * \text{psi} * \text{rho} / (r[n] * \text{omega} * r[w] * \text{eta} * (\text{psi} + \text{varepsilon})) + 12 * \text{sqrt}(-12 \\
& * \text{psi}^4 * \text{rho}^4 * c * (r[w] - \text{omega}) * k[w] * d * (r[n] - \text{eta}) * k[n] / ((\text{psi} + \text{varepsilon})^4 * r[w] * \text{eta} * r[n] \\
& * \text{omega}) - 3 * \text{psi}^2 * \text{rho}^2 * a^2 * (r[c] - \text{psi})^2 * k[c]^2 * b^2 * (r[w] - \text{omega})^2 * k[w]^2 * (1 \\
& + \text{varepsilon} / (\text{psi} + \text{phi}))^2 / ((\text{psi} + \text{varepsilon})^4 * r[c]^2 * \text{omega}^2 * r[w]^2) - 60 * \text{psi}^2 * \text{rho}^2 * a \\
& * (r[c] - \text{psi}) * k[c] * b * (r[w] - \text{omega})^2 * k[w]^2 * (1 + \text{varepsilon} / (\text{psi} + \text{phi})) * c * d * (r[n] - \text{eta}) \\
& * k[n] / ((\text{psi} + \text{varepsilon})^3 * r[c] * \text{omega}^2 * r[w]^2 * \text{eta} * r[n]) + 24 * \text{psi}^2 * \text{rho}^2 * c^2 * (r[w] \\
& - \text{omega})^2 * k[w]^2 * d^2 * (r[n] - \text{eta})^2 * k[n]^2 / ((\text{psi} + \text{varepsilon})^2 * r[w]^2 * \text{eta}^2 * r[n]^2 \\
& * \text{omega}^2) - 12 * a^3 * (r[c] - \text{psi})^3 * k[c]^3 * b^3 * (r[w] - \text{omega})^3 * k[w]^3 * (1 + \text{varepsilon} / (\text{psi} \\
& + \text{phi}))^3 / (r[c]^3 * \text{omega}^3 * r[w]^3 * (\text{psi} + \text{varepsilon})^3) - 36 * a^2 * (r[c] - \text{psi})^2 * k[c]^2 * b^2 \\
& * (r[w] - \text{omega})^3 * k[w]^3 * (1 + \text{varepsilon} / (\text{psi} + \text{phi}))^2 * c * d * (r[n] - \text{eta}) * k[n] / (r[c]^2 * \text{omega} \\
& ^3 * r[w]^3 * (\text{psi} + \text{varepsilon})^2 * \text{eta} * r[n]) - 36 * a * (r[c] - \text{psi}) * k[c] * b * (r[w] - \text{omega})^3 * k[w]^3 \\
& * (1 + \text{varepsilon} / (\text{psi} + \text{phi})) * c^2 * d^2 * (r[n] - \text{eta})^2 * k[n]^2 / (r[c] * \text{omega}^3 * r[w]^3 * (\text{psi} \\
& + \text{varepsilon}) * \text{eta}^2 * r[n]^2) - 12 * c^3 * (r[w] - \text{omega})^3 * k[w]^3 * d^3 * (r[n] - \text{eta})^3 * k[n]^3 \\
& / (r[w]^3 * \text{eta}^3 * r[n]^3 * \text{omega}^3)) ^ (1/3) + (1/3) * \text{psi} * \text{rho} / (\text{psi} + \text{varepsilon});
\end{aligned}$$

$$\begin{aligned}
R := & \frac{1}{6} \left(\frac{8 \psi^3 \rho^3}{(\psi + \varepsilon)^3} + \frac{36 b (r_w - \omega) k_w \left(1 + \frac{\varepsilon}{\psi + \phi} \right) \psi \rho a (r_c - \psi) k_c}{r_w (\psi + \varepsilon)^2 r_c \omega} \right. \\
& - \frac{72 d (r_n - \eta) k_n c (r_w - \omega) k_w \psi \rho}{r_n \omega r_w \eta (\psi + \varepsilon)} \\
& + 12 \left(- \frac{12 \psi^4 \rho^4 c (r_w - \omega) k_w d (r_n - \eta) k_n}{(\psi + \varepsilon)^4 r_w \eta r_n \omega} \right. \\
& - \frac{3 \psi^2 \rho^2 a^2 (r_c - \psi)^2 k_c^2 b^2 (r_w - \omega)^2 k_w^2 \left(1 + \frac{\varepsilon}{\psi + \phi} \right)^2}{(\psi + \varepsilon)^4 r_c^2 \omega^2 r_w^2} \\
& \left. \left. - \frac{60 \psi^2 \rho^2 a (r_c - \psi) k_c b (r_w - \omega)^2 k_w^2 \left(1 + \frac{\varepsilon}{\psi + \phi} \right) c d (r_n - \eta) k_n}{(\psi + \varepsilon)^3 r_c \omega^2 r_w^2 \eta r_n} \right) \right.
\end{aligned} \tag{13}$$

$$\begin{aligned}
& + \frac{24 \psi^2 \rho^2 c^2 (r_w - \omega)^2 k_w^2 d^2 (r_n - \eta)^2 k_n^2}{(\psi + \varepsilon)^2 r_w^2 \eta^2 r_n^2 \omega^2} - \frac{12 a^3 (r_c - \psi)^3 k_c^3 b^3 (r_w - \omega)^3 k_w^3 \left(1 + \frac{\varepsilon}{\psi + \phi}\right)^3}{r_c^3 \omega^3 r_w^3 (\psi + \varepsilon)^3} \\
& - \frac{36 a^2 (r_c - \psi)^2 k_c^2 b^2 (r_w - \omega)^3 k_w^3 \left(1 + \frac{\varepsilon}{\psi + \phi}\right)^2 c d (r_n - \eta) k_n}{r_c^2 \omega^3 r_w^3 (\psi + \varepsilon)^2 \eta r_n} \\
& - \frac{36 a (r_c - \psi) k_c b (r_w - \omega)^3 k_w^3 \left(1 + \frac{\varepsilon}{\psi + \phi}\right) c^2 d^2 (r_n - \eta)^2 k_n^2}{r_c \omega^3 r_w^3 (\psi + \varepsilon) \eta^2 r_n^2} \\
& - \frac{12 c^3 (r_w - \omega)^3 k_w^3 d^3 (r_n - \eta)^3 k_n^3}{r_w^3 \eta^3 r_n^3 \omega^3} \Bigg)^{1/2} \Bigg)^{1/3} - \left(6 \left(\right. \right. \\
& - \frac{1}{3} \frac{a (r_c - \psi) k_c b (r_w - \omega) k_w \left(1 + \frac{\varepsilon}{\psi + \phi}\right)}{r_c \omega r_w (\psi + \varepsilon)} - \frac{1}{3} \frac{d (r_n - \eta) k_n c (r_w - \omega) k_w}{r_n \omega r_w \eta} - \frac{1}{9} \frac{\psi^2 \rho^2}{(\psi + \varepsilon)^2} \Bigg) \Bigg) \\
& \Bigg/ \left(\frac{8 \psi^3 \rho^3}{(\psi + \varepsilon)^3} + \frac{36 b (r_w - \omega) k_w \left(1 + \frac{\varepsilon}{\psi + \phi}\right) \psi \rho a (r_c - \psi) k_c}{r_w (\psi + \varepsilon)^2 r_c \omega} \right. \\
& - \frac{72 d (r_n - \eta) k_n c (r_w - \omega) k_w \psi \rho}{r_n \omega r_w \eta (\psi + \varepsilon)} \\
& + 12 \left(- \frac{12 \psi^4 \rho^4 c (r_w - \omega) k_w d (r_n - \eta) k_n}{(\psi + \varepsilon)^4 r_w \eta r_n \omega} \right. \\
& - \frac{3 \psi^2 \rho^2 a^2 (r_c - \psi)^2 k_c^2 b^2 (r_w - \omega)^2 k_w^2 \left(1 + \frac{\varepsilon}{\psi + \phi}\right)^2}{(\psi + \varepsilon)^4 r_c^2 \omega^2 r_w^2} \\
& - \frac{60 \psi^2 \rho^2 a (r_c - \psi) k_c b (r_w - \omega)^2 k_w^2 \left(1 + \frac{\varepsilon}{\psi + \phi}\right) c d (r_n - \eta) k_n}{(\psi + \varepsilon)^3 r_c \omega^2 r_w^2 \eta r_n} \\
& + \frac{24 \psi^2 \rho^2 c^2 (r_w - \omega)^2 k_w^2 d^2 (r_n - \eta)^2 k_n^2}{(\psi + \varepsilon)^2 r_w^2 \eta^2 r_n^2 \omega^2} - \frac{12 a^3 (r_c - \psi)^3 k_c^3 b^3 (r_w - \omega)^3 k_w^3 \left(1 + \frac{\varepsilon}{\psi + \phi}\right)^3}{r_c^3 \omega^3 r_w^3 (\psi + \varepsilon)^3}
\end{aligned}$$

$$\begin{aligned}
& - \frac{36 a^2 (r_c - \psi)^2 k_c^2 b^2 (r_w - \omega)^3 k_w^3 \left(1 + \frac{\varepsilon}{\psi + \phi}\right)^2 c d (r_n - \eta) k_n}{r_c^2 \omega^3 r_w^3 (\psi + \varepsilon)^2 \eta r_n} \\
& - \frac{36 a (r_c - \psi) k_c b (r_w - \omega)^3 k_w^3 \left(1 + \frac{\varepsilon}{\psi + \phi}\right) c^2 d^2 (r_n - \eta)^2 k_n^2}{r_c^3 \omega^3 r_w^3 (\psi + \varepsilon)^2 \eta^2 r_n^2} \\
& - \frac{12 c^3 (r_w - \omega)^3 k_w^3 d^3 (r_n - \eta)^3 k_n^3}{r_w^3 \eta^3 r_n^3 \omega^3} \Bigg)^{1/2} \Bigg)^{1/3} + \frac{1}{3} \frac{\psi \rho}{\psi + \varepsilon}
\end{aligned}$$

> # Normalized forward sensitivity index technique

> #

seq([j, Re(eval(j*diff(R,j) / R,params))], j in indets(R,name));

;

[a, 0.2779368186], [b, 0.2779368186], [c, 0.2217571744], [d, 0.2217571744], [\eta, -0.2334286048], [\omega, -0.7138485611], [\phi, -0.1175886540], [\psi, -0.1579296918], [\rho, 0.0006120126956], [\varepsilon, -0.02015912070], [k_c, 0.2779368184], [k_n, 0.2217571745], [k_w, 0.4996939930], [r_c, 0.01774064797], [r_n, 0.01167143023], [r_w, 0.2141545685]

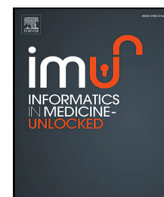
(14)

RESEARCH OUTPUTS

1. Published paper

Erick, B. and Mayengo, M. (2022). Modelling the dynamics of cassava mosaic disease with non-cassava host plants. *Informatics in Medicine Unlocked*. p. 101086.
URL:<https://www.sciencedirect.com/science/article/pii/S2352914822002222>

2. Poster presentation



Modelling the dynamics of Cassava Mosaic Disease with non-cassava host plants

Bahati Erick ^{a,b}, Maranya Mayengo ^{a,*}

^a School of Computational and Communication Science and Engineering, Nelson Mandela African Institution of Science and Technology (NM-AIST), P.O. Box 447, Arusha, Tanzania

^b Mpwapwa Teachers College, P.O. Box 34, Dodoma, Tanzania

ARTICLE INFO

Keywords:

Numerical simulation
Stability analysis
Basic reproduction number
Cassava Mosaic Disease

ABSTRACT

Cassava Mosaic Disease (CMD) is the prominent cassava disease which compromises cassava production in Africa, both qualitatively and quantitatively for many years. In this study, the mathematical model for the dynamics of CMD with Non-cassava host plant population is formulated and analysed. The analysis of basic model properties confirmed the positive boundedness of the model solution for all time $t \geq 0$. Utilizing the next generation matrix the basic reproduction number R_0 is derived and stability of disease-free equilibrium point (DFE) is analysed. Analytical results confirmed that, the disease-free equilibrium point (DFE) is locally asymptotically stable whenever $R_0 < 1$ and unstable otherwise. The sensitivity index analysis identified mortality rate and the carrying capacity of whiteflies as the most sensitive parameters of model. This implies that, any deliberate efforts towards controlling CMD should be directed into reducing the number of whiteflies. This can be implemented by either increasing the mortality rate of whiteflies or reducing their carrying capacity. In view of this, it is clear that deliberate measures such as the use of pesticides and entomopathogenic fungi which increases the parameter value of ω , and removing non-cassava host plants which will eventually decrease the parameter value of κ_w may bring significant results in combating CMD compared to the control of other model parameters. The decision regarding the best approach out of the two requires optimal control and cost-effective analysis of available control strategies. Furthermore, the numerical simulation results suggested that Cassava Mosaic Disease (CMD) can be controlled by increasing mortality rate of whiteflies, and the decreasing in the carrying capacity of whiteflies.

1. Introduction

Cassava (*Manihot esculenta* Crantz) is a Euphorbiaceae family perennial tropical woody plant with consumable starchy roots [1]. The plant was introduced in Africa in the 16th century by Portuguese traders from South America [2]. Although both the roots and the leaves are useful, cassava roots are the most commonly used [3]. While cassava roots are rich in carbohydrates, the leaves are associated with proteins, vitamins B1, B2, C and carotenes [3]. Cassava plant is identified as a potential climate change crop because of its tolerance to unfavourable climatic circumstances such as unreliable rainfall [4]. It is a vital subsistence food crop in Africa, particularly in semi-arid locations where cereal crops fail to grow. In Tanzania, cassava production support around 37% of rural farmers [5].

Cassava production in Africa is hampered by the presence and persistence of plant pests and diseases such as Cassava Mosaic Disease (CMD) and Cassava Brown Streak Disease (CBSD) [6]. The history of CMD incidences in Africa can be traced back to 1894 when it was

first recorded in Tanzania [7]. Studies identify seven different Cassava Mosaic Gemini-viruses (CMGs) and their variants as the causal agents of CMD [8,9] which spread through the use of contaminated cassava stem cuttings and whiteflies (*Bemisia tabaci*) ingestion on plants [10,11]. The effects of CMD in the production of Cassava may not be overemphasized. For instance, available literature reveals that CMD is responsible for the annual loss of more than 34 million tonnes in Africa [12]. The average yield loss is approximated to be between 55% and 77% when contaminated stem cuttings are used and from 35% to 60% when CMD is caused by whitefly [13].

The observable CMD symptoms are highly influenced by the viral species, climatic circumstances, and the susceptibility of the cassava plants. The common symptoms include yellow or light green wilt mosaic leaves, followed by deformation and wrinkling of the leaves [14]. Studies identify at least 64 Solanaceous species and plants such as *Leucana leucocephala*, *Glycine max*, *Ricinus communis* (castor oil plant),

* Corresponding author.

E-mail address: maranya.mayengo@nm-aist.ac.tz (M. Mayengo).

<https://doi.org/10.1016/j.imu.2022.101086>

Received 22 July 2022; Received in revised form 8 September 2022; Accepted 8 September 2022

Available online 13 September 2022

2352-9148/© 2022 The Authors. Published by Elsevier Ltd. This is an open access article under the CC BY-NC-ND license (<http://creativecommons.org/licenses/by-nc-nd/4.0/>).

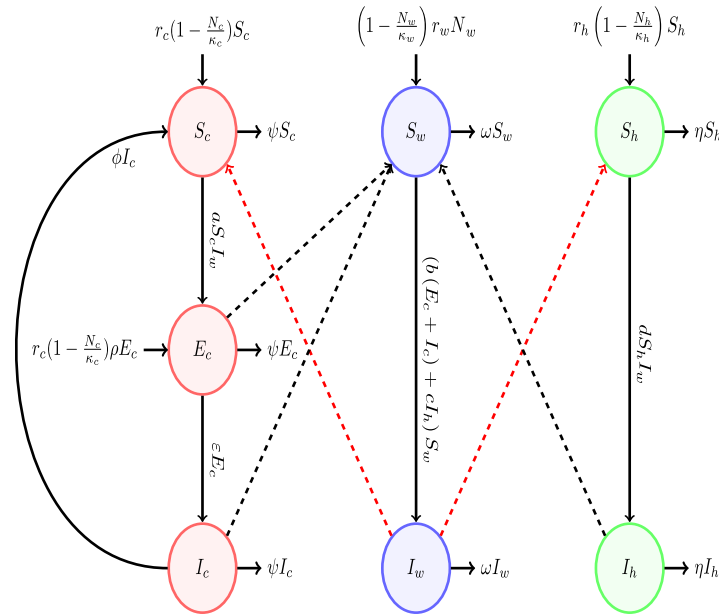


Fig. 1. Cassava Mosaic Disease flow diagram.

Senna occidentalis, *Combretum confertum*, *Manihot glaziovii* which are susceptible to CMGs [10,15–17]. These alternative host plants can be colonized by whiteflies and are commonly found in cassava plots and surrounding areas as leguminous plant species, hedge plants or weeds [15,18,19]. They promote the spread of CMD by acting as the source of CMGs to whiteflies [10,16,17].

Mathematical models provide useful tools to understand the transmission dynamics of CMD. For instance, Holt et al. [20] studied the impacts of different variables on the spread of CMD. The study reveals that, the use of infected cutting tools and elimination of infectious cassava have insignificant effects on the occurrence of the disease. On the other hand, Magoyo et al. [21] modified the work of Holt et al. [20] by including cassava cultivar which can be affected by CMGs through unhealthy cutting only. In this study, the susceptible breed acquired CMGs through unhealthy cutting and whitefly contacts. The study identified death rate, infection rate, whiteflies carrying capacity, and the rate of loss of infected cassava due to disease are the most sensitive parameters in the system.

The effects of whitefly maturation time on the transmission dynamics of CMD was studied by Fahad et al. [22]. The study establishes that, the whitefly maturation time may stabilize epidemiological dynamics. On the other hand, Jittamai et al. [23] includes both planting of infected cuttings and whitefly transmission in the model to identify the most cost-effective method for CMD management. The study establishes that, the spread of the disease is influenced by the density of whiteflies and the number of visited cassava plants. The numerical simulations was used to prove the effectiveness of whiteflies population control in elimination of CMD outbreak at minimum costs.

In this paper, we modify the framework of Jittamai et al. [23] by considering non-cassava host plants population in the transmission dynamics of CMD.

2. Model formulation

We formulated the model consisting three population species; cassava plant (N_c), whitefly (N_w) and non-cassava host plant (N_h). Cassava plant population is divided into Susceptible (S_c), Exposed (infected with

no symptoms) (E_c) and Infected (I_c) population compartments. On the other hand, whitefly population comprises Susceptible (S_w) and Infected (I_w) compartments, similarly non-cassava hosts plant population is categorized into Susceptible (S_h) and Infected (I_h) compartments.

Susceptible cassava plants are recruited logistically at the rate r_c and can acquire CMD through whitefly at the rate a . The exposed cassava plants are replanted logistically depending on the probability of selecting the exposed cassava cuttings ρ . Further, the rate at which exposed plants are converted to infected plants is represented by ϵ . The infected cassava plants are recovered at the rate ϕ and become susceptible to CMD. The model assumes that the cassava plant population is harvested at the rate of ψ .

The whiteflies are recruited logistically at the rate r_w and acquire virus from both exposed and infected cassava plants, and infected non-cassava host plants at the rate b and c respectively. The mortality rate of the whitefly is represented by ω . Susceptible non-cassava host plants are recruited logistically at the rate r_h and acquire CMD through the whitefly at the rate d . Lastly, the non-cassava host plants are harvested at the rate of η . The above information is summarized in the flow diagram presented in Fig. 1 below.

The following assumptions based on characteristics of the CMD were made to the formulated CMD model.

- The replanting rate of cassava plant is higher than its harvesting rate i.e., $r_c - \psi > 0$.
- The recruitment rate of whiteflies is higher than its death rate i.e., $r_w - \omega > 0$.
- The replanting rate of the non-cassava host plant is higher than its harvesting rate i.e., $r_h - \eta > 0$.
- All model populations grow logistically.
- All model parameters and variables are non-negative.
- Cassava plants get CMD through contact with infected whitefly and the of unhealthy cutting.
- Non-cassava host plant gets CMD through contact with infected whitefly only.

The system of differential equations (1) describes the transmission dynamics of CMD by considering all stated assumptions.

$$\begin{cases} \frac{dS_c}{dt} = r_c \left(1 - \frac{N_c}{\kappa_c}\right) S_c + \phi I_c - a S_c I_w - \psi S_c \\ \frac{dE_c}{dt} = r_c \left(1 - \frac{N_c}{\kappa_c}\right) \rho E_c + a S_c I_w - (\psi + \varepsilon) E_c \\ \frac{dI_c}{dt} = \varepsilon E_c - (\psi + \phi) I_c \\ \frac{dS_w}{dt} = \left(1 - \frac{N_w}{\kappa_w}\right) r_w N_w - (b(E_c + I_c) + c I_h) S_w - \omega S_w \\ \frac{dI_w}{dt} = (b(E_c + I_c) + c I_h) S_w - \omega I_w \\ \frac{dS_h}{dt} = r_h \left(1 - \frac{N_h}{\kappa_h}\right) S_h - d S_h I_w - \eta S_h \\ \frac{dI_h}{dt} = d S_h I_w - \eta I_h \end{cases} \quad (1)$$

with initial conditions, $S_c(0) > 0$, $E_c(0) \geq 0$, $I_c(0) \geq 0$, $S_w(0) > 0$, $I_w(0) \geq 0$, $S_h(0) > 0$, $I_h(0) \geq 0$. The equations for the total population of Cassava plants, whitefly, and non-cassava host plants are given by:

$$\begin{cases} \frac{dN_c}{dt} = r_c \left(1 - \frac{N_c}{\kappa_c}\right) S_c + r_c \left(1 - \frac{N_c}{\kappa_c}\right) \rho E_c - \psi N_c \\ \frac{dN_w}{dt} = \left(1 - \frac{N_w}{\kappa_w}\right) r_w N_w - \omega N_w \\ \frac{dN_h}{dt} = r_h \left(1 - \frac{N_h}{\kappa_h}\right) S_h - \eta N_h \end{cases} \quad (2)$$

3. Basic model properties

3.1. Invariant region

Lemma 1. Given the model system (1) in \mathbb{R}_+^7 with the initial conditions $S_c(0) > 0$, $E_c(0) \geq 0$, $I_c(0) \geq 0$, $S_w(0) > 0$, $I_w(0) \geq 0$, $S_h(0) > 0$, $I_h(0) \geq 0$, its solution enters the invariant region $\Omega = (S_c, E_c, I_c, S_w, I_w, S_h, I_h) \geq 0$ in \mathbb{R}_+^7 .

Proof. The box invariant method as used by Chuma [24], Daudi et al. [25] and Nyerere et al. [26] was used to establish the feasible region of the CMD system. We assume the continuity and the Lipschitz properties of its solution for our dynamic system $\frac{dX}{dt} = G(X, t)$, X in \mathbb{R}^n . The model system (1) is reduced to the form,

$$\frac{dX}{dt} = AX + Z$$

where, column vector $X = (S_c, E_c, I_c, S_w, I_w, S_h, I_h)^T$ and

$$Z = \left((r_c \left(1 - \frac{N_c}{\kappa_c}\right) - a I_w) S_c, r_c \left(1 - \frac{N_c}{\kappa_c}\right) \rho, 0, \left(1 - \frac{N_w}{\kappa_w}\right) r_w S_w, 0, r_h \left(1 - \frac{N_h}{\kappa_h}\right) S_h, 0 \right)^T$$

and the Metzler matrix $AX \in \mathbb{R}_+^7$ is defined as,

$$A = \begin{pmatrix} -\psi & 0 & \phi & 0 & 0 & 0 & 0 \\ 0 & -(\psi + \varepsilon) & 0 & 0 & a S_c & 0 & 0 \\ 0 & \varepsilon & -(\psi + \phi) & 0 & 0 & 0 & 0 \\ 0 & 0 & 0 & -Q_1 & \left(1 - \frac{N_w}{\kappa_w}\right) r_w & 0 & 0 \\ 0 & 0 & 0 & Q_2 & -\omega & 0 & 0 \\ 0 & 0 & 0 & 0 & 0 & -(d I_w + \eta) & 0 \\ 0 & 0 & 0 & 0 & 0 & d I_w & -\eta \end{pmatrix} \quad (3)$$

where, $Q_1 = b(E_c + I_c) + c I_h + \omega$ and $Q_2 = b(E_c + I_c) + c I_h$ are simplifying factors.

Since the principal diagonal of a reduced matrix A in Eq. (3) has all negative values, while the off-diagonal has all non-negative values, it proves that, all variables enter and stay in the feasible region Ω . This implies that the formulated model system (1) is well-posed in invariant region Ω .

3.2. Positivity of the solution

From the model equation (1) we have,

$$\frac{dS_c}{dt} = r_c \left(1 - \frac{N_c}{\kappa_c}\right) S_c + \phi I_c - a S_c I_w - \psi S_c \quad (4)$$

$$\frac{dS_c}{dt} \geq -(a I_w + \psi) S_c$$

Separating the variables and integrating both sides, we get

$$\int \frac{dS_c}{S_c} \geq \int -(a I_w + \psi) dt$$

$$\ln S_c \geq -(a I_w + \psi) t + C$$

$$S_c(t) \geq B e^{-(a I_w + \psi)t}$$

If we substitute $t = 0$ as our initial condition, we get

$$S_c(0) \geq B$$

Hence,

$$S_c(t) \geq S_c(0) e^{-(a I_w + \psi)t} \geq 0 \quad \forall t \geq 0$$

Applying the same procedure to all equations of model system (1) for all $t \geq 0$, the following results are established,

$$E_c(t) \geq E_c(0) e^{-(\psi + \varepsilon)t} \geq 0 \quad (5)$$

$$I_c(t) \geq I_c(0) e^{-(\psi + \phi)t} \geq 0 \quad (6)$$

$$S_w(t) \geq S_w(0) e^{-(b(E_c + I_c) + c I_h + \omega)t} \geq 0 \quad (7)$$

$$I_w(t) \geq I_w(0) e^{-\omega t} \geq 0 \quad (8)$$

$$S_h(t) \geq S_h(0) e^{-(d I_w + \eta)t} \geq 0 \quad (9)$$

$$I_h(t) \geq I_h(0) e^{-\eta t} \geq 0 \quad (10)$$

This concludes that, the model system (1) has the positive solution for all $t \geq 0$.

3.3. Existence of equilibria and basic reproduction number

3.3.1. Disease free equilibrium

The equilibrium points of the CMD model (1) is obtained by setting the RHS to be equal to zero and solving the system simultaneously. Thus, we have

$$\begin{cases} r_c \left(1 - \frac{N_c^*}{\kappa_c}\right) S_c^* + \phi I_c^* - a S_c^* I_w^* - \psi S_c^* = 0 \\ r_c \left(1 - \frac{N_c^*}{\kappa_c}\right) \rho E_c^* + a S_c^* I_w^* - (\psi + \varepsilon) E_c^* = 0 \\ \varepsilon E_c^* - (\psi + \phi) I_c^* = 0 \\ \left(1 - \frac{N_w^*}{\kappa_w}\right) r_w N_w^* - (b(E_c^* + I_c^*) + c I_h^*) S_w^* - \omega S_w^* = 0 \\ (b(E_c^* + I_c^*) + c I_h^*) S_w^* - \omega I_w^* = 0 \\ r_h \left(1 - \frac{N_h^*}{\kappa_h}\right) S_h^* - d S_h^* I_w^* - \eta S_h^* = 0 \\ d S_h^* I_w^* - \eta I_h^* = 0 \end{cases} \quad (11)$$

where $(S_c^*, E_c^*, I_c^*, S_w^*, I_w^*, S_h^*, I_h^*)$ is the solution set to the system (11). When $E_c^* = 0$, $I_c^* = 0$, $I_w^* = 0$, $I_h^* = 0$ we have the disease-free equilibrium point, $DFE = (S_c^0, E_c^0, I_c^0, S_w^0, I_w^0, S_h^0, I_h^0)$ given by

$$DFE = \left(\frac{\kappa_c (r_c - \psi)}{r_c}, 0, 0, \frac{\kappa_w (r_w - \omega)}{r_w}, 0, \frac{\kappa_h (r_h - \eta)}{r_h}, 0 \right) \quad (12)$$

3.3.2. Disease Endemic Equilibrium

The equilibrium points at which there is disease infection in model system population is referred to as *Disease Endemic Equilibrium* point (DEE). Considering the system model equation (1), we get, $DEE = (S_c^*, E_c^*, I_c^*, S_w^*, I_w^*, S_h^*, I_h^*)$, where

$$S_c^* = \frac{I_c^* \kappa_c \phi + r_c (\kappa_c - N_c^*)}{\kappa_c (a I_w^* + \phi)}, \quad E_c^* = \frac{a \kappa_c S_c^* I_w^*}{N_c^* r_c \rho + \kappa_c ((\psi + \epsilon) - r_c \rho)},$$

$$I_c^* = \frac{\epsilon E_c^*}{(\psi + \phi)},$$

$$S_w^* = \frac{r_w N_w^* (\kappa_w - N_w^*)}{\kappa_w ((b(E_c + I_c) + c I_h) + \omega)}, \quad I_w^* = \frac{(b(E_c + I_c) + c I_h) S_w}{\omega} \text{ and}$$

$$S_h^* = \frac{\eta I_h^*}{d I_w^*}$$

When the first equation of the system (11) is deployed, we have

$$r_c \left(1 - \frac{N_c^*}{\kappa_c}\right) S_c^* + \phi I_c^* - a S_c^* I_w^* - \psi S_c^* = 0$$

implying that $r_c \left(\frac{\kappa_c - N_c^*}{\kappa_c}\right) S_c^* + \phi I_c^* > 0$, consequently, we have $\kappa_c - N_c^* > 0$. In a similar vein, utilizing the fourth and sixth equations of the system (11) we prove that $\kappa_w - N_w^* > 0$ and $\kappa_h - N_h^* > 0$, respectively. On the other hand, the second equation of the system (11) proves that $r_c \rho N_c^* + (\psi + \epsilon) - r_c \rho > 0$.

3.4. The basic reproduction number, \mathcal{R}_0

The basic reproduction number refers to the number of secondary infections that an infected individual is likely to cause over their infectious life [27]. It is a measure which tells the potentiality of disease to spread within a population. If $\mathcal{R}_0 < 1$, then a few infected individuals introduced into a completely susceptible population will, on average fail to replace themselves. On the other hand, if $\mathcal{R}_0 \geq 1$, then the number of infected individuals will increase with each generation and the disease will spread [28]. We adopt the next generation matrix method proposed by Van den Driessche and Watmough [28], as also used by Mayengo et al. [29] in the computational of \mathcal{R}_0 from the CMD model system (1). The basic reproduction number was obtained by splitting the infected subsystem of the model into the form

$$\frac{dX}{dt} = F_i - \mathcal{V}_i, i = 1, \dots, n,$$

where F_i is the rate of secondary infections increase at i th disease compartment and \mathcal{V}_i is the rate of disease progression and death decrease at i th compartment. The basic reproduction number is given by the dominant eigenvalue (Spectral radius) of the matrix $F\mathcal{V}^{-1}$, thus $\mathcal{R}_0 = \rho(F\mathcal{V}^{-1})$ where, $F = \left[\frac{\partial F_i}{\partial x_j}\right]$ and $\mathcal{V} = \left[\frac{\partial \mathcal{V}_i}{\partial x_j}\right]$ evaluated at DFE point when $x = (E_c, I_c, I_w, I_h)$. Now, considering the model system (1), the infected subsystem are,

$$\begin{cases} \frac{dE_c}{dt} = r_c \left(1 - \frac{N_c}{\kappa_c}\right) \rho E_c + a S_c I_w - (\psi + \epsilon) E_c \\ \frac{dI_c}{dt} = \epsilon E_c - (\psi + \phi) I_c \\ \frac{dI_w}{dt} = (b(E_c + I_c) + c I_h) S_w - \omega I_w \\ \frac{dI_h}{dt} = d S_h I_w - \eta I_h \end{cases} \quad (13)$$

Thus,

$$F_i = \begin{pmatrix} r_c \left(1 - \frac{N_c}{\kappa_c}\right) \rho E_c + a S_c I_w \\ 0 \\ (b(E_c + I_c) + c I_h) S_w \\ d S_h I_w \end{pmatrix} \quad (14)$$

and,

$$\mathcal{V}_i = \begin{pmatrix} (\psi + \epsilon) E_c \\ (\psi + \phi) I_c - \epsilon E_c \\ \omega I_w \\ \eta I_h \end{pmatrix}. \quad (15)$$

The Jacobian matrix for F_i and \mathcal{V}_i evaluated at DFE are given by,

$$F = \begin{pmatrix} r_c \left(1 - \frac{S_c^0}{\kappa_c}\right) \rho & 0 & a S_c^0 & 0 \\ 0 & 0 & 0 & 0 \\ b S_w^0 & b S_w^0 & 0 & c S_w^0 \\ 0 & 0 & d S_h^0 & 0 \end{pmatrix} \quad (16)$$

and

$$\mathcal{V} = \begin{pmatrix} (\psi + \epsilon) & 0 & 0 & 0 \\ -\epsilon & \psi + \phi & 0 & 0 \\ 0 & 0 & \omega & 0 \\ 0 & 0 & 0 & \eta \end{pmatrix}. \quad (17)$$

The computational of \mathcal{V}^{-1} gives,

$$\mathcal{V}^{-1} = \begin{pmatrix} \frac{1}{\psi + \epsilon} & 0 & 0 & 0 \\ \frac{\epsilon}{(\psi + \phi)(\psi + \epsilon)} & \frac{1}{\psi + \phi} & 0 & 0 \\ 0 & 0 & \frac{1}{\omega} & 0 \\ 0 & 0 & 0 & \frac{1}{\eta} \end{pmatrix} \quad (18)$$

consequently as given in Box I. If we let

$$g_{11} = \frac{\psi \rho}{\psi + \epsilon}, g_{13} = a \frac{(r_c - \psi) \kappa_c}{\omega r_c}, g_{31} = b \frac{(r_w - \omega) \kappa_w}{(\psi + \epsilon) r_w} \left(1 + \frac{\epsilon}{\psi + \phi}\right)$$

$$, g_{32} = b \frac{(r_w - \omega) \kappa_w}{(\psi + \phi) r_w}, g_{34} = c \frac{(r_w - \omega) \kappa_w}{\eta r_w} \text{ and } g_{43} = d \frac{(r_h - \eta) \kappa_h}{\omega r_h}$$

and compute $\mathcal{R}_0 = \rho(F\mathcal{V}^{-1})$ we obtain,

$$\mathcal{R}_0 = \frac{1}{6} X + \frac{2}{X} \left(g_{31} g_{13} + g_{43} g_{34} + \frac{1}{3} (g_{11})^2\right) + \frac{1}{3} g_{11} \quad (20)$$

where, $X = (X_0 + 12\sqrt{X_1})^{\frac{1}{3}}$, $X_0 = 4(9g_{31}g_{13} - 18g_{43}g_{34} + 2(g_{11})^2)g_{11}$ and

$$X_1 = -3(g_{11})^2(4g_{34}g_{43}(1 - 2g_{34}g_{43}) + g_{13}g_{31}(g_{13}g_{31} + 20g_{34}g_{43}))$$

$$- 12(g_{13}g_{31})^2(g_{13}g_{31} + 3g_{34}g_{43})$$

$$- 12(g_{34}g_{43})^2(3g_{13}g_{31} + g_{34}g_{43})$$

3.5. Local stability of disease free equilibrium

Theorem 2. The disease-free equilibrium point (DFE) of the CMD model system (1) is locally asymptotic stable when $\mathcal{R}_0 < 1$ and unstable otherwise.

Proof. Following Mayengo et al. [30], we investigate the real part of the eigenvalues of the decomposed Jacobian matrix of the system evaluated at DFE. Thus the result is established as in Box II. The matrix J_{DFE} can be decomposed into the block matrix of the form

$$J_{DFE} = \begin{pmatrix} J_{11} & J_{12} & \mathbf{0} \\ J_{21} & J_{22} & J_{23} \\ \mathbf{0} & J_{32} & J_{33} \end{pmatrix} \quad (22)$$

where $\mathbf{0}$ are zero matrices and

$$J_{11} = \begin{pmatrix} -(r_c - \psi) & -(r_c - \psi) & -(r_c - \psi) + \phi \\ 0 & -(\psi(1 - \rho) + \epsilon) & 0 \\ 0 & \epsilon & -(\psi + \phi) \end{pmatrix},$$

$$J_{22} = \begin{pmatrix} -(r_w - \omega) & -r_w + 2\omega \\ 0 & -\omega \end{pmatrix}, \quad J_{33} = \begin{pmatrix} -(r_h - \eta) & -(r_h - \eta) \\ 0 & -\eta \end{pmatrix}.$$

We can easily observe that, the eigenvalues for matrix J_{11} are $-(\psi + \phi)$, $-(\psi(1 - \rho) + \epsilon)$ and $-(r_c - \psi)$. Based on assumption i, it is

$$\mathcal{FV}^{-1} = \begin{pmatrix} \frac{\psi\rho}{\psi+\varepsilon} & 0 & a\frac{(r_c-\psi)\kappa_c}{\omega r_c} & 0 \\ 0 & 0 & 0 & 0 \\ b\frac{(r_w-\omega)\kappa_w}{(\psi+\varepsilon)r_w}\left(1+\frac{\varepsilon}{\psi+\phi}\right) & b\frac{(r_w-\omega)\kappa_w}{(\psi+\phi)r_w} & 0 & c\frac{(r_w-\omega)\kappa_w}{\eta r_w} \\ 0 & 0 & d\frac{(r_h-\eta)\kappa_h}{\omega r_h} & 0 \end{pmatrix}. \quad (19)$$

Box I.

$$J_{DFE} = \begin{pmatrix} -(r_c-\psi) & -(r_c-\psi) & -(r_c-\psi)+\phi & 0 & -aS_c^0 & 0 & 0 \\ 0 & -(\psi(1-\rho)+\varepsilon) & 0 & 0 & aS_c^0 & 0 & 0 \\ 0 & \varepsilon & -(\psi+\phi) & 0 & 0 & 0 & 0 \\ 0 & -bS_w^0 & -bS_w^0 & -(r_w-\omega) & -r_w+2\omega & 0 & -cS_w^0 \\ 0 & bS_w^0 & bS_w^0 & 0 & -\omega & 0 & cS_w^0 \\ 0 & 0 & 0 & 0 & -dS_h^0 & -(r_h-\eta) & -(r_h-\eta) \\ 0 & 0 & 0 & 0 & dS_h^0 & 0 & -\eta \end{pmatrix} \quad (21)$$

Box II.

clear that $-(r_c-\psi) < 0$ suggesting that the matrix J_{11} has negative real eigenvalues. Similarly, the eigenvalues for matrix J_{22} are $-(r_w-\omega)$ and $-\omega$. Again, utilizing assumption ii we know that $-(r_w-\omega) < 0$ suggesting that matrix J_{22} has negative real eigenvalues. Furthermore, the eigenvalues of matrix J_{33} are $-(r_h-\eta)$ and $-\eta$. Utilizing assumption iii it is clear that matrix J_{33} has negative eigenvalues. This property assures the stability of the diagonal sub-matrices J_{11} , J_{22} , and J_{33} and hence the local stability of the matrix J_{DFE} when $\mathcal{R}_0 < 1$.

4. Sensitivity analysis

The assessment on the contribution of each parameters featured in the computation of \mathcal{R}_0 was conducted by using normalized forward sensitivity index method. Following Kung'aro [31] and Mayengo et al. [32] we establish that;

$$\tau_{u_i}^{\mathcal{R}_0} = \frac{\partial \mathcal{R}_0}{\partial u_i} \times \frac{u_i}{\mathcal{R}_0} \quad (23)$$

where u_i represents the i th parameter of the model as depicted on Table 1.

Applying normalized forward sensitivity index method using the baseline values, we obtain the following sensitivity indices presented in Table 1;

From Table 1 we observe that the natural mortality rate of whiteflies (ω) is the most negative sensitive parameter in the transmission of CMD while the carrying capacity of whiteflies (κ_w) is the most positive sensitive parameter of the CMD model system. Other negative sensitive parameter includes the harvesting rate of the non-cassava host plant (η) followed by the harvesting rate of cassava plant ψ , the CMD latent rate (ε) and the recovering rate of cassava plant (ϕ). Sensitivity index results suggest that, increasing the death rate of whiteflies (ω) and reducing the carrying capacity of whiteflies are the most important control strategies of CMD. Further, we observe that the probability of replanting exposed cassava plant (ρ) have less contribution to the spread of the disease. Thus, any deliberate control efforts with the focus of increasing removal rate of the whiteflies from the field is likely to be of success in the controlling CMD. This can be successfully done by either increasing whiteflies death rate or decreasing their carrying capacity in the non-host cassava plants.

Table 1

Model parameter values and their sensitivity indices.

Parameter	Range	Baseline value	Source	Sensitivity index
r_c	0.025–0.1	0.05day ⁻¹	[33]	0.0177
r_w	0.1–0.3	0.2day ⁻¹	[20]	0.0117
r_h	–	0.02day ⁻¹	Assumed	0.2141
ρ	0–1	0.1	[20]	0.0006
a	0.002–0.032	0.008plant ⁻¹ day ⁻¹	[20]	0.2779
b	0.002–0.032	0.008whitefly ⁻¹ day ⁻¹	[20]	0.2779
c	–	0.008whitefly ⁻¹ day ⁻¹	Assumed	0.2218
d	–	0.008plant ⁻¹ day ⁻¹	Assumed	0.2218
ε	–	0.033day ⁻¹	[33]	–0.0202
ω	0.06–0.18	0.06day ⁻¹	[20]	–0.7138
η	–	0.001day ⁻¹	Assumed	–0.2334
ψ	0.002–0.004	0.003day ⁻¹	[20]	–0.1579
κ_c	0.01–1	0.7m ⁻¹	[20]	0.2779
κ_w	0–350	90plant ⁻¹	[34]	0.4997
κ_h	0.01–1	0.1m ⁻¹	Assumed	0.2218
ϕ	0.002–0.004	0.003day ⁻¹	[33]	–0.1176

5. Numerical simulation and results

Utilizing Runge–Kutta fourth order method by using MATLAB codes, the numerical simulation on the CMD model system (1) was performed and the effects of identified sensitive parameters to the system were illustrated. We simulate the CMD model system (1) using baseline parameter values as shown in Table 1 and $S_c(0) = 0.35$, $E_c(0) = 0.05$, $I_c(0) = 0.05$, $S_w(0) = 40$, $I_w(0) = 10$, $S_h(0) = 0.2$, $I_h(0) = 0.1$ as initial condition values for model variables.

In Fig. 2 we observe that, in the first 100 days the number of susceptible cassava plants decreases from 0.35 per m² to 0.05 per m², remains to this level for sometimes before it stabilizes. It is observed further that, in less than 25 days, the exposed cassava plants attains the maximum value of 0.2 plants per m² before it starts decreasing exponentially to 0.05 plants per m² in 200 days. On the other hand, the infected cassava plant population raises from 0.05 per m² to 0.35 plants per m² in first 100 days.

Fig. 3 shows that, the number of susceptible whiteflies population increases from 40 to approximately 58 susceptible whiteflies per m² within the first 50 days. After 50 days the population of susceptible whiteflies population remain constant at the rate of approximately 58 per m². Conversely, the number of infected whiteflies population

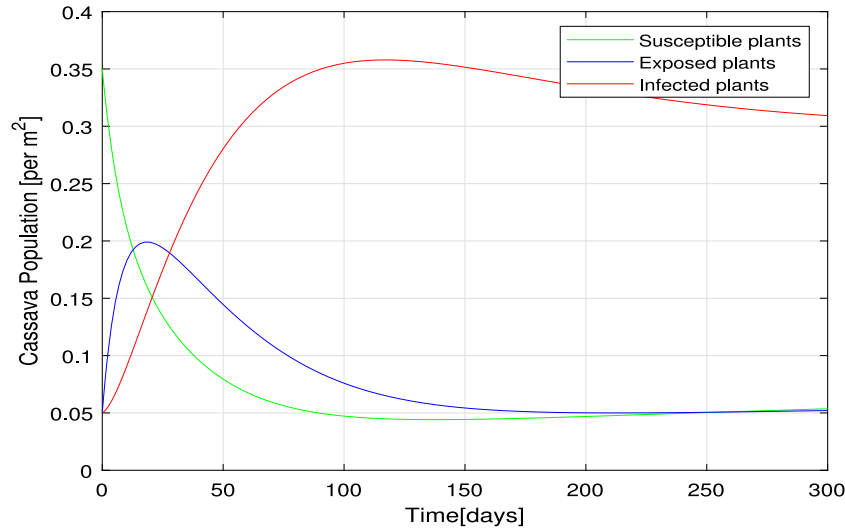


Fig. 2. Cassava population dynamics.

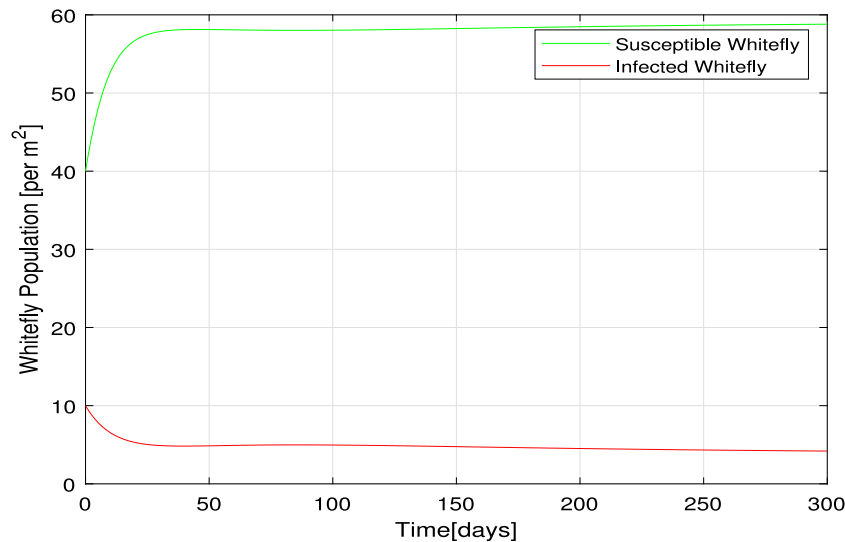


Fig. 3. Whitefly population dynamics.

decreases from 10 to its stability rate of 5 infected whiteflies per m^2 in less than 50 days.

The results in Fig. 4 reveal that, the number of susceptible non-cassava host plants decreases from 0.2 to 0 per m^2 in less than 100 days while the number infected non-cassava host plant increases from 0.1 to its peak value of approximately 0.22 per m^2 in 50 days before it starts decreasing to 0.17 per m^2 in 300 days.

Three scenarios of the model simulation on infected cassava plants, infected whiteflies and infected non-cassava host plants against the variation of different values of mortality rate of whiteflies (ω) are observed in Fig. 5. It is clear that the increase in the mortality rate of whiteflies causes the decrease in number of infected cassava plants, infected whiteflies and infected non-cassava host plants (see Fig. 5). This confirm that controlling the number of whiteflies by increasing its mortality rate is vital in the fight against the spread of the disease.

Fig. 6 portrays the effects of varying the carrying capacity of whiteflies on infected populations. It is observed that, an increase in number

of whiteflies per m^2 leads to the increase in number of infected population of cassava, whitefly and non-cassava host plant. The result portrays that the severity of the CMD can be influenced by the maximum number of whiteflies per m^2 .

6. Conclusion

In this paper, an ordinary differential equation (ODE) model with non-cassava host plant population was formulated and analysed. The analysis of basic model properties confirms that, formulated CMD model has positively bounded solutions for all time $t \geq 0$. Local stability analysis of R_0 confirms that the DFE is asymptotically stable whenever $R_0 < 1$ and unstable otherwise. This implies that, CMD will be endemic when $R_0 \geq 1$, and can be eliminated when $R_0 < 1$. Moreover, the sensitivity analysis on R_0 and numerical simulation of the system model (1) revealed that, mortality rate of whiteflies (ω) and the carrying capacity of whiteflies per m^2 (κ_w) are the most sensitive parameter of the CMD model. This implies that, any deliberate

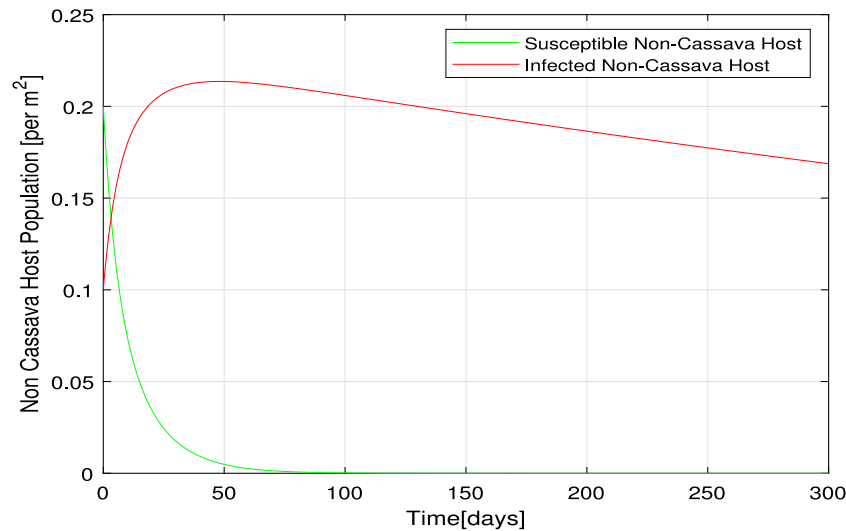


Fig. 4. Non-cassava hosts population dynamics.

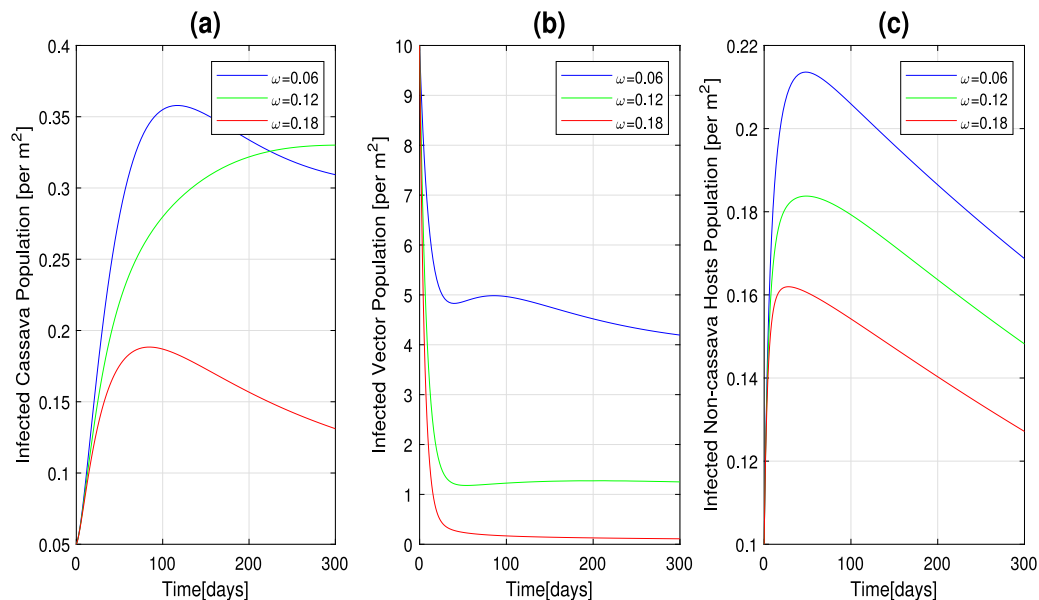


Fig. 5. Infected population of cassava plant (a), infected whiteflies (b) and infected non-cassava host plants (c) against different values of mortality rate of whiteflies.

efforts towards controlling CMD should be directed into reducing the number of whiteflies. This can be implemented by either increasing the mortality rate of whiteflies or reducing their carrying capacity. In view of this, it is clear that measures such as the use of pesticides and entomopathogenic fungi which increases the parameter value of ω , and removing non-cassava host plants which will eventually decrease the parameter value of κ_w may bring significant results in combating CMD compared to the control of other model parameters. The decision regarding the best approach out of the two requires optimal control and cost-effective analysis of available control strategies.

The immediate future study therefore, will be development and analysis of optimal control model on CMD with the aim of minimizing the cost of controlling parameters ω and κ_w . Stochastic modelling approach which incorporates uncertainty in the dynamics of CMD may also be considered.

Declaration of competing interest

The authors declare that they have no known competing financial interests or personal relationships that could have appeared to influence the work reported in this paper.

Data availability

Data used in this study were found from different similar studies and some were assumed.

Acknowledgements

The authors acknowledge the assistance they got from the Nelson Mandela African Institution of Science and Technology (NM-AIST) and the Ministry of Education, Science and Technology (MoEST).

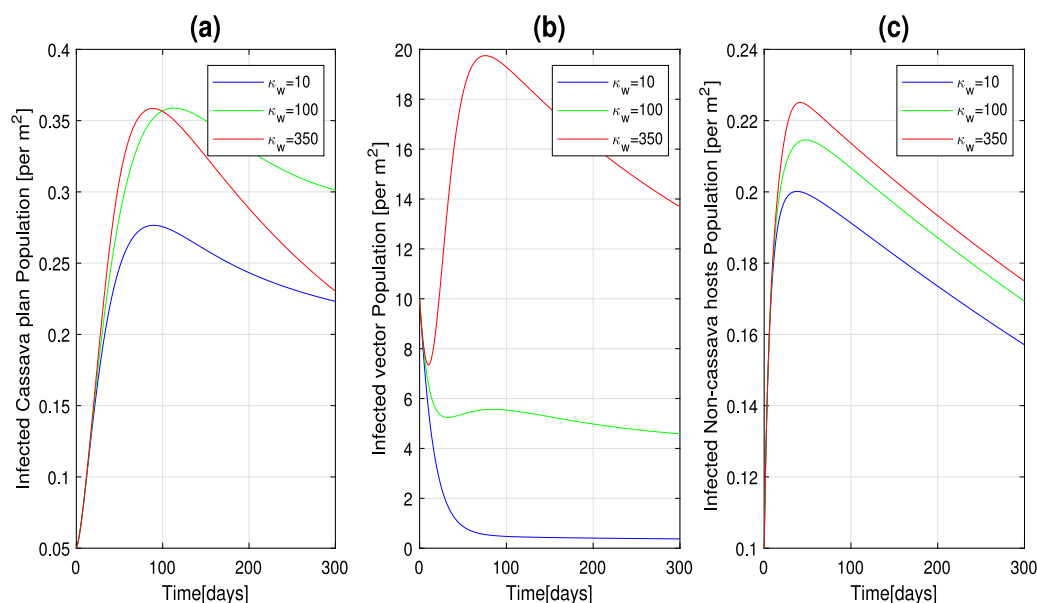


Fig. 6. Infected population of cassava plant (a), infected whiteflies (b) and infected non-cassava host plants (c) against different values of whiteflies carrying capacity.

References

- [1] Alves Alfredo Augusto Cunha. Cassava botany and physiology. Cassava: Biol Prod Util 2002;1:67–89, Publisher: CABI Publishing: Oxon, UK.
- [2] Chapwanya Michael, Dumont Yves. Application of mathematical epidemiology to crop vector-borne diseases: The cassava mosaic virus disease case. In: Teboh-Ewungkem Miranda I, Ngwa Gideon Akumah, editors. Infectious diseases and our planet. Mathematics of planet earth, Cham: Springer International Publishing; 2021, p. 57–95. http://dx.doi.org/10.1007/978-3-030-50826-5_4.
- [3] Fasuyi Ayodeji O. Nutrient composition and processing effects on cassava leaf (*Manihot esculenta*, Crantz) antinutrients. Pak J Nutr 2005;4(1):37–42, ISBN: 1680-5194 Publisher: Citeseer.
- [4] Howeler Reinhardt H. Cassava mineral nutrition and fertilization. Cassava: Biol Prod Util 2002;115–47, Publisher: CAB. International, CIAT: Chatuchak, Bangkok Thailand.
- [5] Mtunguza MK, Beckles DM, Laswai HS, Ndunguru JC, Sinha NJ. Opportunities to commercialize cassava production for poverty alleviation and improved food security in Tanzania. Afr J Food Agric Nutr Dev 2019;19(1):13928–46. <http://dx.doi.org/10.4314/ajfand.v19i1>, Number: 1 URL <https://www.ajol.info/index.php/ajfand/article/view/185568>.
- [6] Hillocks RJ. Cassava virus diseases and their control with special reference to southern Tanzania. Integr Pest Manag Rev 1997;2(3):125–38. <http://dx.doi.org/10.1023/A:1018449017411>.
- [7] Mwakosya Joseph A, Temu Gladness E, Ndunguru Joseph C. Identification and characterization of cassava mosaic begomoviruses in non-crop plants from Unguja and Pemba Islands. Tanzania J Sci 2021;47(5):1870–81.
- [8] Legg, Kumar P Lava, Makesh Kumar T, Tripathi Leena, Ferguson Morag, Kanju Edward, et al. Cassava virus diseases: biology, epidemiology, and management. Adv Virus Res 2015;91:85–142, ISBN: 0065-3527 Publisher: Elsevier.
- [9] Tiendrebeogo Fidele, Lefeuvre Pierre, Hoareau Murielle, Harimalala Mireille, De Bruyn Alexandre, Villemot Brachet Julie, et al. Evolution of African cassava mosaic virus by recombination between bipartite and monopartite begomoviruses. Virol J 2012;9:67. <http://dx.doi.org/10.1186/1743-422X-9-67>.
- [10] Anitha Jose, Makesh Kumar T, Edison S. Potential hosts of Sri Lankan cassava mosaic virus evaluated through whitefly inoculation. J Root Crops 2020;45(2):55–61, Number: 2 URL <https://isrc.in/ojs/index.php/jrc/article/view/564>.
- [11] Macfadyen S, Paull C, Boykin LM, De Barro P, Maruthi MN, Otim M, et al. Cassava whitefly, Bemisia tabaci (gennadius) (Hemiptera: Aleyrodidae) in east African farming landscapes: a review of the factors determining abundance. Bull Entomol Res 2018;108(5):565–82. <http://dx.doi.org/10.1017/S0007485318000032>.
- [12] Legg JP, Owor B, Sseruwagi P, Ndunguru J. Cassava mosaic virus disease in east and central Africa: Epidemiology and management of A regional pandemic. In: Advances in virus research. Vol. 67. Elsevier; 2006, p. 355–418. [http://dx.doi.org/10.1016/S0065-3527\(06\)67010-3](http://dx.doi.org/10.1016/S0065-3527(06)67010-3), URL <https://linkinghub.elsevier.com/retrieve/pii/S0065352706670103>.
- [13] Alaux Jean-Pierre, Fauquet C. African cassava mosaic disease: from knowledge to control. Technical Centre for Agricultural and Rural Cooperation (CTA); 1990.
- [14] Mabasa Kenneth Gaza. Epidemiology of cassava mosaic disease and molecular characterization of cassava mosaic viruses and their associated whitefly (*Bemisia tabaci*) vector in South Africa (Ph.D. thesis), University of the Witwatersrand Johannesburg; 2007.
- [15] Alabi Olufemi J, Ogbé Francis O, Bandyopadhyay Ranajit, Lava Kumar P, Dixon Alfred GO, Hughes Jacqueline d'A, et al. Alternate hosts of African cassava mosaic virus and East African cassava mosaic Cameroon virus in Nigeria. Arch Virol 2008;153(9):1743–7. <http://dx.doi.org/10.1007/s00705-008-0169-8>.
- [16] Badamasi H, Alegbejo MD, Kashina BD, Banwo OO. Alternative hosts of cassava viruses in Kaduna and Sokoto states, Nigeria. Sci World J 2020;15(2):51–5, ISBN: 1597-6343.
- [17] Monde G, Walangululu J, Winter S, Bragard C. Dual infection by cassava begomoviruses in two leguminous species (fabaceae) in yangambi, northeastern democratic Republic of Congo. Arch Virol 2010;155(11):1865–9. <http://dx.doi.org/10.1007/s00705-010-0772-3>, URL <http://link.springer.com/10.1007/s00705-010-0772-3>.
- [18] Milenovic Milan, Wosula Everlyne Nafula, Rapisarda Carmelo, Legg James Peter. Impact of host plant species and whitefly species on feeding behavior of Bemisia tabaci. Front Plant Sci 2019;10:1. <http://dx.doi.org/10.3389/fpls.2019.00001>, URL <https://www.frontiersin.org/article/10.3389/fpls.2019.00001/full>.
- [19] Sseruwagi P, Maruthi MN, Colvin J, Rey MEC, Brown JK, Legg JP. Colonization of non-cassava plant species by cassava whiteflies (*Bemisia tabaci*) in Uganda. Entomol Exp Appl 2006;119(2):145–53, ISBN: 0013-8703 Publisher: Wiley Online Library.
- [20] Holt J, Jeger MJ, Thresh JM, Otim-Nape GW. An epidemiological model incorporating vector population dynamics applied to African cassava mosaic virus disease. J Appl Ecol 1997;34(3):793–806. <http://dx.doi.org/10.2307/2404924>, Publisher: [British Ecological Society, Wiley], URL <https://www.jstor.org/stable/2404924>.
- [21] Magoyo Florence Damascus, Irunde Jacob Ismail, Kuznetsov Dmitry. Modeling the dynamics and transmission of cassava mosaic disease in Tanzania. Commun Math Biol Neurosci 2019;2019:4. <http://dx.doi.org/10.28919/cmbn/3819>, Number: 0, URL <http://www.scik.org/index.php/cmbn/article/view/3819>.
- [22] Fahad Al Basin, Kyrychko YN, Blyuss KB, Ray S. Effects of vector maturation time on the dynamics of cassava mosaic disease. Bull Math Biol 2021;83(8):87. <http://dx.doi.org/10.1007/s11538-021-00921-4>.
- [23] Jittamai Phongchai, Chanlawong Natdanai, Atisattapong Wanyok, Anlam-lert Wanwarat, Buensanteai Natthiya. Reproduction number and sensitivity analysis of cassava mosaic disease spread for policy design. Math Biosci Eng 2021;18(5):5069–93, ISBN: 1551-0018.
- [24] Chuma Furaha. Modeling the dynamics, control and economic loss of Newcastle disease in village chicken: a case of Pwani region in Tanzania (Ph.D. thesis), 2019.
- [25] Daudi Salamida, Luboobi Livingstone, Kgosimore Moathodi, Kuznetsov Dmitry. Modelling the control of the impact of fall armyworm (spodoptera frugiperda) infestations on Maize production. In: Yu Jianshe, editor. Int J Differ Equ Appl 2021;2021:1–16. <http://dx.doi.org/10.1155/2021/8838089>, 1687-9651, 1687-9643, URL <https://www.hindawi.com/journals/ijde/2021/8838089/>.

- [26] Nyerere Nkuba, Luboobi Livingstone, Mpeshe Saul, Shirima Gabriel. Modeling the impact of seasonal weather variations on the infectiology of brucellosis. 2020, <http://dx.doi.org/10.1155/2020/8972063>, URL <https://dspace.nm-aist.ac.tz/handle/20.500.12479/1336>. Accepted: 2021-09-23T12:41:54Z Publisher: Hindawi.
- [27] Heffernan JM, Smith RJ, Wahl LM. Perspectives on the basic reproductive ratio. *J R Soc Interface* 2005;2(4):281–93. <http://dx.doi.org/10.1098/rsif.2005.0042>, ISSN: 1742-5689, 1742-5662. URL <https://royalsocietypublishing.org/doi/10.1098/rsif.2005.0042>.
- [28] Van den Driessche P, Watmough James. Further notes on the basic reproduction number. In: *Mathematical epidemiology*. Springer; 2008, p. 159–78.
- [29] Mayengo Maranya M, Shirima Gabriel M, Chakraverty Snehashish, Kgosimore Moatlhodi, Seshaiyer Padmanabhan, Caiseda Carmen. Mathematical modeling of the dynamics of health risks associated with alcoholism in tanzania: a literature review. *Commun Math Biol Neurosci* 2020;2020.
- [30] Mayengo Maranya M, Kgosimore Moatlhodi, Chakraverty Snehashish. Fuzzy dynamical system in alcohol-related health risk behaviors and beliefs. In: *Soft computing in interdisciplinary sciences*. Springer; 2022, p. 109–27.
- [31] Kung'aro Monica. Mathematical modelling of intra and inter dynamics and control of yellow fever in primate and humna populations (Ph.D. thesis), The Nelson Mandela African Institution of Science and Technology; 2016, URL <https://dspace.nm-aist.ac.tz/handle/20.500.12479/57>. (Accepted: 2019-05-14T14:29:12Z).
- [32] Mayengo Maranya M, Kgosimore Moatlhodi, Chakraverty Snehashish. Fuzzy modeling for the dynamics of alcohol-related health risks with changing behaviors via cultural beliefs. *J Appl Math* 2020;2020:1–9. <http://dx.doi.org/10.1155/2020/8470681>, ISSN: 1110-757X, 1687-0042. URL <https://www.hindawi.com/journals/jam/2020/8470681/>.
- [33] Jeger MJ, Holt J, Bosch FVan Den, Madden LV. Epidemiology of insect-transmitted plant viruses: modelling disease dynamics and control interventions. *Physiol Entomol* 2004;29(3):291–304. <http://dx.doi.org/10.1111/j.0307-6962.2004.00394.x>, URL <https://onlinelibrary.wiley.com/doi/abs/10.1111/j.0307-6962.2004.00394.x>, _eprint: <https://onlinelibrary.wiley.com/doi/pdf/10.1111/j.0307-6962.2004.00394.x>.
- [34] Bokil VA, Allen LJS, Jeger MJ, Lenhart S. Optimal control of a vectored plant disease model for a crop with continuous replanting. *J Biol Dyn* 2019;13(sup1):325–53. <http://dx.doi.org/10.1080/17513758.2019.1622808>, Publisher: Taylor & Francis _eprint.

